VOLUME 39 DECEMBER 1953 NUMBER 12

PROCEEDINGS

OF THE

NATIONAL ACADEMY OF SCIENCES

OF THE

UNITED STATES OF AMERICA

EDITORIAL BOARD

LINUS PAULING, *Chairman* EDWIN B. WILSON, *Managing Editor*

ALEXANDER WETMORE, *Home Secretary* ROGER ADAMS, *Foreign Secretary*

WILLIAM W. RUBEY, *Chairman of the National Research Council*

J. W. BEAMS G. W. BEADLE GREGORY BREIT

R. E. CLELAND E. A. DOISY L. C. DUNN

W. W. RUBEY G. C. EVANS W. F. LIBBY

HARLOW SHAPLEY C. H. GRAHAM J. VON NEUMANN

F. E. TERMAN J. T. PATTERSON PAUL WEISS

Publication Office: Mack Printing Company, Easton, Pa.

Editorial Office and Home Office of the Academy

2101 Constitution Avenue, Washington 25, D. C.

Entered as Second-Class matter June 21, 1920, at the Post-Office at Easton, Pennsylvania, under the Act of August 24, 1912. Accepted for mailing at a special rate of postage provided for in section 1103, act of October 3, 1917. Authorized June 16, 1920.

Published Monthly Price per Annum, $7.50

OFFICERS OF THE ACADEMY

PRESIDENT.....DETLEV W. BRONK
VICE PRESIDENT.....GEORGE W. CORNER
FOREIGN SECRETARY.....ROGER ADAMS
HOME SECRETARY.....ALEXANDER WETMORE
TREASURER.....WILLIAM J. ROBBINS

INFORMATION TO SUBSCRIBERS

Checks covering subscriptions to the PROCEEDINGS OF THE NATIONAL ACADEMY OF SCIENCES at the rate of $7.50 per annum should be made payable to the National Academy of Sciences, and sent to the Treasurer, National Academy of Sciences, 2101 Constitution Ave., Washington 25, D. C. Single numbers $0.75.

Microfilm copies of the PROCEEDINGS are available to subscribers to the paper edition. The microfilm is a positive, furnished on metal reels, suitably labeled, and is distributed at the end of the volume year. Inquiries concerning purchase should be directed to University Microfilms, 313 N. First St., Ann Arbor, Michigan.

Past publications of the NATIONAL ACADEMY OF SCIENCES from 1863 to 1920 and of the NATIONAL RESEARCH COUNCIL from 1916 to 1925 are listed in the Index to the First Ten Volumes of these PROCEEDINGS. This Index appeared as Part 2 of Volume 13, No. 1, January, 1927, and is for sale separately at the price of $1.50. Orders should be sent to the Home Secretary, National Academy of Sciences, 2101 Constitution Ave., Washington 25, D. C.

Past volumes of the PROCEEDINGS may be obtained at five dollars per volume unless the sale of the volume would break a complete set of Volumes I to XXX. Single numbers may be obtained for fifty cents except where the sale of such numbers would break up a complete volume. Beginning with Volume 37 (1951), complete volumes are $7.50, and single numbers $0.75. Only forty complete sets of the PROCEEDINGS are available for sale —Volumes I to XXX price $200.00. Orders should be sent to the Home Secretary, National Academy of Sciences, 2101 Constitution Ave., Washington 25, D. C.

THE NATIONAL ACADEMY OF SCIENCES-NATIONAL RESEARCH COUNCIL also issues technical publications reviewing and correlating recent research. The *Bulletin* and *Reprint and Circular Series* have been replaced by a single publication series, available individually, or by subscription at 25% discount. For a list of available publications, with prices and ordering procedures, address the Publications Office, National Academy of Sciences-National Research Council, 2101 Constitution Avenue, Washington 25, D. C.

PROCEEDINGS
OF THE
NATIONAL ACADEMY OF SCIENCES
Volume 39 December 15, 1953 Number 12

SATELLITES, COMETS, AND INTERPLANETARY MATERIAL

By Gerard P. Kuiper

Yerkes Observatory, University of Chicago

Communicated October 22, 1953

1. In a paper now in press[1] it was shown that the small outer satellites shed by Jupiter, and which later formed the Trojan "asteroids" and the irregular satellites of Jupiter,[2] could not have originated from proto-satellites. Let the mass ratio, proto-satellite to parent planet at the time of formation of the satellite be called m'. Then there is a lower limit to m' which arises as follows.[3] If one considers a series of identical planets but surrounded by nebulae of different densities, then m' will decrease with decreasing density of the nebula; but there is a lower density limit beyond which gravitational instability cannot set in. This limiting density will lead to the smallest possible value of m'; it is of the order of 10^{-4}. Now it can be shown, from the present dimensions of the bodies referred to, that they condensed from cosmic masses about 10^5 times less massive than this lower limit; since small masses are involved in any case, and hence low temperatures during the period of condensation, the possibility of large losses of solid materials through evaporation does not arise. That is, the present masses are reliable indicators of the masses of the initial cosmic clouds that produced them; these are of the order of 200 times the present masses, as follows from a table of cosmic abundances.

The conclusion that outer satellites of Jupiter, since lost,[2] did not originate as proto-satellites means that the density of this part of Jupiter's envelope was too low for gravitational instability to set in. One could probably have anticipated this conclusion since during the earlier stages of protoplanet development, when the nebula had still a large radius, solar tidal friction was a powerful break on the rotation of the outer part of the nebula,[4] preventing it from becoming highly flattened and compressed, and from tending to become unstable gravitationally. For the remainder of this paper these general considerations suffice, without detailed numerical analysis.

It follows that the other protoplanets went through a similar stage as proto-Jupiter, of condensation and sedimentation taking place near the plane of symmetry of the nebular envelopes. In other words, small satellites of a great variety of dimensions formed by a snowballing process near the plane of symmetry of the nebula; they acquired nearly circular orbits of nearly zero inclination. Later in the protoplanet history a similar process occurred in the innermost part of the nebular envelope where the density again fell below the critical value.[1] This is testified by the smallness of the masses of the (close) satellites of Mars; by Jupiter V, only 2.5 radii from the giant planet; and by the innermost satellites of Saturn and Uranus. (The absolute amount of the densities in the innermost part of the planetary envelope was much higher than that in the outermost parts, the critical standard varying with the distance from the planet as r^{-3}, as is true of tidal effects in general.) In all these cases a gravitational collecting process continued after condensation had formed the sediments. Only for the rings of Saturn did this collection process not occur, clearly because it formed inside the Roche limit corresponding to the density of the solid state. The larger satellites, namely the four Galilean satellites of Jupiter, Rhea and Titan of Saturn, and probably the larger of the Uranus satellites formed from genuine proto-satellites; i.e., from gaseous clouds, stable in the tidal field of the parent planet, and giving birth to one satellite each.

2. As the protoplanets lost mass by evaporation[5] they shed the outermost satellites of all sizes. These were deposited into interplanetary space, from which they could be recaptured, or pressed into forced orbits like the Trojans, or scattered through the solar system by planetary perturbations. Because of the third possibility some of these objects may now come close to the earth even if they originated, e.g., in proto-Neptune. It is, therefore, important to examine what such objects might be like.

The effective evaporation of the protoplanets did not begin until the sun had finished contracting to its present equilibrium dimensions and began to radiate powerfully in the ultraviolet and to emit corpuscular radiation. The proto-planets will, therefore, have existed as such roughly 10^8 years, the time scale of the solar contraction, a good fraction of which was spent without sensible heating from the sun. The time interval for unhindered condensation may, therefore, be conservatively estimated as 10^7 years. The Roche density at the distance of Neptune is about 10^{-10} cgs, and the initial mean density of proto-Neptune may be estimated to be 10 times higher or 10^{-9} cgs. In the inner and warmer parts of proto-Neptune only the silicates and metals will have condensed and collected; there the solid fraction will have been about 0.002 by mass. In the colder outer parts H_2O and NH_3 will have condensed also and for the coldest parts probably even CH_4; there the solid fraction will have been about 0.01 by mass. The initial space density of the condensable material will, therefore, have been of the order

of 10^{-11} to 10^{-12}. Since the size to which condensations grow is

$$r = \frac{v}{4}\frac{\rho_N}{\rho_C}t, \qquad (1)$$

in which v is the mean velocity of the molecules relative to the condensation[6] and t the available time, we find, with $\rho_N = 10^{-12}$, $\rho_C = 1$, $v = 1.6 \cdot 10^4$ (corresponding to $T = 20°$K., $\bar{\mu} = 20$), and $t = 10^7$ years $= 10^{14.5}$ sec., $r \simeq 10$ km.

Thus, in the coldest and most tenuous parts proto-Neptune objects will have formed with radii from about 100 meters to 10 km. composed of ices (in the form of very loose snow) and silicate and metal grains. These bodies will resemble comet heads in composition and size. In the inner parts which are denser and warmer, larger objects will have grown, largely composed of silicates and metals but with some admixture of H_2O snow. These objects would probably resemble the present satellite Nereid.

It follows that all four Jovian planets will have produced comet-like objects. The problem remains whether some of these were later shed into interplanetary space. This problem is complicated; the result depends on the size of the object and the time scale of contraction of the protoplanet envelope. This is seen as follows. The gaseous envelope will in part be held up by a radial pressure gradient; the sediment will not be supported by this gradient and will initially fall inward to seek an orbit around the planet suitable for its angular momentum. In doing so it will increase its angular velocity over that of the surrounding gas which does not move in free circular orbits. Thus it will lose angular momentum to the gas and continue to spiral inward. Therefore, all particles smaller than a given size will spiral inward, and build in time the nucleus of the planet. The larger particles will be less affected by the resisting medium, the friction depending on the diameter of the body to a power less than 3; they will lose, therefore, a smaller fraction of their initial angular momentum and spiral in more slowly. If now the planet loses mass fast enough by evaporation, once the sun has become bright, the object may even increase its distance from the planetary nucleus. After the boundary of the envelope has fallen inside the object, the further increase from the planet will be governed by the law derived before[7] and the object may be shed into interplanetary space.

Since the time scales of the decreasing planetary envelopes are not yet known to any precision, no precise prediction can be made as to the lower limit in size that will be set free for each of the planets. In the case of Jupiter we know empirically that small satellites have been set free down to the limit of detection, something like $r = 8$ km.

The production of comets by the outer planets must be in addition to the production in the outer parts of the solar nebula.[8, 9] This addition is wel-

come because from the beginning there has been some doubt as to whether the mass of Pluto was sufficient to cause the initial dispersal of comets in the required frequency.[10] The question of the mass of Pluto is no more settled today than when its role in the dispersal process was first considered. It is hoped that further light will be shed on this problem by a photometric study now underway. (If the period of rotation is found to be of the order of a day or less, it is very probable that Pluto formed as a planet; if the period is of the order of a week or more, it almost certainly formed as a satellite of Neptune, showing the slow rotation of an outer satellite. In the latter case, the small mass inferred from the measured diameter would in a general way be confirmed.) At any rate, there is reason to doubt Pluto's ability to have dispersed quite enough objects from the comet zone outside Neptune.

It appears then that *the comets observed during the present epoch probably belong to different genetic groups:* solar-nebula comets, Neptune comets, Uranus comets, etc. Because of the above-mentioned processes and time scales relevant to the shedding of these bodies, some differences in composition are likely to exist between these groups, particularly in the carbon content.

3. It is of interest to examine next the analogous problems for the Earth and Venus. Such objects of Icarus, Adonis, Hermes, and Apollo, find their most natural explanation as freed minor satellites of the earth. The smallness of these bodies ($r \sim 1$ km.) then testifies that the outer parts of proto-Earth were of a density very far below the critical Roche density. Venus, being still closer to the Sun and retarded even more in its rotation, will presumably have produced even smaller objects. One characteristic of such former satellites can be confidently predicted: they will be extremely fragile structures, having been formed in a region of very low effective gravity. If such a body would strike the Earth, not much more than a vast dust cloud might remain. Possibly the Siberean "meteorite" of 1908 was such a body.

4. One is forced to conclude that *two different mechanisms of satellite formation have been operative.* The large satellites developed from proto-satellites, which in turn resulted from the break-up of a gaseous nebula by gravitational instability. This mechanism allows in principle the computation of the proto-satellite masses from the distances between the resulting satellite orbits. The small satellites, on the other hand, developed in nebulae which were below the limiting density, ρ', permitting gravitational instability to set in. They grew by accretion and no simple prediction can be made of the resulting masses, except that they will depend on the amount of solid material available in the nebular zone in question, and will be smaller than corresponds to proto-satellites formed from a nebula at the limiting density ρ'.

The satellite masses show[1] that there is no distinct gap between the two genetic groups. This probably arises from the fact that even when the nebular density is below ρ' a condensation with $r \gg 1$ km. will acquire a gaseous envelope that will accelerate the accretion process, and that in the final stages may become so large as to simulate a proto-satellite. For instance, if the Roche density should be 10^{-6}, the nebular density 10^{-8} or 10^{-9}, and the density of the solid condensation 1, this body will be able to retain a "massless" envelope of about 100 times its own radius, and a compressed envelope of slightly greater radius. If there is a small relative motion between the condensation and the nebula, the envelope will suffer losses to the nebula but will be replenished on the leading edge. If the condensation should reach $r \cong 100$ km., the envelope would have become quite resistant to disruption by collisions. Evaporation would not take place because of the small mean free path (roughly 1 cm.) in the surrounding nebula.

The rate of accretion for a substantial condensation will be increased not merely by the enlarged cross section owing to its envelope. It has been remarked that small condensed grains will spiral inward toward the planet owing to friction with the surrounding nebula which rotates at a slightly slower rate, the nebula being partly supported by a radial pressure gradient. Once the sediments become concentrated toward the plane of symmetry as a result of inelastic collisions (a process that is expected to take place at a cosmically rapid rate), further spiralling inward will often lead to capture by the envelopes of large condensations already present. As long as the protoplanet envelope exists, therefore, *the smallest condensations will be swept up by the larger ones*, though not necessarily with complete efficiency. Genuine proto-satellites will also sweep up grains condensed farther out from the planet.

5. The process outlined in the preceding paragraph may have played some role in the formation of the rings of Saturn. A fraction of the materials of which the rings are composed may have condensed in the zone of the inner satellites and have been prevented from spiralling in still further when Saturn's envelope dissipated. The particles of the three subdivisions of the ring may then differ in size.

Possible further consequences are the relatively low mean densities of Jupiter III and IV, and of the Moon. If the loss by the Earth of silicates as compared to iron is real, as seems likely,[11] one is led to assume that the silicates evaporated from the surface of a molten earth during the period of highest central temperature. A fraction of the resulting oxides will have condensed in the outer parts of proto-Earth. The resulting grains of $r \cong 10^{-5}$ cm. could have been driven away into interplanetary space by solar radiation pressure.[12] Larger particles would have spiralled in toward the Earth, with a fraction attaching themselves to small outer satellites,

since lost (see above); while some of the material would have been acquired by proto-Moon. If the period of evaporation lasted long enough, eventually an appreciable fraction of the silicates could thus have been permanently lost to the Earth. It is stressed that these applications of section 4 are at present without direct confirmation. Even more speculative is the remark that the materials from which the present tektites are formed, originated in this manner on the earth and were subsequently lost to interplanetary space. The only justification from the remark is that it provides a dynamically possible origin for these bodies. One might perhaps further assume that they were remolten and degassed during subsequent close approaches to the Sun, prior to the recent collisions of some of them with the Earth.

The bearing of section 4 on the origin of the asteroids is discussed in the following paper.[13]

[1] Kuiper, G. P., *Vistas in Astronomy* (in press), Cambridge University Press, 1954, edited by A. Beer.

[2] "On the Origin of the Irregular Satellites," these PROCEEDINGS, **37,** 717 (1951).

[3] *Astrophysics*, J. A. Hynek, editor, McGraw-Hill Book Co., 1951, p. 398, eq. (48).

[4] *Ibid.*, Chapter 8, Part III.

[5] *La Physique des Comètes*, Louvain, 1953, Section 31: "Comets and the Dissipation of the Solar Nebula," by G. P. Kuiper.

[6] Reference 3, p. 370, eq. (2).

[7] Reference 2, p. 719.

[8] "On the Origin of the Solar System," these PROCEEDINGS, **37,** 13 (1951).

[9] Ref. 3, pp. 359f, 400–402.

[10] *Ibid.*, p. 401. The mass of Pluto may be about $10^{-7}\odot$.

[11] E.g., *The Atmospheres of the Earth and Planets*, 2nd ed., University of Chicago Press, 1952, p. 330f.

[12] *Ibid.*, p. 335.

[13] Kuiper, G. P., "Note on the Origin of the Asteroids," these PROCEEDINGS, **39,** 1159–1161 (1953).

NOTE ON THE ORIGIN OF THE ASTEROIDS

BY GERARD P. KUIPER

YERKES OBSERVATORY, UNIVERSITY OF CHICAGO

Communicated October 22, 1953

In the preceding paper[1] it was found that the satellites have originated by two different processes, depending on whether the planetary envelopes in which they formed were gravitationally stable or unstable. One is forced to this conclusion by the smallness of a number of satellite masses, which are some 10^5 times smaller than is compatible with their origin from proto-satellites. In these cases the planetary envelope clearly did not break up by gravitational instability; it must have had a density below the critical limit which separates gravitationally stable from unstable nebulae.

This clarification of the satellite problem suggests a re-examination of the planet problem, in particular that of the planets of small mass, the asteroids. The hypothesis made before[2] was based on the assumption that gravitational instability, clearly operative in the formation of the 8 major planets, was also responsible, though in modified form, for the formation of the original group of minor planets. This assumption seemed natural on grounds of simplicity and uniformity. The modification definitely called for by the small masses of the asteroids was considered to be the result of the perturbations by massive proto-Jupiter, which would tend to prevent the formation of a single, large protoplanet in the asteroid zone if the density of the solar nebula was not greatly in excess of the limiting density; but which might allow the formation of several small and more stable protoplanets. That this could definitely happen was not demonstrated; it appears doubtful to the writer now that the anticipated development could arise from gravitational instability alone. The amplification of density fluctuations of comparatively small wavelengths could have occurred only if condensation products would have locally raised the mean density to greatly increased values. The hypothesis was made to preserve uniformity in the processes of planet formation, but without detailed proof. It has become clear that uniformity does not exist in satellite formation and it appears necessary to abandon it also between planets and asteroids.

There is another argument against the old hypothesis of asteroid formation. The present masses of the largest asteroids are of the order of 10^{-10} $M_\odot$. In the earlier paper referred to[2] it was shown that a lower limit exists for the mass of a protoplanet formed by gravitational instability. The numerical value derived before, 2.10^{-5} $M_\odot$, was based on a greatly simplified model. Subsequent unpublished studies confirm the existence of the lower limit, but show its value to be dependent upon the uncertain initial temperature of the solar nebula; the numerical value is estimated to be of

the order of 10^{-4} $M_\odot$ or somewhat larger. Now the mean internal temperature of a protoplanet of mass M and radius R is proportional to M/R, with the coefficient dependent upon the degree of central concentration of the mass; this follows from the virial theorem. Therefore, if the protoplanets were built approximately on the same model, the internal temperatures at the time they attained the same mean density, varied as R^2 or $M^{2/3}$. Hence, for corresponding phases of development, the smaller masses had much the lower internal temperatures and, as judged from present masses, no large mass losses by evaporation could have occurred from the original asteroids; because even the earth, which now has a mass 10^4 times greater, did not suffer any excessive losses.

On the basis of the preceding paragraph one may estimate how large the cosmic masses were from which the original asteroids formed; one finds 10^{-7} to 10^{-8} $M_\odot$. This is 10^3 to 10^4 times smaller than the lower limit of protoplanet masses. The interpretation of this discordance is undoubtedly the same as that for the analogous situation of the small satellites: both groups were formed by accretion in gravitationally stable nebulae.

A rough test of the accretion hypothesis may now be made. The radius of the condensation, r, is given by

$$r = \frac{v}{4}\frac{\rho_N}{\rho_C} t, \qquad (1)$$

in which the nebular density may be estimated to be 10^{-2} of the Roche density, or 10^{-9} cgs. The condensable material will have an average space density of about 0.003 of this, so that $\rho_N = 3.10^{-12}$ cgs. Further, $\rho_C = 2$, while we may estimate $T = 100°$K., $\mu = 50$, and hence $v = 2.2\ 10^4$; then, with $t = 10^7$ years $= 3.10^{14}$ sec., $2r = 50$ km.

The radial density gradient in the solar nebula was extremely small and the condensate, even the part contained in small grains, will not have moved out of the asteroid zone until the sun got its present brightness (after about 10^8 years) and the small particles started spiralling in toward the sun under the Poynting-Robertson effect. The accretion by the asteroids did, therefore, not stop with the dissolution of the solar nebula, and, in fact, it must be still continuing today, though at a reduced rate because of the removal of all original particles smaller than about 10 cm. The value of 50 km. computed with $t = 10^7$ years must, therefore, be corrected upward by one or two orders of magnitude. It is concluded that the original asteroids might indeed have attained the size of Ceres, the largest, which has $2r = 800$ km.; about a dozen asteroids are as large as $2r = 300$ km. Furthermore, before the solar nebula dissolved there may have been a period where the accretion rate was temporarily increased by the formation of gaseous envelopes around the condensations.[1]

On the accretion hypothesis the number of original asteroids cannot be

clearly determined, but it is expected to be rather large, say 10–100 in the observable region. Collisions within the asteroid ring will have started much earlier, and will have been more frequent later on, than was considered on the basis of the old hypothesis which assumed the number of original asteroids to have been of the order of 5 to 10. Furthermore, not all *small* asteroids need be *fragments* of collisions; on the old hypothesis the production of small asteroids from protoplanets would have been even more artificial than of Ceres. From current photometric studies the writer has gained the general impression that the accretion hypothesis fits the empirical data very well. As these studies progress several empirical tests (periods of rotation; position in space of rotational axes; maximum amplitudes of light variation and shapes of the bodies) will be possible concerning predictions of a more elaborate theory of asteroid origin and development.

[1] These PROCEEDINGS, **39**, 1153–1158 (1953).

[2] *Astrophysics*, J. A. Hynek, editor, the McGraw-Hill Book Co., New York, 1951, pp. 398–400 and Fig. 10, p. 395.

MAGELLANIC CLOUDS, VIII. ON THE POPULATION CHARACTERISTICS OF THE TWO CLOUDS

BY HARLOW SHAPLEY

HARVARD COLLEGE OBSERVATORY

Communicated October 5, 1953

Because of the differences between the Magellanic Clouds in form, brightness, and amount of nebulosity and dust, I suggested some time ago that the future of the Small Cloud perhaps lies in the direction of the dwarf open spheroidal galaxies in Sculptor and Fornax and that the Large Cloud may go the way of the barred spirals.[1] The Small Cloud's population at its center is possibly intermediate between populations I and II (Baade's nomenclature); its "sixteen-day" cepheids remind one of the cepheids in globular clusters, but their light curves, we have found,[2] are in general not alike.

The suggestion of a difference between the two Clouds in population characteristics has been carried further by others. Baade had already proposed[3] that the Large Magellanic Cloud has an essentially pure population I. Gascoigne and Kron have suggested that the Small Cloud is predominantly population II, and accordingly they propose that the hundreds of cepheids in the Small Cloud may be of the W Virginis type,[4] whereas those of the Large Cloud are classical cepheids. If such a difference could be established it would be of high importance in questions of

the life history of galaxies. Heretofore the Clouds have been considered a physical pair, and not separated in space by some 80 k.l.y. as the hypothesis would require.

The following comparative data show of course that the Clouds undoubtedly differ from each other in some respects, such as in the abundance of supergiant blue stars and of diffused nebulosity; the Large Cloud is about four times the Small Cloud in volume, also in luminosity, and presumably therefore in mass. But the comparisons also show that basically the Clouds are a pair of similar irregular galaxies, neither dwarfs nor giants, with closely comparable populations; their distances apparently differ by only a few thousand light years.

In the Small Cloud are several hundred variables that conform as closely as should be expected with a single period-luminosity relation. The scatter is due almost entirely to Cloud thickness and localized space absorption. If its cepheids actually were members of the W Virginis subclass, as the variables with periods greater than a day in globular clusters appear to be,[5] then the Small Cloud is at but half the distance of the Large Cloud and a star of given type should appear $1^m.5$ brighter in the Small Cloud than in the Large. Thus the novae, irregular red variables, and long-period variables would be conspicuously brighter (apparent magnitude) in the Small Cloud. Also, if there were any classical cepheids in the Small Cloud, they should on this hypothesis be most easy to discover and observe because their apparent magnitudes, say for periods of ten days, would be between 13 and 14, available even to the patrol cameras; but such variables have not been identified.

In the following paragraphs we intercompare the apparent magnitudes for objects of six special types in the two Clouds, in addition to the cepheids with periods in excess of a day.

Novae.[6]—Using the same apparent magnitude standards for the two Clouds, we have the following magnitudes at maximum for the eight novae now in our records.

DESIGNATION	SMALL CLOUD	DESIGNATION	LARGE CLOUD
Nova Tuc 1897	$11^m.4$	Nova Dor 1926	$12^m.4$
Nova Tuc 1927	11.4	Nova Dor 1936	10.8
Nova Tuc 1951	11.0	Nova Dor 1937	10.65
Mean	11.3	Nova Dor 1948	13.8:
		Nova Men 1951	11.95
		Mean	11.7

Within the observational uncertainty the novae attain about the same apparent magnitude at maximum in the two Clouds, but this evidence by itself is not decisive.

Supergiant Red Variables.[7]—From results published from the Harvard

Observatory we have for 99 red irregular variables the following mean apparent magnitudes at maximum.

	SMALL CLOUD	NUMBER	LARGE CLOUD	NUMBER
All studied	$14^{m}.52$	31	$14^{m}.39$	68
Seventeen brightest	13.87	17	...	..

The second entry for the Small Cloud recognizes the fourfold greater population of the Large Cloud. Similar adjustments are shown for the following types.

Long-Period Variables.[8]—From their high frequency per unit area we conclude that the 22 long-period variables in the Cloud fields, with one or two possible exceptions, are actual Cloud members. The mean maximum magnitudes are:

	SMALL CLOUD	NUMBER	LARGE CLOUD	NUMBER
All measured	$15^{m}.20$	11	$14^{m}.13$	11
Three brightest	14.33	3	...	..

Eclipsing Binaries.[9]—The apparent magnitudes at maximum of the Beta Lyrae type of eclipsing binary that we have found and studied in the 30 Doradus nebulosity of the Large Cloud may be somewhat dimmed by the accompanying dust; the mean magnitude at maximum for that Cloud in the following tabulation should possibly be brightened somewhat in comparing it with the mean for the Small Cloud.

	SMALL CLOUD	NUMBER	LARGE CLOUD	NUMBER
All found	$15^{m}.39$	26	$14^{m}.94$	24
Six brightest	14.42	6	...	..

Blue Supergiant Stars.[10]—The survey of hottest stars (Classes B, O, and P Cygni) is certainly incomplete in both Clouds and the mean magnitudes carry little weight, except to show for the B stars consistency with the foregoing data.

	SMALL CLOUD	NUMBER	LARGE CLOUD	NUMBER
All classified	$10^{m}.4$	7	$11^{m}.2$	150
Twenty-eight brightest	..	..	10.3	28

Globular Star Clusters.[11]—The three clusters that are most definitely identified as globular in the Small Cloud provide useful evidence of the comparable distances of the two Clouds; but it is probable that further study will reveal fainter globular clusters in both systems. Total photographic magnitudes are tabulated.

SMALL CLOUD	NUMBER	LARGE CLOUD	NUMBER
$11^{m}.07$	3	$11^{m}.12$	10

We conclude from the foregoing comparisons of six types of objects that the Clouds are at essentially the same distances. Using the values adjusted to allow for the larger population of the Large Cloud, we have the following summary:

TYPE OF OBJECT	SMALL MINUS LARGE	WEIGHT
Novae	−0.4	1
Irregular variables	−0.52	2
Long-period variables	+0.40	2
Eclipsing binaries	−0.52	1
Blue supergiants	+0.1	1
Globular clusters	−0.05	2
Ten-day cepheids	+0.1	4
Weighted mean	−0.06 ± 0.3 (m.e.)	

The last entry, the average ten-day cepheid, is derived from the period-magnitude curve of figure 2. The mean difference of magnitude for the seven items corresponds to a difference in distance (Small Cloud nearer) of less than 3 per cent, or five thousand light years on the revised scale—far within the error.

Cepheid Variables.—To examine further the suggestion that the Small Cloud's cepheids may belong to population II (W Virginis type) and therefore be much fainter intrinsically than the classical cepheids of the Large Cloud, we can work directly with the variables. Two tests can be made. The first, which was completed five years ago,[12] appears to be definitive. We selected 40 cepheids from the Small Cloud and 49 from the Large Cloud for a special study of magnitudes, amplitudes, and light curves. For each Cloud there is a wide spread in period and apparent luminosity. Period-luminosity relations, therefore, based on the same apparent magnitude standards, are obtained separately for the two Clouds. Figure 1 shows the results; open circles refer to stars of the Large Cloud, dots to those of the Small Cloud. No adjustment of zero point to allow for slightly different distances has been made. The resulting plot is of course closely similar to earlier period-luminosity relations based on hundreds of variables less precisely studied in the two Clouds. Most of the scatter around the smooth mean curve can be attributed to the thickness of the Clouds, and to local patches of obscuring material. Contributions to the scatter from measuring errors, Eberhard effect, and undetected doubling are minor for the 89 selected variables. Again we conclude that the cepheids have essentially the same apparent magnitudes and the same absolute luminosity in the two Clouds.

The light curves of the 89 variables have been published in detail;[13] they do not show systematic differences between the two Clouds, or show among the variables of the Small Cloud the characteristics of W Virginis type cepheids.

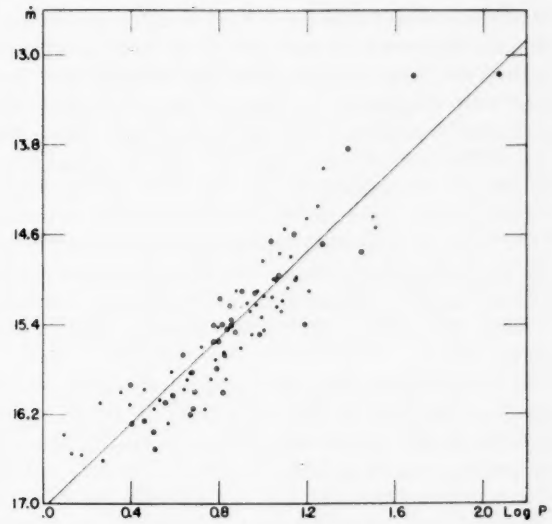

FIGURE 1

Period-magnitude relation for 39 selected cepheids in the Large Cloud (open circles) and 49 selected cepheids in the Small Cloud (dots). Ordinates are median apparent photographic magnitudes; abscissae, logarithms of periods.

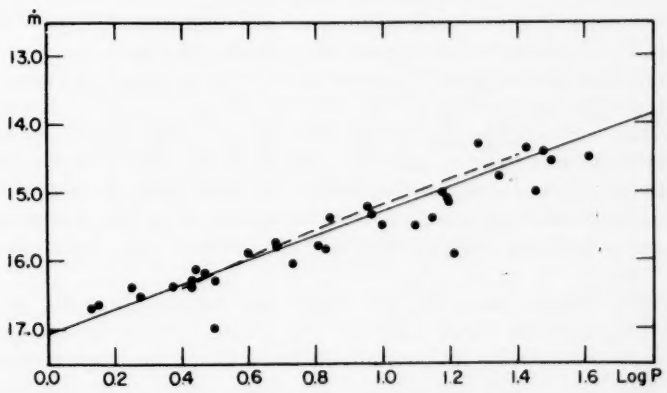

FIGURE 2

Period-magnitude relation for 34 cepheids in the core of the Small Cloud (dots) and the broken-line representation for 122 cepheids in the bar (axis) of the Large Cloud. Coordinates as in figure 1.

To clarify one point that has entered the Gascoigne and Kron discussion, it should be noted that we have been unable to verify on Harvard plates the three periods less than a day reported by Dartayet and Dessy.[14] If their variables were accepted as members of the Small Cloud, the assignment of its stars to population II would be supported. But on the basis of our studies of the distribution of high-latitude RR Lyrae type variables that are members of the galactic system,[15] we should expect in the area covered by the Cloud at least half a dozen such variables in the magnitude interval 17 to 18, and some of these superposed stars may fall in the regions examined by the Cordoba observers. The true RR Lyrae type members of the Small and Large Clouds are almost certainly those 19th magnitude variables discovered by Thackeray[16] in the globular clusters that appear to be Cloud members.

The second test compares the period-magnitude relation of the "core" of the Small Cloud with that for the bar (axis) of the Large. Both regions have high stellar density and in this respect approach the conditions in the galactic nucleus and in globular clusters. The core has but a few cepheids with periods between four and ten days, the usually predominant length, but several with longer periods. The periods that are less than four days may well be those of stars superposed from the outer regions of the Cloud. In figure 2 the 34 plotted points refer to all the core variables[17] for which we have periods. One of the two points that fall farthest below the standard period-magnitude curve refers to a variable that is alongside, a nebulous patch, and the other may be similarly affected. The longer-period stars of the core are on the average fainter than what is normal for the whole Cloud by nearly two tenths of a magnitude. This deficiency indicates the concentration of space absorption in the core.

The broken line in figure 2 is a mean curve based on 122 cepheid variables located in the bar of the Large Cloud.[18] The close agreement of the curves is further evidence that the Clouds are essentially equidistant and alike in cepheid characteristics, except for the singular richness of the Small Cloud in cepheids with periods between one and three days. Another feature that awaits further study and clarification is the difference in color for the two Clouds reported from the photoelectric work by Gascoigne and Kron.[19]

Bright Nebulae.—In 1925 Miss Wilson and I published a list of 278 nebulosities in the Small Cloud.[20] The paper appears to have been generally overlooked. As a result, the Small Cloud has been considered relatively free of dust and gas, and therefore perhaps genetically related to pure population II objects. My evidence for the transparency of the Small Cloud[21] should not be overvalued because of the conspicuous irregularities, in some parts of the sky, in the areal population of faint galaxies.

In an unpublished[22] new study at Harvard of the Shapley-Wilson

nebulosities, by Mrs. Nail, Whitney, and Wade, 125 of these objects have been identified as H-alpha emission nebulae. It is well known that such nebulae are extremely uncommon in population II aggregations.

Summary.—An intercomparison of the magnitudes of the novae, star clusters, blue stars, nebulae, and four types of variable stars indicates that the distances of the Magellanic Clouds are essentially the same, their populations not unlike, and their cepheids all of the "classical" type. Certain peculiarities in the integrated colors of the Clouds and of the cepheids in the Small Cloud, reported recently by Gascoigne and Kron, remain incompletely explained; but it hardly appears possible to clarify the situation by proposing that the hundreds of cepheids of the Small Cloud are of the W Virginis type while those of the Large Cloud are "classical" and 1.5 magnitudes more luminous.

[1] *Pub. Mich. Obs.*, **10,** 83 (1951): *Harvard Reprint* Series II-37.

[2] These PROCEEDINGS, **26,** 546 (1940): *Harvard Reprint* 207; these PROCEEDINGS, **28,** 203–204 (1942): *Harvard Reprint* 241; these PROCEEDINGS, **39,** 353 (1953): *Harvard Reprint* 372.

[3] Baade, W. A., *Pub. Mich. Obs.*, **10,** 13 (1951).

[4] Gascoigne, S. C. B., and Kron, G. E., *Pub. Ast. Soc. Pac.*, **65,** 32 (1953).

[5] "Note on the Extragalactic Distance Scale," a communication presented at the Boulder, Colo., meeting of the American Astronomical Society, August, 1953; see also Paper X in this series (in press). The variables are more fully treated in an important unpublished thesis by Halton C. Arp.

[6] *Harv. Obs. Bull.* 912 (1940), 915 (1941), 920 (1951); *Harv. An. Card* 1143 (1951) Nova Tuc 1951 and Nova Men 1951 were discovered by K. G. Henize at Michigan; Nova Dor 1948, unpublished.

[7] *Harv. Obs. Bull.* 846 (1927), 905 (1937), 921 (1952); these PROCEEDINGS, **34,** 175 (1948); *Harvard Reprint* 306; these PROCEEDINGS, **37,** 144 (1951): *Harvard Reprint* 346; *Ast. J.*, **55,** 249 (1951): *Harvard Reprint* Series II-36.

[8] These PROCEEDINGS, **34,** 175 (1948): *Harvard Reprint* 306; these PROCEEDINGS, **37,** 142 (1951): *Harvard Reprint* 346; *Harv. Obs. Bull.* 921 (1952).

[9] *Harv. Obs. Bull.* 916, 19 (1942); these PROCEEDINGS, **34,** 177 (1948): *Harvard Reprint* 306; these PROCEEDINGS, **39,** 1–5 (1953): *Harvard Reprint* 368.

[10] *Henry Draper Catalogue; Henry Draper Extension; Harv. Obs. Bull.* 801 (1924).

[11] These PROCEEDINGS, **39,** 355 (1953): *Harvard Reprint* 372.

[12] *Proc. Am. Philos. Soc.*, **92,** 310–323 (1948): *Harvard Reprint* Series II-25; *Proc. Am. Philos. Soc.*, **93,** 44 (1948): *Harvard Reprint* Series II-29.

[13] *Harv. Ann.*, **90,** No. 10 (1940); *Ibid.*, **109,** No. 11 (1948).

[14] Dartayet, M., and J. L. Dessy, *Ap. J.*, **115,** 281–283 (1952).

[15] These PROCEEDINGS, **25,** 423–428 (1939): *Harvard Reprint* 173; *Harv. Obs. Bull.* 920, 14 (1951).

[16] Thackeray, A. D., and A. J. Wesselink, *Nature*, **171,** No. 4355, 693 (1953).

[17] *Harv. Obs. Bull.* 916, 1–2 (1942); these PROCEEDINGS, **28,** 202 (1942): *Harvard Reprint* 241.

[18] *Harv. Circ.* 439 (1940); *Harv. Obs. Bull.* 921 (1952).

[19] Gascoigne, S. C. B., and Kron, G. E., *Pub. Ast. Soc. Pac.*, **65,** 35 (1953).

[20] *Harv. Circ.* 275 (1925); 276 (1925).

[21] These PROCEEDINGS, **37,** 133–138 (1951): *Harvard Reprint* 345.

[22] "Nebulosities of the Small Magellanic Cloud," a communication presented at the Boulder, Colo., meeting of the American Astronomical Society, August, 1953; see also Paper IX in this series, these PROCEEDINGS, **39**, 1168–1176 (1953).

MAGELLANIC CLOUDS, IX. THE NEBULOSITIES OF THE SMALL CLOUD

BY VIRGINIA MCKIBBEN NAIL, CHARLES A. WHITNEY, AND CAMPBELL M. WADE

HARVARD COLLEGE OBSERVATORY

Communicated by Harlow Shapley, October 12, 1953

The presence of hydrogen-emission nebulosity in the Small Magellanic Cloud is strikingly illustrated on several plates made with a 3-inch $f/1.5$ Zeiss-Sonnar camera, exposed from four to six hours. Red sensitive (103 a-E) Eastman plates were used with a red glass filter (Corning 2403) in conjunction with an H-alpha interference filter. This camera, kindly lent to Harvard's Boyden Station by Mr. Richard S. Perkin, has been effective in the study of emission details in the Milky Way. The scale is too small, however, to show the detailed structure in the Cloud's nebulosity. From an examination of a 90-minute red (103 a-E) plate and a 60-minute blue (103 a-O) plate, both made with the Baker-Schmidt telescope, we find that the nebulosities have the characteristics of Galactic H(II) regions.

Table 1 is a catalog of the emission nebulosities in the Small Magellanic Cloud. In the first column is the new assigned number; the second, the number published in the NGC or IC catalogues or in Harvard Circulars 275 and 276.[1] The early work of Shapley and Wilson was based on long-exposure blue plates and is affected by the color characteristics of the Bruce telescope. Not all the objects described by them as nebulous could be found; a few were identified as galaxies and a few as open clusters, but 125 of the 152 objects in table 1 were in the Shapley-Wilson lists. We have included in this catalogue only those objects which on the red plate show nebulosity or which have definite non-stellar images. The objects found during the course of this investigation have no numbers in the second column.

The third column of table 1 gives the position in X and Y coordinates, as described in *Harvard Annals*, **60**, No. 4 (1907). The fourth gives the dimensions in parsecs with the Cloud's distance taken as 50 kpc. In the fifth is a short description, and the last column gives the type in the Bok-Wade classification. The criteria are structure, or shape, and surface brightness. The apparent and linear sizes of the nebulae and the spectral type and luminosity of the exciting star do not enter into the classification. A summary of the Bok–Wade system follows (p. 1171).[2]

TABLE 1

CATALOG OF EMISSION NEBULOSITIES IN THE SMALL MAGELLANIC CLOUD

SERIAL NUMBER	CATALOG NUMBER	POSITION X	POSITION Y	DIMENSIONS IN PARSECS	DESCRIPTIVE REMARKS	TYPE
1	91	7054″	5669″	...	Faint wisp, nebulous star	V
2	93	7526	6311	2 × 6	Irregular nebula near star	II
3	N 176	7944	8046	10 × 10	Nebula between two stars	II
4	...	8699	5427	...	Nebulous star	V
5	N 220	9186	7284	6 × 6	Two or more stars involved in nebulosity	II
6	N 222	9240	7351	4 × 4	Irregular nebulosity, central condensation	II
7	N 231	9234	7471	10 × 5	Irregular nebulosity two condensations	II
8	5	9736	6103	2 × 3	Two stars involved	II
9	6	9750	8142	2 × 2	Nebulosity around group of three stars	II
10	7	9774	8164	2 × 1	Nebula between two stars	II
11	...	9906	9108	8.5 × 4	Very faint patch	II
12	105	9912	8808	...	Nebulous star	V
13	N 241	9973	7194	4 × 4	Several stars involved in nebulosity	II
14	N 242	9996	7174	1 × 1	Nebulosity between two stars	II
15	107	10281	8170	4 × 4	Nebulosity around four stars	II
16	...	10339	7804	...	Bright nebulous star	V
17	8	10373	8008	4 × 2	Nebulous cluster	II
18	N 249	10430	8525	30 × 25	Nebulosity with condensations	II
19	N 248	10440	7444	8 × 15	Nebula around and between stars	II
20	9	10513	6261	...	Nebulous star	V
21	...	10529	8423	17 × 3	Very faint nebulous wisps	II
22	10	10546	10308	6 × 8	Irregular nebulosity	II
23	N 256	10596	6982	6 × 6	Nebulous cluster	II
24	111	10604	12214	3 × 3	Small nebula, three condensations	V
25	N 261	10703	8455	16 × 20	One or two stars involved in nebulosity	II
26	115	11044	8331	80 × 80	Nebulous patch, limits vague	II
27	15	11067	8026	4 × 4	Crescent-shaped nebulosity	II
28	N 267	11123	7841	30 × 30	Irregular nebulous patch	II
29	117	11136	7073	4 × 4	Small, irregular patches	V
30	17	11139	7974	8 × 8	Circular nebula with a central star	III
31	N 269	11228	6921	4 × 4	Part of circle, one bright star	IV:
32	119	11238	5717	3 × 4	Two stars in faint nebulosity	II
33	120	11251	7730	8 × 8	Irregular nebulous patch	II
34	122	11334	8375	4 × 5	Arc of circle, central star	IV
35	...	11367	8329	...	Nebulous star	V
36	...	11385	8438	...	Nebulous star	V
37	18	11388	7534	...	Nebulous star	V
38	123	11430	7950	8 × 12	Nebulous patch	II
39	125	11452	7492	...	Nebulous star	V
40	126	11464	9418	...	Elongated nebulous star	V
41	127	11498	9528	3 × 3	Small group nebulous (?) stars	V
42	...	11545	8228	...	Nebulous star	V
43	20	11550	9104	1 × 2.5	Nebula (?) between two stars	II
44	...	11597	10544	...	Nebulous star	V
45	...	11614	10522	...	Nebulous star	V
46	128	11632	7921	...	Nebulous star	V
47	...	11636	10504	8 × 2	Crescent shaped, uniformly bright nebulosity	II
48	129	11642	7633	4 × 8	Faint crescent-shaped nebula near two stars	II
49	130	11702	9294	45 × 50	Nebulous patch	II
50	131	11730	7755	...	Nebulous star	V
51	132	11734	7446	3 × 3	Nebulous mass, uniformly brighter in middle	V

SERIAL NUMBER	CATALOG NUMBER	POSITION X	POSITION Y	DIMENSIONS IN PARSECS	DESCRIPTIVE REMARKS	TYPE
52	24	11740″	8118″	4 × 4	Faint nebulous patch	II
53	133	11762	8934	2 × 2	Nebulous patches and stars	II
54	134	11764	9000	4 × 4	Round nebula, bright star off center	I
55	27	11826	9846	4 × 4	Nebulous (?) group	II
56	28	11859	8126	3 × 4	Uniformly bright nebulosity	II
57	...	11889	9536	...	Nebulous star	V
58	135	11957	6721	...	Irregular, nebulous star	V
59	136	12068	8037	4 × 7	Nebulous patch with condensations	II
60	32	12100	9037	1 × 3	Group of nebulous stars (?)	V
61	137	12106	7131	2.5 × 8	Three stars in wisp	II
62	33	12152	11955	...	Nebulous star	V
63	34	12157	10564	...	Nebulous stars	V
64	...	12243	10020	...	Bright nebulous star	V
65	140	12265	8684	2.5 × 6	Nebulous wisps	II
66	141	12310	9140	...	Nebulous star	V
67	142	12321	9602	...	Nebulous star (?), wisp (?)	V
68	37	12322	8938	2.5 × 2.5	Nebula plus three or four stars	II
69	143	12365	7374	2 × 6	Several stars involved in nebulosity	II
70	144	12382	9234	30 × 40	Faint extended nebulosity	II
71	40	12399	10196	4 × 4	Nebulous patch and stars	II
72	42	12446	14668	4 × 6	Three stars in nebulous wisp	II
73	43	12461	9713	3 × 3	Nebulous patch, bright stars	II
74	N 299	12471	11777	6 × 6	Nebulous cluster	II
75	146	12518	10074	3 × 3	Round nebula, central star	III
76	147	12569	10114	...	Nebulous star	V
77	149	12631	10761	1 × 2.5	Nebulous star involved in faint nebulosity	V
78	N 306	12704	11623	6 × 6	Nebulous patch and stars	II
79	150	12730	9950	5 × 5	Round nebula, central star	III
80	151	12734	7826	...	Nebulous star	V
81	153	12851	10807	3 × 4	Nebulous patch and stars	II
82	45	12877	12083	3.5 × 5.5	Irregular nebula with condensations	II
83	47	12931	7356	...	Nebulous stars	V
84	155	12981	7799	2.5 × 2.5	Faint regular patch of nebulosity near star	II
85	156	13007	7035	2 × 2	Fan-shaped nebulosity	II
86	...	13059	12803	...	Nebulous star	V
87	157	13065	12559	...	Nebulous star	V
88	160	13257	11415	...	Nebulous star	V
89	55	13600	11535	4 × 4	Bright, round nebula with three stars in center	II
90	165	13655	7326	34 × 34	Very faint patch	II
91	...	13656	9089	...	Nebulous star	V
92	167	13742	10922	1 × 2.5	Nebulous star, faint wisp	V
93	...	13763	10101	30 × 35	Faint extended patch	II
94	168	13775	7894	2.5 × 3	Faint nebulous patch	II
95	58	13796	12484	...	Nebulous star	V
96	...	13800	7106	...	Nebulous star	V
97	169	13801	10149	5 × 5	Circular nebula with central star in nebulosity no. 93	III
98	59	13829	11408	...	Nebulous star	V
99	60	13839	10081	6 × 5	Nebulous group, three nebulous stars	II
100	61	13921	10908	...	Nebulous star	V
101	N 346	14055	11874	80 × 100	Very bright nebulous group	I
102	171	14060	10286	2 × 2	Nebulous (?) group	II
103	...	14128	12102	...	Nebulous star	V
104	I 1611	14230	11277	6 × 1	Nebulosity with involved stars	II
105	177	14464	15045	3 × 3	Faint nebulous patch faint central star	II
106	178	14486	8304	2.5 × 4	Faint nebulous spot	II
107	182	14601	13964	3 × 3	Nebulous star	V
108	184	14725	5505	20 × 20	Loose cluster, faint nebulosity	II

SERIAL NUMBER	CATALOG NUMBER	POSITION X	POSITION Y	DIMENSIONS IN PARSECS	DESCRIPTIVE REMARKS	TYPE
109	65	14746"	10434"	4 × 6	Three nebulous stars	V
110	66	14749	13034	...	Bright nebulous star	V
111	186	14908	7467	...	Nebulous star	V
112	187	14984	7625	...	Two nebulous stars	V
113	...	15057	11010	3 × 2	Faint wisps between two stars	II
114	69	15166	11485	2.5 × 4	Nebula between two stars	II
115	191	15281	13113	4 × 4	Round nebula, central star	III
116	N 371	15288	12253	80 × 80	Loose cluster, faint nebulosity	II
117	192	15294	9082	...	Two nebulous stars	V
118	193	15333	7894	1 × 2	Two or three nebulous stars	V
119	...	15408	12193	4 × 4	Round nebula, central star, in NGC 371	III
120	70	15410	10120	...	Nebulous star	V
121	195	15482	6525	2 × 3	Nebulosity around stars	II
122	196	15486	10218	4 × 4	Nebula between two stars	II
123	...	15500	9080	...	Nebulous star	V
124	197	15533	11796	4 × 6	Nebulous group some condensations	II
125	199	15550	9861	...	Nebulous star	V
126	72	15576	11876	...	Nebulous star	V
127	201	15579	8676	2.5 × 4	Wisp near bright star	II
128	N 395	15759	12490	30 × 40	Nebulous patch with condensations	II
129	I 1624	15795	12293	6 × 8	Nebulous patch	II
130	I 1626	15848	7744	...	Nebulous stars (?)	V
131	205	15934	11208	8 × 8	Small dense group of nebulous stars (?)	V
132	206	15945	12609	1 × 4	Star in wisp	II
133	208	16048	7956	...	Two or three nebulous stars (?)	V
134	210	16220	12744	...	Nebulous speck	V
135	77	16269	10734	2.5 × 2.5	Irregular nebula	II
136	I 1644	16652	8082	5 × 6	Small nebula near bright star	II
137	79	16678	12419	51 × 51	Faint nebulous patch with condensations	II
138	I 1641	16700	13244	2 × 2	Nebulous (?) cluster	II
139	...	16722	10685	...	Nebulous star	V
140	...	16772	10638	...	Nebulous star	V
141	...	16787	11070	...	Nebulous star	V
142	...	16798	12419	4 × 6	Arc and central star, in nebulosity no. 137	IV
143	227	17393	11022	1.2 × 8	Nebulous wisp in cluster	II
144	...	17422	14816	...	Nebulous star	V
145	I 1662	17456	7078	4 × 4	Irregular nebulous patch	II
146	228	17522	7014	...	Faint nebula beside star	V
147	I 1655	17786	14778	12 × 16	Nebula and four stars	II
148	N 456	17824	7665	40 × 40	Nebulous triangular group	II
149	232	17955	7743	4 × 4	Round nebula, central star	III
150	N 460	18096	7489	4 × 8	Wisps with nebulous condensations	II
151	...	18100	7460	20 × 40	Nebulous patch	II
152	...	18937	9000	...	Nebulous star	V

Type I: Irregular nebulae of very high surface brightness. Messier 8 is typical for this class.

Type II: Irregular nebulae of low to moderate surface brightness. NGC 6604 is a typical member of this class.

Type III: A spherical H(II) region, with the exciting star near the geometrical center. An excellent example is the nebula surrounding NGC 6383.

Type IV: An incomplete ring. A typical example is NGC 2327.

Type V: This new type has been added by us to indicate objects for which the images are almost stellar.

The numbers and percentages of the various types are given in table 2, with a reference to an example of each type from the Milky Way and from the Small Cloud. We shall discuss each type as found in the Cloud in detail.

Type I.—NGC 346 is the only Type I object in our list. It is the most conspicuous feature in the northern part of the Small Cloud. The marked difference in surface brightness between NGC 346 and the other nebulosities is apparent on the PZ plates (Zeiss-Sonnar) where NGC 346 is a very intense concentrated mass. On the ADH blue and red plates faint lanes of dark material are visible, but globules would be too small for detection in the Cloud with available equipment. HD 5980 (Oep) is associated with

TABLE 2

DISTRIBUTION OF NEBULOSITIES AMONG TYPES

TYPE	NUMBER	PER CENT	EXAMPLE	
			GALAXY	SMALL CLOUD
I	1	0.7	Messier 8	NGC 346
II	79	52.0	NGC 6604	NGC 249
III	7	4.6	NGC 6383	30
IV	3	2.0	NGC 2327	34
V	62	40.8	...	51

TABLE 3

DISTRIBUTION OF LONGEST AXES OF NEBULOSITIES

TYPE	DIMENSION IN PARSECS					
	<3	3–6	7–10	11–14	15–18	>18
I	0	0	0	0	0	1
II	11	37	13	1	3	14
III	0	6	1	0	0	0
IV	0	3	0	0	0	0
V	2	7	1	0	0	0

this nebulosity. It has a photographic absolute magnitude of -7.9 (the provisional distance modulus for the Small Cloud,[3] uncorrected for absorption, is taken as $18^m.9$), and a red index of $-0^m.24$. Other early type stars have been identified with the nebulosity through the following method. The known B stars of the Small Cloud were measured on ADH plates (four blue and five red with a red filter). The magnitudes were based on an unpublished photoelectric sequence of Dr. Ivan King. The mean red index for these seven B stars is $-0^m.43 \pm 0^m.11$. Unfortunately, on the objective prism plates available in Cambridge, the subclassification of these B stars could not be made; we assume that this red index of $-0^m.43$ refers on the average to a B4 or B5 star and that all stars with a negative red index of half a magnitude or greater are early B stars. Five stars in the nebulosity of NGC 346 have red colors ranging from $-0^m.33$ to $-1^m.17$. The brightest

magnitude is 12.87 ($M = -6.0$), about two magnitudes fainter than the Oep star. The star next in brightness is more than a magnitude fainter. The number of faint blue stars convincingly identified with this nebulosity is limited by the limiting magnitude of the red sequence, $15^m.7$. There is an indication that NGC 346 is similar to the constellations of the Large Magellanic Cloud[4] in respect to association with blue stars, but is smaller in extent.

Type II.—This type contains the largest group of the emission nebulosities—52 per cent. Although the exact boundaries of the wisps are hard to ascertain, approximate sizes have been measured with a fine scale and a mi-

TABLE 4

BRIGHTEST BLUE STARS IN TYPE II NEBULOSITIES

CATALOG NUMBER	PHOTOGRAPHIC MAGNITUDE	ABSOLUTE PHOTOGRAPHIC MAGNITUDE	RED INDEX
47	12.24	−6.7	$-1^m.66$
127	13.85	−5.1	−0.83
17	13.89	−5.0	−0.41
107	14.60	−4.3	−0.50:
129	14.67	−4.2	−0.81
128	14.70	−4.2	−0.93
148	14.80	−4.1	−0.55

TABLE 5

MAGNITUDE AND COLOR OF CENTRAL STAR IN TYPE III NEBULOSITIES

CATALOG NUMBER	DIAMETER IN PARSECS	PHOTOGRAPHIC MAGNITUDE	RED INDEX
30	8 × 8	13.81	$-0^m.65$
75	3 × 3	14.90	+0.34
79	5 × 5	15.60	−0.19
97	5 × 5	14.93	−0.07
115	4 × 4	15.25	−0.33
119	4 × 4	15.42	+0.94
149	4 × 4	14.95	+0.15

croscope. The sizes in parsecs were computed using as the revised distance to the Small Cloud 50 kiloparsecs (space absorption, $+0^m.4$). Table 3 shows the distribution of the largest dimension for the Type II objects. Most of them are between three and six parsecs in greatest diameter; only eight are more extended than 18 parsecs. The largest approaches the size of NGC 346 but the very low surface brightness makes the nebula inconspicuous. Only on the small scale plates are the limits well defined. The stars involved in this type of nebulosity are not the most luminous in the Cloud. Only two B stars are identified in the Type II regions. Table 4 lists the seven brightest stars with large negative red indices. As found in the study of the constellations of the Large Cloud, several of these stars are

excessively blue, but only three are brighter than $-4^{M}.5$. Even in the most extended patches only two or three stars are found to have negative red indices. The material is too much affected by selection and by the limiting magnitude of the sequence to read into the results the existence of O–B associations.

Type III.—On the red ADH objective prism plates the Type III nebulosities appear as spheres in H-alpha. Since the spectra of the central stars are unknown, the red index must be taken as a rough criterion of spectral type; only two of the central stars may be as early as B. Number 30 has the brightest absolute magnitude, -5.1, as seen from Table 5.

Type IV.—Type IV is difficult to separate from Type II. There are only two objects that appear to qualify fully and another is doubtful. All the stars associated with this type are too faint for color measurements.

Type V.—Type V contains 41 per cent of the total number of nebulous objects in the Small Cloud. Only ten have dimensions that are measurable with some certainty, and all but one are less than six parsecs in diameter. Most of the images are stellar in size. Some of the brighter nebulous stars have bright emission lines of hydrogen and the forbidden lines of oxygen II and III as seen on the ADH objective prism plates. Their diameters, of about one parsec, and their spectra seem to give some evidence that these particular objects are large planetary nebulae. The exact nature of the fuzzy objects showing no bright spectral lines is unknown. For those bright enough for the measurement of colors, the red indices range from $-0^{m}.11$ to $+1^{m}.48$, with the brightest absolute magnitude of $-6^{M}.3$. The majority are fainter than $-4^{M}.0$, with some as faint as $-2^{M}.0$.

All the tabulated nebulosities are marked on a print of the Small Magellanic Cloud. It is seen that these objects roughly outline the shape of the central mass of the Cloud. There is little difference between the distribution of Type II and Type V objects. The numbers of the other types are too small for significance in respect to distribution. Only toward the so-called "wing" of the Cloud is there marked nebulosity outside the main body. The preliminary work of Henize and Miller[5] on the bright line objects in the Small Cloud does not permit ready comparison with our results.

In conclusion we may say that some of the bright stars in the Small Magellanic Cloud are B stars that are not obviously associated with nebulosity. On the other hand there are a number of extremely blue stars (presumably early B) associated with the hydrogen emission. Because of the irregular structure of the Cloud it is very difficult to be sure of dark material. There are, however, several cepheids that fall considerably below the period-luminosity curve,[6] thus suggesting some local obscuration, i.e., within the Cloud. At this time it would be hasty to presume the existence of developing spiral structure on the basis of the extent or location of the emission nebulosity.

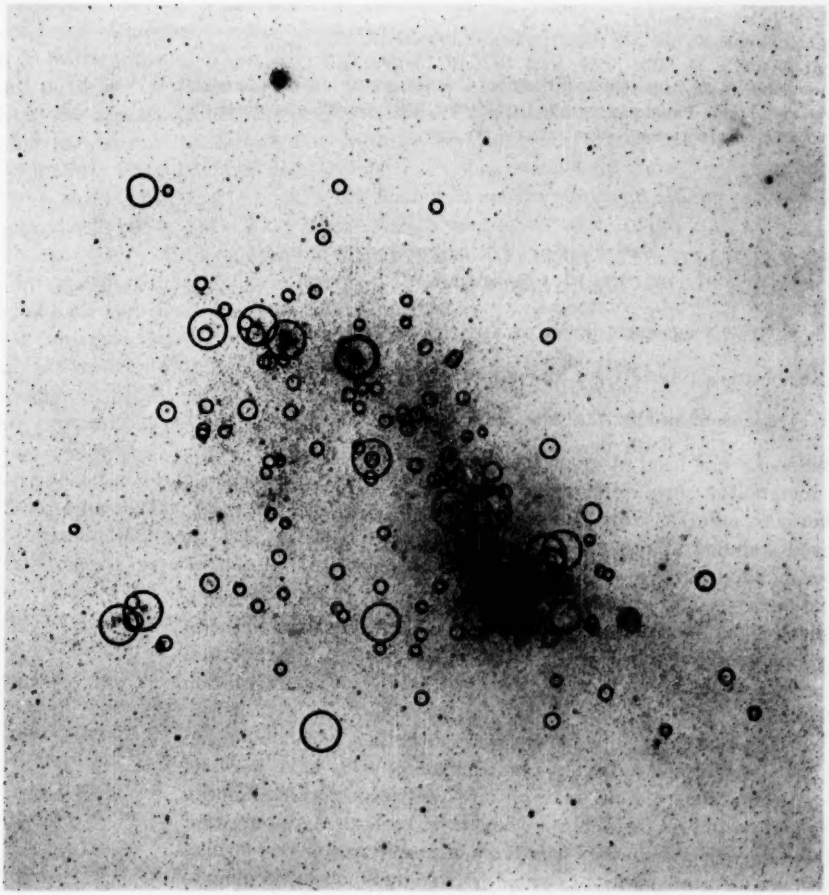

FIGURE 1

Distribution of hydrogen emission nebulosity in the Small Magellanic Cloud. The six groups in table 3 are represented respectively by six different sizes of circles.

[1] Shapley, H., and Wilson, H., *Harv. Circ.* 275 (1925), 276 (1925).

[2] Report of the Second Conference on the Gas Dynamics of Cosmic Clouds, held at Cambridge, England, July 6–11, 1953 (in preparation).

[3] These PROCEEDINGS, **39**, 349–357 (1953): *Harvard Reprint* 372. A slightly greater value is obtained in the following paper of this series in a discussion of the bright stars in Magellanic globular clusters.

[4] These PROCEEDINGS, **39**, 358–362 (1953): *Harvard Reprint* 373.

[5] Henize, K. G., and F. D. Miller, *Pub. Mich. Obs.*, **10**, 75–78 (1951).

[6] These PROCEEDINGS, **28**, 192–199 (1942): *Harvard Reprint* 240. In the preceding paper of this series, these PROCEEDINGS, **39**, 1161–1168 (1953), Dr. Shapley notes the evidence of some space absorption concentrated in the core.

*THE ENZYMATIC SYNTHESIS OF PORPHYRINS FROM PORPHOBILINOGEN**

BY LAWRENCE BOGORAD† AND S. GRANICK

ROCKEFELLER INSTITUTE FOR MEDICAL RESEARCH, NEW YORK

Communicated by D. A. MacInnes, October 1, 1953

Porphobilinogen has been of great interest to students of pyrrole and porphyrin metabolism since its discovery[1] in 1931 as a constituent of the urine of humans suffering from the hereditary disease acute porphyria. On prolonged standing at room temperatures, or much more quickly on heating, porphobilinogen gives rise to uroporphyrin with yields as high as 40%.[2] The highest yields of uroporphyrin are obtained under acid conditions. Other as yet incompletely identified products are also formed.[3] Recently porphobilinogen has been isolated and crystallized;[2] structural studies[4–6] indicate that it is a monopyrrole, probably of the configuration shown in figure 6.

Several unsuccessful attempts to determine whether porphobilinogen may be a precursor of the naturally occurring porphyrins have been reported.[7–9] Alternative possible relationships between porphobilinogen and pyrrole and porphyrin metabolism which have been advanced are that the compound may be a degradation product of porphyrins or that it may be some product associated with abnormal pyrrole metabolism peculiar to acute porphyria. The evidence presented in the present paper demonstrates that porphobilinogen can be used as a precursor in the biosynthesis of naturally occurring porphyrins, including protoporphyrin, by frozen and thawed preparations of Chlorella cells. Also, it has been possible to interrupt the enzyme system in these preparations in such a way that no detectable amount of protoporphyrin is formed, but instead uroporphyrin I is accumulated. Other experiments are described in which enzymatic por-

phyrin synthesis from porphobilinogen has occurred in the cell-free supernate of frozen and thawed Chlorella cells.

The relationship of these findings to the general problem of porphyrin biosynthesis and the porphyria diseases will be discussed.

Methods and Materials.—Porphobilinogen was isolated by Westall's[2] method from the urine of a patient with acute porphyria.‡ The Chlorella used in these experiments were grown on a solid (agar) medium containing glucose and inorganic salts in diphtheria toxin bottles, each bottle containing one liter of medium. The cultures were grown at 30°C. in darkness for four days and were then grown under fluorescent light for a 15 to 20-hr. period preceding harvest. The final yield of cells was about 10 cc. of packed cells per bottle. The cultures were harvested by washing the cells from the surface of the agar with distilled water. The cells were then packed by centrifugation and were frozen in the centrifuge tube in a dry ice–alcohol bath and thawed by immersing the tube in warm water. The cells were subjected to two cycles of freezing and thawing and then diluted with one-half volume of 0.25 *M* sucrose. Aliquots of diluted suspensions were capable of using porphobilinogen for the production of porphyrins, including protoprophyrin, with the addition of only the substrate to the suspension. However, in the experiments described in this paper other items were added as described below.

Rat liver mitochondria were prepared in isotonic sucrose, essentially according to the method described by Schneider.[14]

Porphobilinogen was assayed by the Ehrlich *p*-dimethylaminobenzaldehyde reaction. The optical density of the pyrrole-*p*-dimethylaminobenzaldehyde complex was measured at 555 mμ (molar extinction for the complex = 27,400).[13] This reagent couples with free α-positions of pyrroles and multi-pyrrolic compounds; for this reason the data given below for decrease in concentration of porphobilinogen in incubated preparations should, more strictly, be considered a decrease in number of free α-positions.

Quantitative analyses of porphyrins were made spectrophotometrically using a Cary recording spectrophotometer. Qualitative analyses of porphyrin products were made by several methods of paper chromatography.[10–13]

Experiments and Results.—Growing intact normal green and mutant Chlorella cells were used in several attempts to demonstrate the utilization of porphobilinogen for the production of porphyrins, including chlorophyll. In some experiments there was a greater decrease in porphobilinogen concentration in the presence of cells than in the controls; however, no porphyrins other than the ones normally produced by the particular strain could be recovered. These normal products were present in such abundance originally that any relatively small increase in them would have been difficult to detect.

Frozen and thawed preparations of normal green Chlorella prepared as described above proved very suitable for these experiments. Normal green Chlorella were used because porphyrins other than the chlorophylls, if present, occur in quantities too small to detect, particularly in the amounts of tissue required in each experiment. On the other hand it was found, as had been anticipated, that porphyrin biosynthesis from porphobilinogen, as far as could be determined, stopped short of chlorophyll, and so the new products could be separated readily from the chlorophyll initially present.

The system which was most active in synthesizing from porphobilinogen the greatest quantity of porphyrins with fewer than 8 carboxyl groups per molecule in a typical experiment contained the following components in a final volume of 4 cc.: 2 cc. of frozen and thawed diluted Chlorella suspension (prepared as described above); 0.2 cc. of rat liver mitochondria preparation[14] (this volume of mitochondria suspension is approximately equal to that obtained from 1.5 g. of rat liver); adenosine triphosphate (final concentration 5×10^{-4} *M*); $MgCl_2$ (final concentration 2×10^{-3} *M*); and phosphate buffer pH 7.6 (final concentration 0.095 *M*). The pH generally fell to about pH 7 by the end of a 20-hr. incubation period under these conditions. Penicillin and streptomycin were found to be without effect on the system; these two compounds were added to a final concentration of 125 mg. per liter each to inhibit bacterial growth.

With an initial porphobilinogen concentration of about 200 μg. per cc., no porphobilinogen was detectable in the suspension at the end of a 20-hr. incubation period at 30°C. (see below for kinetic experiments). In various experiments the new porphyrin present could account for from 50 to 70% of the porphobilinogen initially present.

Controls lacking the frozen and thawed Chlorella material usually still contained about 75% of the initial porphobilinogen at the termination of the experiment, and the porphyrin formed non-enzymatically in these controls could account for only about 8% of the porphobilinogen that had disappeared. Controls containing all the components listed above but lacking porphobilinogen contained no detectable porphyrins, other than chlorophylls and chlorophyll degradation products, at the end of the 20-hr. incubation period.

At the termination of the incubation period the following procedure was employed to isolate the newly formed porphyrins. The suspension (4 cc.) was centrifuged and the supernatant fluid collected. The sedimented solids were twice resuspended in water and recentrifuged, the three supernatant fractions were combined (total volume 7 cc.) and centrifuged at 14,000× G in the cold for 1 hr. Aliquots of the clarified supernates were taken for porphobilinogen assays, for the spectrophotometric quantitative assay, and for the qualitative analysis of porphyrins by paper chromatography.

In some cases these aqueous extracts were fractionated further. The extract was first washed with ether and the ether was discarded. Following this, acetic acid was added to bring the solution to about pH 4. The ether-soluble components were then extracted with ether (or in some cases ethyl acetate). Porphyrins with 2, 3, 4, 5, 6, and 7 COOH groups per molecule were detectable in such fractions by paper chromatography. Porphyrins with 4 and with 5 carboxyl groups per molecule were most abundant. The pigment which remained in the aqueous phase, usually only uroporphyrin, was concentrated by adsorption on talc; it was eluted from the talc with a small amount of concentrated NH_4OH.

The washed sedimented material from the centrifugations described above (approximately 1 cc.) was extracted with acetone and then with acetone (10 cc.) concentrated HCl (0.1 cc.). This fraction contained water-insoluble porphyrins, including chlorophyll degradation products. The ether-soluble components of this acetone-HCl fraction were then

TABLE 1

PORPHYRINS NEWLY FORMED FROM PORPHOBILINOGEN IN REACTION MIXTURE CONTAINING FROZEN AND THAWED CHLORELLA

FRACTION	PORPHYRINS PRESENT[a]	TOTAL PORPHYRIN SYNTHESIZED, %
Aqueous	Uroporphyrin[b]	28
	2, 3, 4,[c] 5, 6, 7	52
Acetone-HCl (2*N* HCl)	2, 4,[c] 5	6
	Protoporphyrin	14

[a] Numbers refer to number of —COOH groups per porphyrin molecule, estimated on the basis of paper chromatography by Nicholas-Rimington method.[10]

[b] Mostly uroporphyrin I. Uroporphyrin III formed earlier in the incubation has apparently been converted to porphyrins with fewer carboxyl groups per molecule.

[c] Largely coproporphyrin III.

transferred into 20 cc. of ether, the ether was washed with water and then extracted twice with 5 cc. of 2*N* HCl. This hydrochloric acid solution then contained the water-insoluble porphyrins formed from porphobilinogen during the incubation period plus a trace of pheophytins. The 2*N* HCl fraction was extracted once with ether, which was discarded. This contained the pheophytins. Then saturated sodium acetate was added to the aqueous-HCl solution to bring it to pH 4 and the porphyrins were extracted into ether. The ether solution was washed with water, concentrated in vacuo, and made to a final volume of 5 cc. The porphyrins present in these solutions were estimated quantitatively by spectrophotometry and qualitatively by paper chromatography. This fraction will subsequently be designated in this paper as the "2*N* HCl" fraction.

Table 1 shows the distribution of porphyrins, except chlorophylls and their degradation products, in the aqueous fraction and in the 2*N* HCl

fraction derived from the acetone-HCl extracts at the end of a 20-hr. incubation period at 30°C. In the particular experiment cited the newly formed porphyrins accounted for about 60% of the porphobilinogen. Only uroprophyrin and protoporphyrin were isolated free of other porphyrins. The uroporphyrin was characterized by the solubility characteristic of the free acid, by the HCl number of the octamethyl ester, by its absorption spectrum, and by the behavior of the compound and its methyl ester on paper chromatography. The protoporphyrin was separated from the other porphyrins of the 2*N* HCl fraction by ether-HCl partition and was characterized by its HCl number; by paper chromatography by the Nicholas-Rimington method, which showed the porphyrin possessed two free carboxyl groups per molecule; by its behavior on paper chromatography, by a method to be published elsewhere, by its absorption spectrum, which indicated two vinyl groups per molecule; and by the ability of *Hemophilus influenzae* to grow, i.e., to insert iron into the porphyrin ring, and to reduce nitrate in the absence of any source of heme or porphyrin other than this compound.[15]

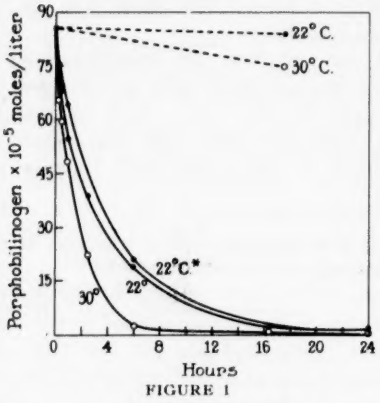

FIGURE 1

Change in concentration of porphobilinogen in the presence (solid lines) and absence (broken lines) of frozen and thawed Chlorella preparation. See text for other components. Incubation temperatures are shown.

* Preparation heated at 55°C. for 60 minutes prior to addition of porphobilinogen and incubation, showing that the rate of porphobilinogen disappearance is essentially unchanged. Aliquots of the same preparation of frozen and thawed Chlorella cells were used in each treatment shown.

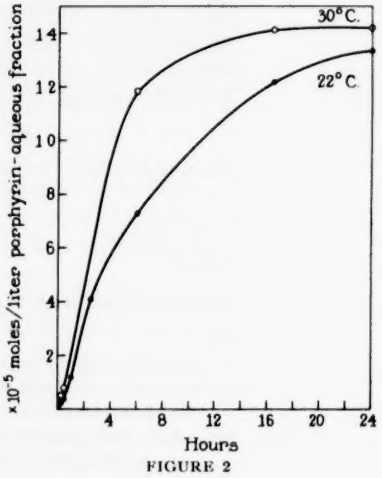

FIGURE 2

Course of appearance of porphyrins (aqueous fraction) during course of incubation.

Paper chromatography of the fraction from acetone-HCl which appears to be a mixture of porphyrins with 2, 4, and 5 carboxyl groups per molecule indicated the presence of a monovinyl-monohydroxyethyl-deuteroporphyrin of the type recovered from a Chlorella mutant.[16, 17]

The principal possible source of error in the percentage figures of table 1 arises from the lack of information on the extinction coefficients for the porphyrins with 3, 5, 6, and 7 carboxyl groups per molecule in the mixture. Extinction coefficients for coproporphyrin were used in calculating the amount of porphyrin present in fractions containing mixtures of pigments in which coproporphyrin III was generally the most abundant single porphyrin. It is probable that the extinction coefficients of the other porphyrins in these mixtures are very similar or almost identical to the extinction coefficient of coproporphyrin.

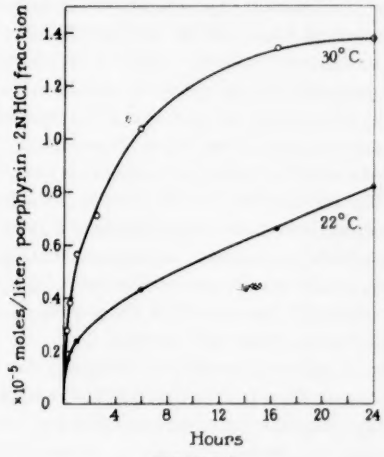

FIGURE 3

Course of appearance of porphyrins (2 *N* HCl fraction) during course of incubation.

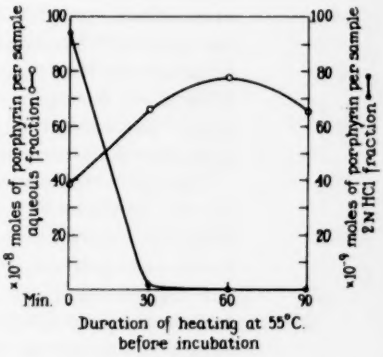

FIGURE 4

Effect of heating frozen and thawed Chlorella cell preparation at 55°C. for varying periods of time on amount of porphyrins synthesized from porphobilinogen on subsequent incubation at 30°C. for 20 hours.

The change in concentration of porphobilinogen in the presence of frozen and thawed Chlorella cells, rat liver mitochondria, ATP, etc., is shown in figure 1. One portion of the preparation was incubated at 30°C. and another aliquot at 22°C. The initial concentration of porphobilinogen was 86.75×10^{-6} *M*. At the end of 1 hr. at 30°C. the concentration of porphobilinogen had been reduced by 44%, after 6 hr. the porphobilinogen concentration was only 3% of the initial concentration. On the other hand, in the control, without frozen and thawed Chlorella cell preparation, the

porphobilinogen concentration was still 88% of the initial concentration after 17.5 hr. at 30°C.

The temperature coefficient calculated on the interval 22° to 30°C. over the first 6 hr. was 1.54 for the enzyme-mediated disappearance of porphobilinogen.

The course of the appearance of porphyrins is shown in figure 2 for the total porphyrins in the aqueous fraction, and in figure 3 for the total porphyrins extractable by 2*N* HCl from among the ether soluble components of the acetone-HCl fraction. These data are from the same experiment for which the porphobilinogen uptake data are given in figure 1. Studies of the coproporphyrin tetramethyl ester by paper chromatography[11] revealed it to be the III isomer. In similar experiments it was found that the uroporphyrin present at the end of 4 hr. was the III isomer, but at 20 hr. the uroporphyrin present was almost entirely type I. Evidently all the uroporphyrin III had been converted to porphyrins higher in the biosynthetic chain during the interval between the 4th and 20th hr. (see Discussion). Protoporphyrin was detectable at the end of 30 minutes. No products other than the porphyrins listed in table 1 have been identified as yet.

The Effect of Heating.—The effect of heating Chlorella cell preparations on the biosynthesis of porphyrins from porphobilinogen was studied. Boiled preparations were completely inactive. However, heating at 55°C. for 60 minutes resulted in essentially no decrease in the rate of porphobilinogen disappearance (Fig. 1) although the nature of the porphyrin produced and the yield of porphyrin were both drastically altered.

Figure 4 shows the effect of different periods of heating the Chlorella preparation at 55°C. on the amounts of porphyrins (exclusive of chlorophyll and its degradation products) present in the aqueous and in the acetone-HCl (2*N* HCl) fractions at the end of a 20-hr. incubation period at 30°C. In this experiment a five-day old culture of Chlorella was harvested and the cells were frozen and thawed, as described above. Phosphate buffer, sucrose, and $MgCl_2$ were added and after an aliquot was removed as an unheated control other aliquots were heated for 30 minutes, 60 minutes, and 90 minutes, respectively. At the end of the heating period rat liver mitochondria, ATP, porphobilinogen, streptomycin, and penicillin were added. The entire mixture was then incubated and finally analyzed in the usual way. At the end of the 20-hr. incubation period no porphobilinogen was detectable in any of the treatments. The final yield of total porphyrin for the Chlorella control which was not heated was about 55% while the preparation heated for 1 hr. at 55°C. yielded porphyrin in such an amount as to account for about 90% of the porphobilinogen had that disappeared. Another striking feature of the synthesis by the heated preparations was that, unlike the control, no ether-soluble porphyrin could be detected and an analysis of the ether-insoluble porphyrin revealed it to be almost ex-

clusively uroporphyrin I. The isomer number was determined by paper chromatography of the octamethyl ester by the method of Falk and Benson.[12]

Experiments with Extracts of Frozen and Thawed Chlorella Cells.—A suspension of a frozen and thawed Chlorella cell preparation plus one-half volume of cold 0.25 *M* sucrose was permitted to stand at 0° for 30 minutes and was then centrifuged in the cold at 14,000× G for 1 hr. The supernatant liquid at the termination of the centrifugation was optically clear. When an aliquot of the supernate was incubated with porphobilinogen no detectable porphobilinogen remained in the mixture at the end of the 20-hr. incubation period. The total yield of porphyrin was about 45% of that to be expected from the amount of porphobilinogen consumed. The aqueous fraction contained 93% of the total porphyrin and included uroporphyrin I, uroporphyrin III, a smaller amount of material which behaved as a tetracarboxylic porphyrin on paper chromatography, and a trace of porphyrin which behaved as a dicarboxylic porphyrin. The spectrum of the 2*N* HCl fraction derived from the acetone-HCl fraction suggested the presence of predominantly a divinyl porphyrin. Paper chromatography revealed the presence of a porphyrin which behaved as protoporphyrin in this system.

Kinetic studies of changes in porphobilinogen concentration and porphyrin production with such supernate fractions have not been made so it is not yet possible to relate the activity of the supernate to that of the complete frozen and thawed Chlorella cell preparations.

Activity of Other Tissues. A few preliminary experiments to test the ability of other tissues to produce porphyrins from porphobilinogen have been performed. Rat liver mitochondria alone, homogenized whole rat liver, and frozen and thawed yeast cells each appear to be inactive with respect to this system in our experiments. On the other hand, frozen and thawed leaf tissue of market spinach proved to be active in porphobilinogen uptake and in the production of at least the water-soluble porphyrins. A frozen and thawed preparation of a pale green Chlorella mutant (No. 571) lacking carotinoids proved quite active in both porphobilinogen uptake and in producing about the same spectrum of porphyrins as described in the experiments with similar preparations of the cells of the normal green alga.

Discussion.—It has been shown unequivocally here for the first time that porphobilinogen can be used for the enzymatic synthesis of biologically active and important porphyrins, such as protoporphyrin.

It is very highly probable that in the course of preparing the cell material, as well as during the incubation period, some enzymes are more readily inactivated than others. That this is the case is apparent from the fact that one gets an array of porphyrins rather than just more chlorophyll. Indeed, from the point of view of experimentation, this disruption of the normal pattern is of great value.

The clearest example of the differential inactivation of components of this enzyme system is seen in the experiments in which frozen and thawed Chlorella cell preparations were heated at 55°C. before incubation with porphobilinogen. It seems that here an early but not the initial step in the assembling of the porphyrin is sharply affected. The initial step, as measured by the decrease in porphobilinogen concentration, appears to be very little affected by this heat treatment (Fig. 1). However, the total yield of porphyrin, as calculated on the basis of porphobilinogen disappearance, is considerably higher (about 90%) than in unheated preparations (about 50 to 70%). This suggests that in systems with unheated preparations part of the non-porphyrin products, or the porphyrin products which we have failed to find and measure, may arise from enzymatic activity subsequent to the coupling step performed by the enzyme or enzymes resistant to heating at 55°C.

Probably the most unique feature of the activity of these preparations heated at 55°C., in contrast to unheated ones, is the fact that the porphyrin product is almost exclusively uroporphyrin I. (In this regard it is interesting to note that in congenital porphyria uroporphyrin I is the major porphyrin excreted.) In unheated preparations the uroporphyrin present at the end of a 24-hr. incubation period was also found to be almost entirely the I isomer; however, the uroporphyrin present in a suspension incubated for 4 hr. was found to be almost exclusively the III isomer. So it appears that the enzyme which controls this critical step, i.e., the formation of the type III rather than the type I isomer, breaks down completely during the course of a 24-hr. incubation period and that the uroporphyrin III formed earlier in the incubation is almost entirely used up in the production of other porphyrins.

What is the critical step which determines which isomer of uroporphyrin will be formed? Cookson and Rimington have found that the uroporphyrin which is formed when porphobilinogen is boiled in acid solution is almost entirely the III isomer.[4] It has been suggested that perhaps an intermediate tripyrrylmethane, similar to compounds described by Corwin and Andrews[18, 19] as intermediates in the organo-chemical synthesis of dipyrroles, may be formed and that this may then split to give fragments which can recombine to form uroporphyrin III.

However, an alternative hypothesis is suggested which would account more satisfactorily for formation of uroporphyrin III by heating porphobilinogen in acid solution, and for the fact that in nature only porphyrins of the I and III isomer series have been found. This hypothesis postulates a branched "T" tetrapyrrylmethane as an intermediate (Fig. 5). If this tetrapyrrylmethane splits at "B" (formula T) two kinds of dipyrrylmethanes (4 and 5) are formed. The only porphyrin which could be formed by the condensation of 4 and 5 is uroporphyrin III. A split at "A" (formula T)

would result in the production of two fragments to give uroporphyrin I as the only possible porphyrin product.

Two possible series of steps by which the synthesis of "T" might proceed are shown in figure 5. In (X) it is suggested that straight-chain tripyrrylmethane (3) is formed by the linear condensation of porphobilinogen molecules under the influence of enzyme(s) E-1. The over-all reaction consists of the formation of a carbon-to-carbon bond with the splitting out of ammonia, a principle of condensation not heretofore met with biochemically. Then through the action of enzyme E-2 a molecule of porphobilinogen is added to formula 3 at "G" to form "T." If this latter enzyme is not

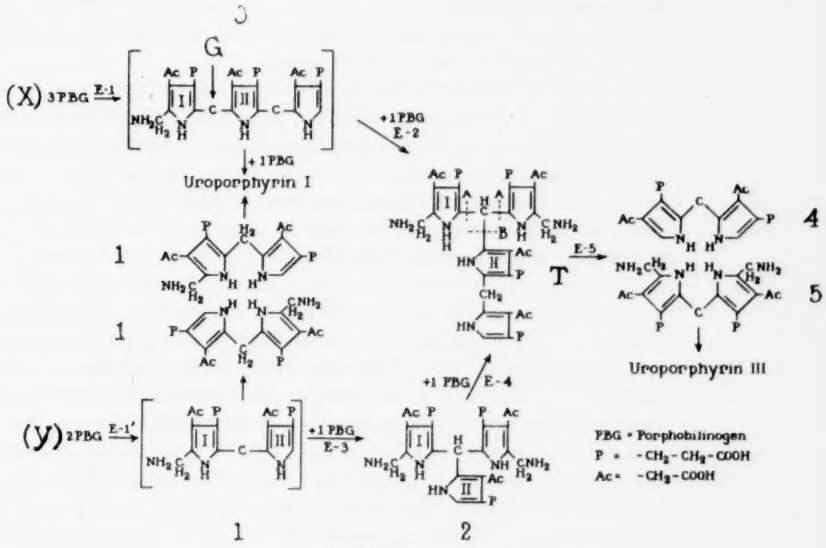

FIGURE 5

functioning, straight-chain tripyrrylmethane would accumulate, one molecule of the tripyrrylmethane could then condense with one molecule of porphobilinogen to give a molecule of uroporphyrin I. In the alternative sequence (Y), it is suggested that first a dipyrrylmethane (1) is formed and then two molecules of porphobilinogen are added in a series of enzymatically mediated steps to form "T." Here, if enzyme(s) E-3 is not functioning, dipyrrylmethanes would accumulate; these could combine with one another to form only uroporphyrin I.

Some of the structures for postulated intermediates in figure 5 are shown as amines. It may well be, however, that oxidative deamination precedes coupling of pyrroles and —CHO should be written in place of $-CH_2NH_2$ in several of the compounds shown. If coupling follows the conversion of

porphobilinogen to the aldehyde there is a direct analogy to the work of Corwin and Andrews[19] and the dipyrrylmethane shown in (Y) should be written as a dipyrrylcarbinol aldehyde.

The data presented in this paper support the idea, previously suggested from studies of Chlorella mutants, isotope studies, and the studies of porphyrins excreted by porphyria patients, that protoprophyrin arises via the intermediates shown in figure 6. They also demonstrate again the similarity of the biosynthetic pathways of the porphyrins in Chlorella and in animals, for here the substrate used by the enzymes of Chlorella for the production of porphyrins is a compound recovered from the urine of a patient with acute porphyria.

The nature of the action of added rat liver mitochondria on this enzyme system will be discussed in a later paper.

London[20] has reported the synthesis of the end product, heme, from glycine and acetate in preparations of hemolyzed avian erythrocytes. The present paper reports for the first time, however, the biosynthesis of intermediate porphyrins even in cell-free extracts. The fact that at least some of the enzymes active in these syntheses are quite soluble suggests that the isolation of individual enzymes may be possible. The ready separation of activity by heating makes this possibility even more promising.

Summary.—It has been shown that porphobilinogen recovered from the urine of a patient with acute porphyria can be used in the biosynthesis of a number of porphyrins including protoporphyrin by a preparation of frozen and thawed normal green Chlorella cells. These syntheses, in which porphobilinogen was used as a substrate, also can be carried out by optically clear cell-free extracts of normal green Chlorella. Frozen and thawed Chlorella cell preparations heated at 55°C. are incapable of synthesizing detectable amounts of porphyrins other than uroporphyrin I. A new hypothesis concerning the synthesis of porphyrins from porphobilinogen non-enzymatically and enzymatically via a "T" tetrapyrrylmethane is presented and discussed.[21]

* This is the tenth in a series of papers on porphyrins and related compounds. Presented Sept. 6, 1953 at the meetings of the American Chemical Society at Chicago.

† Merck Fellow in the Natural Sciences of the National Research Council, 1951–1953. Present address: Department of Botany, University of Chicago.

‡ We are indebted to Dr. T. F. Yü, Mt. Sinai Hospital, New York, for cooperation in helping us to obtain the urine from which the porphobilinogen was isolated.

[1] Sachs, P., *Klin. Wschr.*, **10,** 1123 (1931).

[2] Westall, R. G., *Nature*, **170,** 614 (1952).

[3] Brockman, P. E., and Gray, C. H., *Biochem. J.*, **54,** 22 (1953).

[4] Cookson, G. H., and Rimington, C., *Nature*, **171,** 875 (1953).

[5] Kennard, O., *Ibid.*, **171,** 876 (1953).

[6] Granick, S., and Bogorad, L., *J. Am. Chem. Soc.*, **75,** 3610 (1953).

[7] Waldenström, J., *Acta Med. Scand.*, Suppl. 82 (1937).

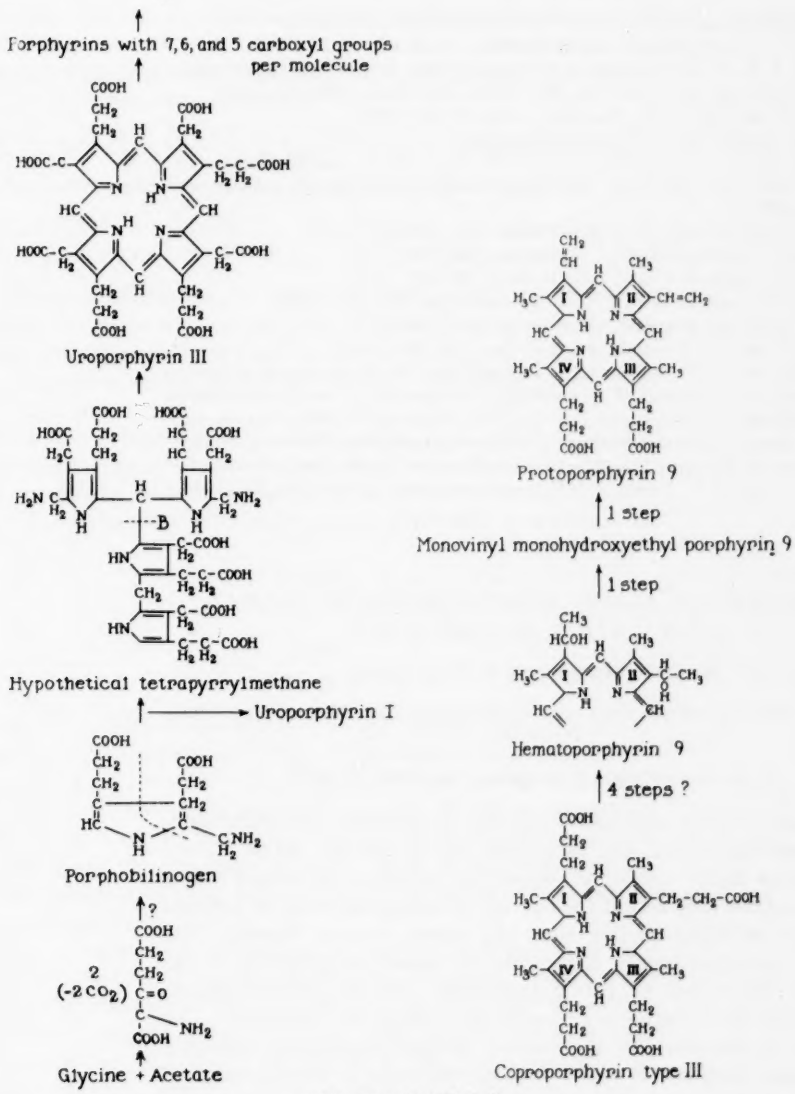

FIGURES 6 (*a*) AND 6 (*b*)

A scheme for the biosynthesis of porphyrins. Porphobilinogen was used as the substrate in the experiments described in this paper. Most of the porphyrins listed, up to and including protoporphyrin,[17] were found in the mixtures in which porphobilinogen was incubated with a preparation of frozen and thawed Chlorella cells.

[8] Waldenström, J., and Wendt, S., *Z. Physiol. Chemie*, **259**, 157 (1939).
[9] Prunty, F. T. G., *Biochem. J.*, **39**, 449 (1945).
[10] Nicholas, R. E. H., and Rimington, C., *Scand. J. Clin. Lab. Investig.*, **1**, 12 (1949).
[11] Chu, T. C., Green, A. A., and Chu, E. J. H., *J. Biol. Chem.*, **190**, 643 (1951).
[12] Falk, J. E., and Benson, A., *Biochem. J.*, **53**, XXXII (1953).
[13] Bogorad, L., and Granick, S. (unpublished data).
[14] Schneider, W. C., chapter in Umbreit, W. W., Burris, R. H., and Stauffer, J. F. S., *Manometric Techniques and Tissue Metabolism*, Burgess Publishing Co., Minneapolis, Minn., 1949, 227 pp.
[15] Gilder, H., and Granick, S., *J. Gen. Physiol.*, **31**, 103 (1947).
[16] Bogorad, L., and Granick, S., *J. Biol. Chem.*, **202**, 793 (1953).
[17] Granick, S., Bogorad, L., and Jaffe, H., *Ibid.*, **202**, 801 (1953).
[18] Corwin, A. H., and Andrews, J. S., *J. Am. Chem. Soc.*, **58**, 1086 (1936).
[19] Corwin, A. H., and Andrews, J. S., *Ibid.*, **59**, 1973 (1937).
[20] London, I. M., and Yamasaki, M., *Fed. Proc.*, **11**, 250 (1952).
[21] Note added in proof. Subsequent to the completion of this manuscript a note appeared in which the synthesis of uroporphyrin, coproporphyrin, and protoporphyrin from porphobilinogen by preparations of hemolyzed chicken erythrocytes was reported. The authors also described the synthesis of mainly coproporphyrin from porphobilinogen by supernatant fractions from hemolyzed erythrocyte preparations centrifuged at high speeds. (Falk, J. E., Dresel, E. I. B., and Rimington, C., *Nature* **172**, 292 (1953).)

*COMPETITION AMONG IONIC SPECIES IN CATION ACTIVATION OF ENZYMES**

BY C. E. HAGEN AND P. C. JACKSON

BUREAU OF PLANT INDUSTRY, SOILS, AND AGRICULTURAL ENGINEERING, BELTSVILLE, MARYLAND

Communicated by S. B. Hendricks, September 29, 1953

Activation of many enzymes is ascribed to formation of catalytically active complexes of the enzyme-protein and a specific cation. Since ligands are not highly specific in complexing cations, it is evident that a number of cations may inhibit the enzyme by competing with the activating ions for available binding sites. In many systems, however, the activating cation at higher concentrations causes inactivation of the enzyme.[1, 2] The effect of cation hydrolysis and the enzyme-protein complexes with the resulting ionic species are considered in this paper. An explanation is presented for the distinct cation concentration optimum and its correct position is found without reference to measurement of enzymatic activities.

The equilibrium between manganese and L-leucine aminopeptidase,[3] for example, has been represented as

$$\text{Protein} + \text{Mn}^{++} \rightleftharpoons (\text{Mn}^{++}\cdot\text{protein}), \qquad (1)$$

an apparently self-evident expression which needs to be examined in detail with respect to Mn^{++}. When the products of hydrolysis of a metal are considered, the total concentration would include Mn^{++}, $Mn(OH)_2$, $(MnOH)^+$ and (Mn·protein).

$$[\Sigma Mn] = [Mn^{++}] + [MnOH^+] + [Mn(OH)_2] + [Mn\cdot protein] \quad (2)$$

so that the mathematical expression for equation (1) becomes:

$$(K)\,[Protein]\{[\Sigma Mn] - [MnOH^+] - [Mn(OH)_2] - [Mn\cdot protein]\} = [Mn\cdot protein]. \quad (3)$$

In view of these considerations, an explanation for specific cation activation of enzymes is presented which considers complexing by an enzyme-protein of the ionic species arising from the hydrolysis of the activating cation, and self-competition of the polyvalent cations. The latter proved particularly important.

Derivation and Discussion of Equations.—The mass action expression for the association of a divalent cation, M^{++}, with an enzyme-protein, E, where the binding sites are monovalent and independent, is shown by equation (4); an enzyme with paired monovalent sites is expressed by equation (5)

$$K = \frac{[E_2M]}{[E]^2\,[M]} \quad (4)$$

$$K = \frac{[EM]}{[E]\,[M]} \quad (5)$$

The enzymatic activity in the presence of non-limiting substrate is proportional to the concentration of the enzyme-cation complex, E_2M or EM. According to equation (4), for ideal solutions in which only [E] is limiting, the logarithm of the enzymatic activity, $[E_2M]$, is proportional to the logarithm of the enzyme concentration. With paired monovalent sites, equation (5), the enzymatic activity, [EM], is proportional to the enzyme concentration. Paired monovalent sites are inferred from numerous enzyme concentration curves.[1, 4, 5]

According to equation (5), [EM] would increase with increasing concentrations of cation until the enzyme becomes saturated. Other possibilities must be considered, however, since measurements[1, 2] show that increasing concentrations of the activating cation produce an increase in activity followed by inhibition. The nature of the curves suggests that at increased concentrations, the cations compete for the positions required for the formation of the active complex, EM, by increasing the probability of formation of an inactive complex, $E(M^+)_2$, as described by equation (6)

$$E^{--} + M^{++} \underset{}{\overset{k_1}{\rightleftharpoons}} (EM)^{\pm} \quad (EM)^{\pm} + M^{++} \underset{}{\overset{k_2'}{\rightleftharpoons}} E(M^+)_2. \quad (6)$$

The effective concentration of activating cation is limited by the hydrolysis of the cation, as shown by equations (7) and (8).

$$M^{++} + H_2O \rightleftharpoons (MOH)^+ + H^+ \quad (7)$$

$$(MOH)^+ + H_2O \rightleftharpoons M(OH)_2 + H^+. \quad (8)$$

Formation of $(MOH)^+$ ion introduces the possibility that it, too, is bound by the enzyme site to form a complex, $E(MOH)_2$, equation (9).

$$E^{--} + (MOH)^+ \underset{}{\overset{k_1''}{\rightleftharpoons}} (EMOH)^- \quad (EMOH)^- + (MOH)^+ \overset{k_2''}{\rightleftharpoons} E(MOH)_2. \quad (9)$$

The uncharged hydroxide, $M(OH)_2$, is not considered to be bound by the enzyme site.

The several reactions are shown in the following scheme:

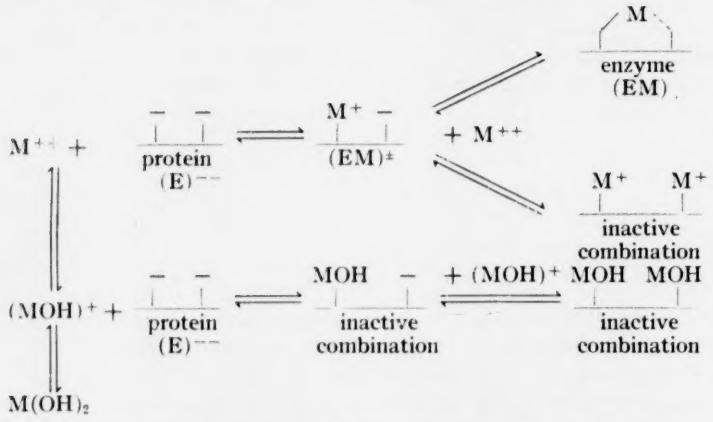

The enzymatic system at constant temperature, constant pH and non-limited substrate is described by the following equations:

Cation Hydrolysis:

$$K_{1h} = \frac{[MOH^+][H^+]}{[M^{++}]} \quad (10)$$

$$K_{2h} = \frac{[M(OH)_2]\,[H^+]}{[MOH^+]} \quad (11)$$

Protein-cation Dissociation:

$$K_{1d} = \frac{[E^{--}]\,[M^{++}]}{[EM]} = \left\{\frac{[E^{--}]\,[M^{++}]}{[EM^{\pm}]}\right\} \cdot \left\{\frac{[EM^{\pm}]}{[EM]}\right\} = k_1 k_2 \quad (12)$$

$$K_{2d} = \frac{[E^{--}]\,[M^{++}]^2}{[E(M^+)_2]} = \left\{\frac{[E^{--}]\,[M^{++}]}{[EM^{\pm}]}\right\} \cdot \left\{\frac{[EM^{\pm}]\,[M^{++}]}{[E(M^+)_2]}\right\} = k_1k_2' \tag{13}$$

$$K_{3d} = \frac{[E^{--}]\,[MOH^+]^2}{[E(MOH)_2]} = \left\{\frac{[E^{--}]\,[MOH^+]}{[EMOH^-]}\right\} \cdot \left\{\frac{[EMOH^-]\,[MOH^+]}{[E(MOH)_2]}\right\} = k_1''k_2''. \tag{14}$$

Enzyme Conservation:

$$[E] = [E^{--}] + [EM] + [E(M^+)_2] + [E(MOH)_2]. \tag{15}$$

Cation Conservation:

$$[M] = [M^{++}] + [MOH^+] + [M(OH)_2] + [EM] + 2[E(M^+)_2] + 2[E(MOH)_2]. \tag{16}$$

In equations (10)–(16) there are seven variables; [EM], $[E(M^+)_2]$, $[E(MOH)_2]$, $[MOH^+]$, $[M(OH)_2]$, $[M^{++}]$, and $[E^{--}]$; and three parameters, $[H^+]$, [M] and [E]. These equations may be partially combined and solved by mapping, or all variables except EM, the active complex, eliminated. The latter gives the cubic equation:

$$\alpha(EM)^3 + \beta(EM)^2 + \gamma(EM) - \mu = 0 \tag{17}$$

where α, β, γ, and μ are the following functions of the parameters and the several equilibrium constants:

$$\alpha = 4(K_{1d})^3\{(K_{1h})^2(K_{2d}) + (K_{3d})[H^+]^2\}^2 - (K_{1d})(K_{2d})(K_{3d})[H^+]^2 \times \{(K_{1h})^2(K_{2d}) + (K_{3d})[H^+]^2\}$$

$$\beta = 2(K_{1d})(K_{2d})(K_{3d})[H^+]^2[E]\{(K_{1h})^2(K_{2d}) + (K_{3d})[H^+]^2\} - (K_{2d})^2 \times (K_{3d})^2[H^+]^2\{[H^+]^2 + (K_{1h})[H^+] + (K_{1h})(K_{2h})\} + 4(K_{1d})^2 \times (K_{2d})(K_{3d})\{[H^+]^2 + (K_{1h})[H^+] + (K_{1h})(K_{2h})\}\{(K_{1h})^2(K_{2d}) + (K_{3d})[H^+]^2\}$$

$$\gamma = (K_{1d})(K_{2d})(K_{3d})[H^+]^2[M]\{[M] - 2[E]\}\{(K_{1h})^2(K_{2d}) + (K_{3d}) \times [H^+]^2\} + (K_{2d})^2(K_{3d})^2[H^+]^2\{[M] + [E]\}\{[H^+]^2 + (K_{1h})[H^+] + (K_{1h})(K_{2h})\} + (K_{1d})(K_{2d})^2(K_{3d})^2\{[H^+]^2 + (K_{1h})[H^+] + (K_{1h}) \times (K_{2h})\}$$

$$\mu = (K_{2d})^2(K_{3d})^2[H^+]^2[E][M]\{[H^+]^2 + (K_{1h})[H^+] + (K_{1h})(K_{2h})\}.$$

Equation (17) shows that when [E] and $[H^+]$ are maintained constant, [EM], the concentration of the active enzyme, increases to a maximum and then decreases as the cation concentration is increased. One should note that $[E(M^+)_2]$ and $[E(MOH)_2]$ continue to increase and the sum of the two asymptotically approaches complete enzyme saturation. Since the coefficients α and β are not functions of [M], they are constant when

[E] and [H$^+$] are maintained constant. Initially, as cation concentration is increased, [EM] increases because μ varies directly with [M] and the terms in γ containing [M] and [M]^2 are insignificant. With further increases of cation, the [M] term in γ is significant and [EM] becomes constant. This describes the optimal concentration of EM. With even greater increases of cation, the [M]^2 term becomes significant and the result is reduced concentrations of EM. The location of the peak of maximum [EM] value is determined by the dissociation and hydrolysis constants, with the sharpness of the peak depending on the relative values of the dissociation constants.

In the expressions for α, β, and γ the $(K_{1h})^2(K_{2d})$ term in equation (17) reflects the effect of the formation of $E(MOH)_2$, and the $(K_{3d})[H^+]^2$ term, the $E(M^+)_2$ complex. Thus, if $(K_{1h})^2(K_{2d})$ is insignificant in comparison to $(K_{3d})[H^+]^2$, inhibition of EM due to formation of $E(MOH)_2$ is negligible, and the inhibition is due to formation of $E(M^+)_2$.

TABLE 1

HYDROLYSIS AND DISSOCIATION CONSTANTS AT 25°C.

CONSTANT[a]	DIVALENT METAL		
	MANGANESE	MAGNESIUM	COBALT
K_1 hydrolysis	1×10^{-13}[b]	5×10^{-12}	1×10^{-12}
K solubility product	5×10^{-14}	9×10^{-12}	3×10^{-15}
K_2 hydrolysis (calc.)	1×10^{-2}	5×10^{-6}	1×10^{-2}
K_1 dissociation	1×10^{-5}	5×10^{-4}	1×10^{-6}
K_2 and K_3 dissociation	1×10^{-7}	5×10^{-6}	1×10^{-9}

[a] All constants were rounded out to the nearest half power.

[b] The K_{1h} of cobalt, nickel, and zinc change by two factors of ten from 100° to 25°C. The same extrapolation was applied to approximate the K_{1h} of manganese at 25°C. The K_{1h} of manganese at 100°C. is 2×10^{-11}.[7]

Whenever the terms $(K_{1h})[H^+]$ and $(K_{1h})(K_{2h})$ are insignificant compared to $[H^+]^2$, and $(K_{1h})^2(K_{2d})$, as compared to $(K_{3d})[H^+]^2$, the enzymatic activity is independent of the hydrogen-ion concentration. This condition may hold only in a limited region. The general dependence of cation activities on [H$^+$] is given by equation (17), but the consequences of this dependence on [H$^+$], as a variable influencing enzymatic activity, requires consideration of enzyme hydrolysis which is not considered here.

Hydrolysis and Dissociation Constants.—The K_{1h} for each metal, table 1, is an average of several values obtained from literature.[6-8] Where the value of K_{2h} was not available, an apparent constant was calculated, and designated as such, from the solubility product as follows:

$$K_{2h} = \frac{(K_w)^2[\text{soluble } M(OH)_2]}{(K_{sp})(K_{1h})}. \qquad (18)$$

Since the solubility of the undissociated metal hydroxides has not been determined, it was assumed that these substances are completely ionized.

From previous considerations, the enzyme-protein has been inferred to have paired monovalent sites, with an imposed limitation on both positions of equal association values. From statistical and electrostatic considerations, however, the relative stability of the metal complex with the first position would be expected to be greater than that with the second. An internally unbiased scheme has been devised for an approximation of these constants. A number of dissociation constants for each metal with organic acids, amino acids, and peptides were calculated from an average of chelate stability constants.[9] In each case, the dissociation constant of the enzyme-metal complex, K_{1d}, K_{2d}, and K_{3d}, was assumed to be a factor

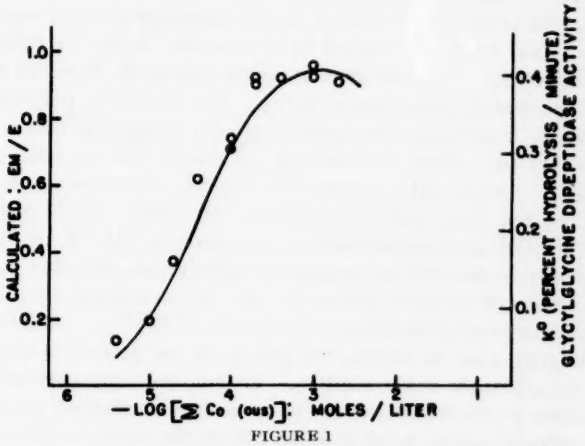

FIGURE 1

Activation of glycylglycine dipeptidase by cobalt, at pH 7.8. The solid line describes the curve derived from equation (17). The points are taken from the experiments of Smith.[10]

of ten smaller than this average, since it appears likely that the dissociation of a protein-metal complex would be smaller than these averages. Only orders of magnitude are important.

Since the two positions of the paired monovalent site exist in the same molecule, they do not have independent freedom for orientation with respect to the divalent cation. When the first position is occupied by a divalent cation, the position of the second limits bonding to the same cation and the relative value of k_2 is greatly increased. The dissociation constant of EM, K_{1d}, in this treatment, is considered to be that of the first position, k_{1d}.

Estimation of the stability of $E(MOH)_2$ relative to $E(M^+)_2$ necessitates consideration of the effect of hydrogen bonding. If the juxtaposition of

groups which can form hydrogen bridges is unfavorable, or are blanked out by interformation of hydrogen bonding between the ketoimino linkage and amino and carboxyl side chains, no difference in stability would be expected between the two complexes. From these, and from entropy considerations, the simplifying assumption has been made that K_{2d} and K_{3d} for the enzymes have the same order of magnitude, table 1. A different situation is met in cation binding by clays where $K_{2d} > K_{3d}$ which enhances formation of the complex with the basic ion.

Agreement with Experimental Observations.—Agreement between observed enzymatic activities and values calculated from equation (17) are shown in figures 1, 2, and 3, at various metal concentrations. In figure 1, and curve (*a*) of figure 2, further increases of metal would cause the theoretical curve to descend in the manner shown by figure 3 and curve (*b*) of figure 2; experimental results, however, were not available beyond the metal concentration shown. The change in pH from 7.6 to 7.8, figure 2, translocates the curve to greater manganese concentrations. Since higher pH values decrease $[M^{++}]$ relative to the concentrations of $(MOH)^+$ and $M(OH)_2$, greater total metal concentration is required to produce the same effect as at lower pH values. In all of the cases studied, $[MOH^+]$ is insignificant as compared to $[M^{++}]$ up to pH 10; consequently, unless the enzyme has an affinity for $(MOH)^+$ greater by several factors of ten (6 or greater, at pH 8, in most cases) than it has for M^{++}, the inactivation is caused by formation of $E(M^+)_2$. Although additional binding may be exerted by groups of the protein moiety on the metal, it apparently is not limiting. Enzyme concentrations affect only the absolute concentrations of the metal-enzyme complexes but not their concentrations relative to each other. With the values of the constants given, the slopes of the metal concentration curves would change only at enzyme concentrations greater than 10^{-5} *M*. Therefore, concentrations of 10^{-8} *M* were used for calculations. The agreement of equation (17) with experimental results indicates that the effect of buffers is insignificant in the systems studied, as was expected from their probable dissociation constants. The theoretical metal concentration curves agree, so far as tested, with experimental results on enzymes other than the examples presented.

The assumption that EM is the active complex is supported by the fact that $[E(MOH)_2]$ or $[E(M^+)_2]$ never decreases with increasing [M]. If the $(MOH)^+$ affinity for the enzyme is greater than that of M^{++}, then it must be greater by a factor of 10^6, which is unlikely, in order to describe the experimental results. In addition, experimental results do not support the likelihood that the dissociation constant for EM is equal to, or smaller than, the dissociation constant for $E(MOH)_2$ or $E(M^+)_2$.

Although the system presented does not include all the possible inter-

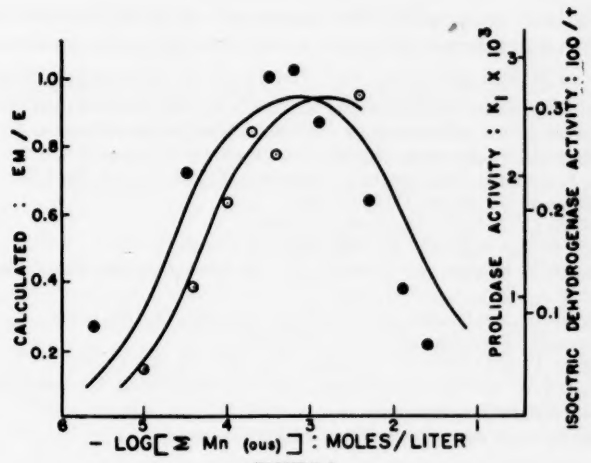

FIGURE 2

Activation by manganese of prolidase, at pH 7.8 (curve (a), open circles), from Adams, *et al.*,[1] and of isocitric dehydrogenase, at pH 7.6 (curve (b), solid circles), from Adler, *et al.*[1] The solid lines describe the respective curves derived from equation (17).

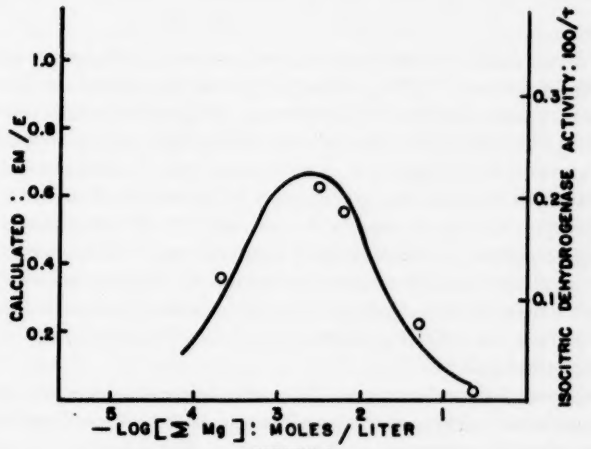

FIGURE 3

Activation of isocitric dehydrogenase by magnesium, at pH 7.6. The solid line describes the curve derived from equation (17). The points are taken from the experiments of Adler, *et al.*[1]

actions of the components, the agreement with experimental results indicates that it describes the mechanism for cation activation of enzymes.

* This investigation was supported in part by the U. S. Atomic Energy Commission.

† Although the active concentration of $M(OH)_2$ in the solid phase is generally assumed to be constant, as the entire mass per unit volume does not participate in a reaction, this treatment has admitted the $M(OH)_2$ as a variable in the equation.

[1] Adler, E., v. Euler, H., Gunther, G., and Plass, M., *Biochem. J.*, **33**, 1028 (1939).

[2] Malstrom, B. G., *Nature*, **171**, 392 (1953).

[3] Smith, E. L., *J. Biol. Chem.*, **163**, 15 (1946).

[4] Adams, E., and Smith, E. L., *Ibid.*, **198**, 671 (1952).

[5] Ochoa, S., in Sumner and Myrback, *The Enzymes*, Academic Press, New York, 1951, p. 1220.

[6] Gayer, K. H., and Garrett, A. B., *J. Am. Chem. Soc.*, **74**, 1436 (1952).

[7] Kullgren, C., *Z. Physik. Chem.*, **85**, 466 (1913).

[8] Stock, D. I., and Davies, C. W., *Trans. Far. Soc.*, **44**, 856 (1948).

[9] Martell, A. E., and Calvin, M., *Chemistry of the Metal Chelate Compounds*, Prentice-Hall, New York, 1952, p. 514.

[10] Smith, E. L., *J. Biol. Chem.*, **173**, 571 (1948).

---

*ENZYMATIC REACTIONS IN PURINE DECOMPOSITION BY PREPARATIONS OF CLOSTRIDIUM ACIDI-URICI**

BY NORMAN S. RADIN† AND H. A. BARKER

DEPARTMENT OF PLANT BIOCHEMISTRY, UNIVERSITY OF CALIFORNIA, BERKELEY

Communicated October 26, 1953

Clostridium acidi-urici ferments several purines including uric acid, xanthine, and guanine.[1, 2] The products of these fermentations are mainly acetic acid, carbon dioxide, and ammonia. Experiments with cell suspensions and C^{14}-labeled uric acid have established the source of some of the carbon atoms in the products.[3] Also various types of evidence have been obtained which indicate that glycine may be an intermediate in the purine fermentation. Glycine is readily decomposed by cell suspensions when a fermentable purine is simultaneously supplied, and it is formed from uric acid by a physiologically similar bacterium, *C. cylindrosporum*.[2] These and other lines of evidence indicate that the mechanism of purine decomposition by these bacteria is somewhat similar to the mechanism of purine synthesis in animals.[4]

Up to now all experiments on the purine fermentation have been done with intact cells. This report describes the anaerobic conversion of xanthine to glycine, ammonia, carbon dioxide, and formate by dried cell suspensions and cell-free extracts of *C. acidi-urici*. The enzymatic decomposition of glycine, serine, pyruvate, and formate by extracts is also reported.

Experimental Methods.—Clostridium acidi-urici, strain 9 a,[1] was grown on a medium containing the following constituents in grams per liter of distilled water: uric acid 2.5, yeast autolysate 1, K_2HPO_4 1, $MgSO_4 \cdot 7H_2O$ 0.05, $CaSO_4 \cdot 2H_2O$ 0.005, $FeSO_4 \cdot 7H_2O$ 0.002, $Na_2S \cdot 9H_2O$ 0.10, and Na_2CO_3 1. The uric acid was neutralized to pH 8 with NaOH at 100° before being added to the medium. The sulfide and carbonate were added after autoclaving the remainder of the medium, and then the pH was adjusted to 7.4 with 1 *N* H_2SO_4. The medium was incubated in 5- to 20-liter bottles or flasks filled to the neck. The inoculum was 5 to 10 volume per cent of a 14–18 hour culture. After 16–18 hours at 30° when most of the urate was decomposed but before spore formation was appreciable, the cells were harvested with a Sharples centrifuge, washed twice with an oxygen-free solution containing 0.2 per cent KCl, 0.2 per cent NaCl, and 0.03 per cent $Na_2S \cdot 9H_2O$ neutralized to pH 7.6, and resuspended in a quantity of water equal to 0.5 volume per cent of the culture. A thin layer of the bacterial suspension was dried in a vacuum desiccator over calcium chloride at room temperature overnight. The yield of dried cells was 150 to 200 mg. per liter of culture.

Most experiments were done with a 3 per cent suspension of dried cells in water containing 0.03 per cent sodium sulfide and 0.1 *M* TRIS (tris-(hydroxymethyl)aminomethane) buffer, pH 7.7. Active cell-free extracts were made by incubating a 5 per cent cell suspension (without TRIS buffer) in vacuo for one to three hours at 20–25°C. and then centrifuging 5 minutes at 10,000 r. p. m. in a Servall type SS-1 angle centrifuge at 5°C. Another method consisted of shaking 250 mg. of dried bacteria with 5 ml. of 0.03 per cent sodium sulfide solution and 5 gm. of 0.15 mm. diameter glass beads in an evacuated tube for 40–50 minutes at a rate of 20 strokes per second. The beads were separated by low-speed centrifugation and then the extract was clarified by centrifuging at high speed. The cell-free extracts contained from 25 to 45 per cent of the dry weight of the cells.

Flavin adenine dinucleotide (FAD) was prepared by the method of Warburg and Christian.[5] The purity was not determined but the preparation was shown to activate resolved D-amino acid oxidase apoenzyme. Crystalline catalase in saturated ammonium sulfate (Worthington Biochemicals) was dialyzed and the resulting solution was diluted 1:10 with water. Sodium glyoxylate was prepared by adding 6.9 g. H_5IO_6 in 15 ml. of water to 5.5 g. of tartaric acid in 5 ml. water at 0°. After 1 hour the resulting glyoxylic acid was extracted in a continuous extractor with ether. After removal of ether, the acid was diluted with an equal volume of water, carefully neutralized to pH 5.0 with saturated NaOH at 0° and the sodium salt was precipitated by addition of 3 volumes of acetone. N-formylglycine was made by the method of du Vigneaud;[6] imidazole-4-carboxylic acid by the method of Pyman.[7]

Ammonia was estimated by steam distillation from borax solution and titration with acid. Acetic acid was steam distilled from acid solution and titrated. Formic acid was separated from the reaction mixture by lyophilization and then was determined by the method of Grant[8] with omission of the sulfosalicylic acid treatment. Glycine was estimated by the method of Alexander, *et al.*,[9] and pyruvate by the method of Friedemann and Haugen.[10] The method of Bratton and Marshall[11] was used to estimate amino imidazoles. Oxygen and carbon dioxide were determined by the usual Warburg manometric method.

RESULTS

Decomposition of Urate and Xanthine.—Dried cell suspensions and cell-free extracts decompose uric acid in the absence of oxygen to form carbon dioxide, ammonia, and other products. With most preparations, the rate of fermentation was increased significantly by addition of glycine or pyruvate (table 1). These compounds are known to serve as reducing

TABLE 1

INFLUENCE OF GLYCINE AND PYRUVATE ON URATE DECOMPOSITION

The indicated substrates and 130 μM. TRIS buffer pH 7.7, were in the main compartment of the manometer vessel in 0.6 ml. water. One side-arm contained 25 mg. dried cells suspended in 0.4 ml. water and the other contained 0.2 ml. 1 *N* H_2SO_4 which was mixed with the other constituents after 80 minutes to liberate bound carbon dioxide. Gas phase: N_2. Temp. 36°.

SUBSTRATES ADDED	CO_2 FORMED,[a] μM	NH_3 FORMED,[a] μM
Expt. A		
Glycine, 10 μM	1.5	1.3
Lithium urate, 9 μM	6.9	10.4
Glycine + urate	10.8	14.2
Expt. B		
Sodium pyruvate, 30 μM	3.6	0.8
Urate, 20 μM	9.6	11.2
Pyruvate + urate	18.3	17.3

[a] Corrected for a blank without substrates. The blank values in Expt. A, CO_2 1.5 μM, NH_3 14.3 μM; in Expt. B, CO_2 3.7 μM, NH_3 17.6 μM.

agents, under the influence of enzymes present in the preparation. In several experiments pyruvate proved to be more effective than glycine in stimulating carbon dioxide and ammonia formation from urate. Sodium sulfide and formate were ineffective when tested at the same levels.

The stimulatory effect of reducing agents on uric acid decomposition by enzyme preparations, which has been observed previously with cell suspensions, indicates that uric acid may be reduced to xanthine. Support for this idea was provided by the observation that all preparations which decompose uric acid also attack xanthine. Several preparations,

obtained from cells grown on urate, decomposed xanthine much more rapidly than urate, presumably as a result of the loss of ability to reduce urate. In this connection it is significant that xanthine may be decomposed by cell-free extracts and dried cell preparations both in the presence and absence of oxygen, whereas urate decomposition is quickly and totally inhibited by oxygen. This is consistent with the theory that a reductive step is essential for urate but not for xanthine breakdown.

Products Formed from Xanthine.—The main products of anaerobic xanthine decomposition by dried cell suspensions are carbon dioxide, ammonia, glycine, and formate (table 2). The same products are formed by cell-free extracts. The observed yields of carbon dioxide, ammonia, and glycine are roughly in accordance with the equation

$$1 \text{ xanthine} \xrightarrow{H_2O} 3 \text{ ammonia} + 2 \text{ carbon dioxide} + 1 \text{ formate} + 1 \text{ glycine} \quad (1)$$

which represents a non-oxidative decomposition of xanthine. The yield of formate is considerably lower than would be expected. The agreement between the equation and the experimental data might be better if a correction could be made for the probably incomplete utilization of xanthine. Unfortunately the quantity of xanthine decomposed was not determined directly.

TABLE 2

PRODUCTS OF XANTHINE DECOMPOSITION

A suspension of 20 mg. dried cells in 0.8 ml. 0.1 *M* TRIS buffer pH 7.7 was incubated with 10 μM of xanthine at 36° in the main compartment of a Warburg vessel. 0.2 ml. of 1 *N* H_2SO_4 was added from a side arm after 100 minutes. Atmosphere: N_2.

PRODUCT	QUANTITY FORMED,[a] μM
Ammonia	24.2[b]
Carbon dioxide	19.9
Glycine	8.1
Formate	4.0

[a] Corrected for a blank without xanthine.
[b] Determined in a parallel experiment.

The above-mentioned compounds are not the only products formed from xanthine by cell-free extracts. Evidence has been obtained for the accumulation of small amounts of several substances that give colored reaction products either spontaneously or after reaction with the Bratton-Marshall reagents for detecting diazotizable amines. When the Bratton-Marshall (B-M) test was applied directly to reaction mixtures initially containing xanthine, an intense reddish-orange color was obtained which is quite different from the violet color obtained with aromatic amines such as sulfanilamide or with 4-amino, 5-carboxamido-imidazole. Cell-free extracts incubated in the absence of xanthine give a violet color in the Bratton-Marshall test, but the color is much less intense than the orange color obtained from the products of xanthine decomposition. Since amino purines and pyrimidines do not react in the B-M test, the formation of the orange reaction product may be taken to indicate the formation of an amino imid-

azole not identical with 4-amino, 5-carboxamido-imidazole, which has been implicated in purine synthesis by bacteria and animals.[12]

Attempts to detect the unknown compound(s) on paper chromatograms were unsuccessful when phenol or lutidine were used as developing agents, but were successful with butanol-acetic acid-water (74:19:50). The enzyme mixture was deproteinized by addition of 4 volumes of ethanol and the supernatant was concentrated in vacuo to dryness. The residue was dissolved in a minimum amount of water, and a few lambda of the resulting solution was applied to the paper. On developed chromatograms a yellow spot was often visible at R_f 0.50. Under a Mineralite UV light, a yellow fluorescent spot was seen just under this and overlapping it. On spraying the paper with the Bratton-Marshall reagents, an orange spot appeared in the same area. In one experiment a faint red spot at R_f 0.18 was also observed with the Bratton-Marshall reagent which was absent from the blank without xanthine. Most chromatograms also showed faint violet spots at R_f 0.79, 0.41, and 0.36, but these were not dependent upon the presence of xanthine in the reaction mixture. None of these spots corresponds with 4-amino, 5-carboxamido-imidazole (R_f 0.88) or *p*-aminobenzoic acid (R_f 0.54).

Since it seemed possible that 4-amino, 5-carboxy-imidazole would be an intermediate in xanthine decomposition (see Discussion), an attempt was made to prepare this compound by hydrolysis of the corresponding amide or ethyl ester. The latter was synthesized by the method of Cook, *et al.*[13] Both compounds proved to be refractory to hydrolysis by either dilute acid or alkali. Therefore more vigorous treatment was applied by heating the ethyl ester in 80 per cent sulfuric acid at 100° for 2.5 hours. As a result of this treatment the Bratton-Marshall reaction color changed from violet to orange without any great reduction in absolute intensity. After removal of the sulfuric acid with barium chloride and neutralization the reaction mixture was chromatographed on paper with the butanol-acetic acid-water solvent. On spraying the paper with the Bratton-Marshall reagents an intense spot developed with the same orange color and the same R_f 0.50 as the enzymatic reaction product derived from xanthine. Several other spots of varying colors and lesser intensities also appeared on the chromatogram.

A direct comparison of the enzymatic and chemically prepared products on the same chromatogram also showed that the corresponding spots at R_f 0.50 gave identical reaction colors with ninhydrin (brown) and diazotized sulfanilic acid followed by sodium carbonate (brown). These results indicate that the main product of acid hydrolysis of 4-amino, 5-carbethoxy-imidazole is probably the same as the enzymatic product of xanthine decomposition. Although actual identity of the compound is not established by these experiments, it is probably either 4-amino, 5-carboxy-imidazole or 4-amino-imidazole.[17]

Possible Intermediates Between Xanthine and Glycine.—Several compounds that might be intermediates in the conversion of xanthine to glycine, formate, ammonia, and carbon dioxide, or are otherwise structurally related to purines, were tested by incubating them either with a dried cell suspension or a cell-free extract in the presence of 0.1 *M* TRIS buffer and in the absence of oxygen and looking for production of carbon dioxide, ammonia, or glycine. The following compounds were tested: N-formyl glycine, formamide, 5-carboxy-imidazole, 4-amino-5-carboxyamino-imidazole, parabanic acid, alloxan, isodialuric acid, uramil, allantoic acid, allantoin, and hydantoic acid. All were found to be inactive both in the presence and absence of 30 μm. per ml. of glycine.

Oxidation of Glycine.—Since glycine had previously been implicated as an intermediate in urate fermentation and had been shown to be a good reducing agent, the oxidation of glycine was studied, using oxygen as the ultimate electron acceptor.

When glycine and methylene blue are incubated anaerobically with dried cells, the dye is quickly reduced, but admission of air restores the blue color and the uptake of oxygen quickly stops. In order to maintain oxygen uptake for an hour or more it is necessary to add FAD and catalase. A high glycine concentration is also desirable. The following reaction mixture was found to be favorable for observing glycine oxidation: 30 mg. dried cells, 360 μm. glycine, 120 μm. TRIS buffer pH 7.7, 250,000 units of dialyzed crystalline catalase, 0.2 μm. methylene blue, and approximately 40 μg. FAD in a total volume of 1.0 ml. Larger amounts of methylene blue or catalase caused some inhibition. Under the above conditions the initial rate of oxygen uptake was usually in the range from 15 to 40 μm. per 30 mg. cells per hour. The rate falls off with time and usually stops after 60 to 90 minutes.

TABLE 3

OXIDATION OF GLYCINE

30 mg. dried cells, 360 μM glycine, 120 μM TRIS-HCl buffer, pH 7.7, 250,000 units dialyzed crystalline catalase, 0.2 μM methylene blue, and approximately 40 μg FAD in a total volume of 1.0 ml. were shaken for 45 minutes in air at 36°C. All values are corrected for a blank without glycine.

COMPOUND	QUANTITY, μM
Oxygen	−8.0
Ammonia	12.2
Acetate	3.7
Formate	0.9[a]
Carbon dioxide	12.6

[a] Determined in a parallel experiment.

The products of glycine oxidation were found to be ammonia, acetate, carbon dioxide and a little formate (table 3). If ammonia is taken as a measure of glycine decomposition and the formate production is disregarded, the data are roughly in agreement with equation 2, although the yield of

$$2CH_2NH_2COOH + O_2 \longrightarrow 2NH_3 + 2CO_2 + CH_3COOH \qquad (2)$$

acetate is low (61%). Neither glyoxylic acid nor other keto acid could be detected in the reaction mixture by means of 2,4-dinitrophenylhydrazine.

Serine Decomposition.—Serine is readily converted to pyruvate and ammonia by dried cells in the absence of oxygen. In a typical experiment, 20 mg. dried cells and 174 μm. DL-serine were incubated in 1 ml. 0.1 M TRIS buffer pH 7.7 for 75 minutes at 30°. 83 μm. of ammonia were formed, corresponding to 95 per cent of one of the optical isomers; 69 μm. of pyruvate and 9.5 μm. of carbon dioxide were also produced. Pyruvate was identified by paper chromatography,[14] by isolation of the 2,4-dinitrophenylhydrazone and comparison of its absorption spectrum with an authentic sample, and by application of the rather specific quantitative method of Friedemann and Haugen.[10] The carbon dioxide was probably formed by secondary decomposition of pyruvate (see below). The serine dehydrase appears to attack only one optical isomer since in several experiments not more than half the DL-serine was decomposed. DL-Threonine and L-cysteine are not deaminated anaerobically by dried cell preparation of *C. acidi-urici*.

Pyruvate Oxidation.—Pyruvate is attacked quite slowly when added to a buffered suspension of dried cells under either aerobic or anaerobic conditions. However, when the aerobic reaction mixture is supplemented with methylene blue, catalase, and FAD, a fairly rapid oxidation occurs. Under the conditions described in table 3, except that the glycine was replaced by 30 μm. of pyruvate, 20.6 μm. of carbon dioxide, and 11.2 μm. of oxygen were produced and taken up, respectively, in 38 minutes. The experiment was terminated before oxygen uptake had stopped. Acetic acid, recovered from the reaction mixture, was identified by Duclaux distillation. It may be concluded that *C. acidi-urici* possesses an active enzyme system for the oxidation of pyruvate to acetate and carbon dioxide.

Formate was found to be rapidly oxidized under conditions suitable for glycine and pyruvate oxidation. Compounds shown not to be oxidized in this system are acetate, glycolate, glyoxylate, α-keto glutarate, succinate, fumarate, lactate, acetaldehyde, formaldehyde, and methylamine.

DISCUSSION

Considerable evidence has accumulated which indicates that the first step in the fermentation of urate by *Clostridium acidi-urici* is its reduction to xanthine. This view is supported by the observation that enzyme preparations always decompose xanthine at least as fast as urate, and several preparations, derived from bacteria grown on urate, decompose xanthine but not urate. Furthermore, oxidizing agents like oxygen are preferentially inhibitory to urate breakdown, whereas reducing agents, like pyruvate and glycine, preferentially accelerate the utilization of urate. Dr. J. V. Beck and his collaborators have obtained evidence by the method of

simultaneous adaption which indicates that uric acid, guanine, and hypoxanthine are all degraded via xanthine.[15]

The main products of xanthine decomposition by dried cells and cell-free extracts are ammonia, carbon dioxide, glycine, and formate.[18] Since these same compounds serve as substrates for purine synthesis in animals,[4] a general similarity between the degradative and synthetic processes is indicated. However, there is one conspicuous difference between the two processes, namely that hypoxanthine or a derivative is the initial product of purine synthesis, whereas xanthine appears to be the key compound for purine breakdown by *Clostridium acidi-urici*.

The accumulation of one or more products of xanthine decomposition that react with the Bratton-Marshall reagents and diazotized sulfanilic acid and consequently appear to be amino imidazoles, suggests that the purine ring is initially broken at the carbon nitrogen bond between the 1-6, 1-2, or 2-3 positions. The non-reactivity of 4-amino, 5-carboxamido-imidazole, which could be formed by rupture of either the 1-2 or 2-3 bonds, points toward an initial attack on the 1-6 bond to yield 4-ureido, 5-carboxy-imidazole. This compound could be decomposed to yield 4-amino, 5-carboxy-imidazole, and 4-amino-imidazole. The paper chromatographic evidence suggests that one of these two compounds is formed enzymatically from xanthine. The non-reactivity of 5-carboxy-imidazole indicates that carbon 6 of the purine is probably removed before or simultaneously with the amino group derived from position 3. The amino imidazole may then be broken down by a series of steps to glycine, ammonia, and formate. This would be somewhat analogous to the formation of ammonia, formate, and glutamic acid from urocanic acid by *Pseudomonas fluorescens*.[16] Formamide and N-formyl glycine are not attacked by the enzyme system, and therefore cannot be precursors of formate.

Since neither glycine nor formate accumulate in fermentations by living bacteria, they must be further decomposed. Both glycine and formate have been shown to be oxidized by dried cell preparations, using oxygen or methylene blue as acceptors. The products of glycine oxidation, namely ammonia, carbon dioxide, and acetate, are the normal fermentation products of purines. Previously reported tracer experiments[3] have established that glycine-2-C^{14} oxidation involves a condensation of two methylene carbons to give doubly labeled acetate. The accumulation of a little formate during glycine oxidation indicates the formation of a C_1 unit that may condense with glycine to give serine. So far attempts to demonstrate the latter reaction directly have been unsuccessful, but its occurrence under suitable conditions has not been excluded. Serine is rapidly converted to pyruvate and ammonia under anaerobic conditions, and pyruvate is oxidized readily to acetate and carbon dioxide. These results are consistent with, but do not establish, a participation of serine in the conversion of glycine to acetate.

Summary.—Dried cell preparations and cell-free extracts of *Clostridium acidi-urici* have been shown to decompose uric acid, xanthine, glycine, serine, pyruvate, and formate. The main products of xanthine decomposition are glycine, formate, ammonia, and carbon dioxide. In addition, one or more amino-imidazoles are formed in appreciable amounts. 4-Amino, 5-carboxamido-imidazole is neither formed nor decomposed in this system.

Glycine is oxidized in the presence of suitable electron carriers to acetate, carbon dioxide, and ammonia. Serine is converted to pyruvate anaerobically and the latter is oxidized to acetate and carbon dioxide.

The mechanism of purine fermentation has been discussed in the light of these observations.

* This work was supported in part by a research grant from the U. S. Public Health Service and a contract with the Atomic Energy Commission.

† A. E. C. Fellow, 1949–1950. Present address: U. S. Veterans Administration Research Hospital, Chicago, Ill.

[1] Barker, H. A., and Beck, J. V., *J. Bact.*, **43**, 291 (1942).

[2] Barker, H. A., and Beck, J. V., *J. Biol. Chem.*, **141**, 3 (1941).

[3] Karlsson, J. L., and Barker, H. A., *Ibid.*, **178**, 891 (1949).

[4] Sonne, J. C., Buchanan, J. M., and Delluva, A. M., *Ibid.*, **173**, 69 (1948).

[5] Warburg, O., and Christian, W., *Biochem. Z.*, **298**, 150 (1938).

[6] du Vigneaud, V., and Irish, O. J., *J. Biol. Chem.*, **122**, 349 (1938).

[7] Pyman, F. L., *J. Chem. Soc.*, **109**, 186 (1916).

[8] Grant, W. M., *Anal. Chem.*, **19**, 206 (1947).

[9] Alexander, B., Landwehr, G., and Seligman, E. M., *J. Biol. Chem.*, **160**, 51 (1945).

[10] Friedemann, T. E., and Haugen, G. E., *Ibid.*, **147**, 415 (1943).

[11] Bratton, A. C., and Marshall, E. K., *Ibid.*, **128**, 537 (1939).

[12] Shive, W., *Fed. Proc.*, **12**, 639 (1953).

[13] Cook, A. H., Davis, A. C., Heilbron, I., and Thomas, G. W., *J. Chem. Soc.*, 1071 (1949).

[14] Cavallini, D., Frontali, N., and Toschi, G., *Nature*, **163**, 568 (1949); **164**, 792 (1949).

[15] Beck, J. V., *Bact. Proc.*, 136 (1950).

[16] Tabor, H., Mehler, A. H., Hayaishi, O., and White, J., *J. Biol. Chem.*, **196**, 121 (1952).

[17] Dr. J. C. Rabinowitz (unpublished) has recently obtained evidence that 4-amino, 5-carboxy-imidazole is rapidly converted to 4-amino-imidazole by dilute acid. Therefore the main product of acid hydrolysis of the 4-amino, 5-carboxy-imidazole ethyl ester, which gives the orange spot at R_f 0.50, is probably 4-amino-imidazole.

[18] W. Bradshaw and J. V. Beck, *Bact. Proc.*, 86, (1953), have shown independently that extracts of *Clostridium acidi-urici* convert xanthine to these products.

EFFECT OF AMINO ACIDS, ESPECIALLY ASPARTIC AND GLUTAMIC ACID AND THEIR AMIDES, ON THE GROWTH OF DATURA STRAMONIUM EMBRYOS IN VITRO*

BY DENISE PARIS,† J. RIETSEMA, S. SATINA, AND A. F. BLAKESLEE

GENETICS EXPERIMENT STATION, SMITH COLLEGE, NORTHAMPTON, MASSACHUSETTS

Communicated October 5, 1953

Experiments on the growth of plant embryos have indicated the importance of organic nitrogen compounds in the culture medium. Sanders and Burkholder[13] showed that embryos of *Datura stramonium* and *D. inoxia*, in the pre-heart and early heart stage, develop well only in a medium to which a complex nitrogen source has been added; e.g., casein hydrolysate at 400 p.p.m. On the other hand, on media with only one or a few amino acids, embryos grow to a very limited extent.

Little attention has been given to the stage of development of the embryos with respect to their nitrogen requirements. It has been found for embryos of *D. stramonium*[9] and for *D. ceratocaula* (unpubl.) that the sucrose requirements are largely determined by the stage of development. Whether anything comparable to this change in sucrose requirements takes place with the need for organic nitrogen is not known. Experiments have been designed in order to collect data on this subject.

In a recent publication, Rijven[10] showed that embryos of *Capsella bursa-pastoris* grow at least as well in vitro when glutamine is the only nitrogen source present as when a mixture of amino acids has been added. This amide, however, has not been tested on Datura before. The importance of asparagine for plant tissue and organ cultures has been stressed frequently.[1, 2, 4] Therefore, experiments have been made in order to obtain information regarding the possibility of glutamine and asparagine as key substances in the metabolism of *D. stramonium* embryos.

Materials and Methods.—Embryos of *Datura stramonium* (standard Line I) obtained from capsules of self-pollinated flowers were used. The excised embryos were grown according to previously described method,[9] for eight days in a dark incubator at 26°C. The basal medium consisted of water, which had been doubly distilled over glass, mineral salts,[9] trace elements (one drop of a Berthelot solution, according to Morel,[7] per 200 ml. of nutrient solution) and 0.8 per cent Bacto-Difco agar. Sucrose was added in concentrations of 8, 4 and 2 per cent, depending on the stage of development of the embryos. Embryos smaller than 0.3 mm. (early heart stage) were grown on 8 per cent sucrose, those between 0.3 and 0.8 mm. (early heart to torpedo stage) on 4 per cent sucrose, and older embryos on 2 per cent sucrose (cf. Rietsema, *et al.*[9]). To this basal medium, amino acids‡ were added. As a rule the sucrose and agar-salt solutions were sterilized

separately by autoclaving at 110°C. for 20 minutes, whereas the amino acids and casein hydrolysate were added after Seitz filtration. The pH was adjusted to 6.0.

Effect of Casein Hydrolysate in Relation to the Stage of Development.—In order to establish the relation between the stage of development and the amino acid requirements, embryos varying from pro-embryos, 0.08 mm.

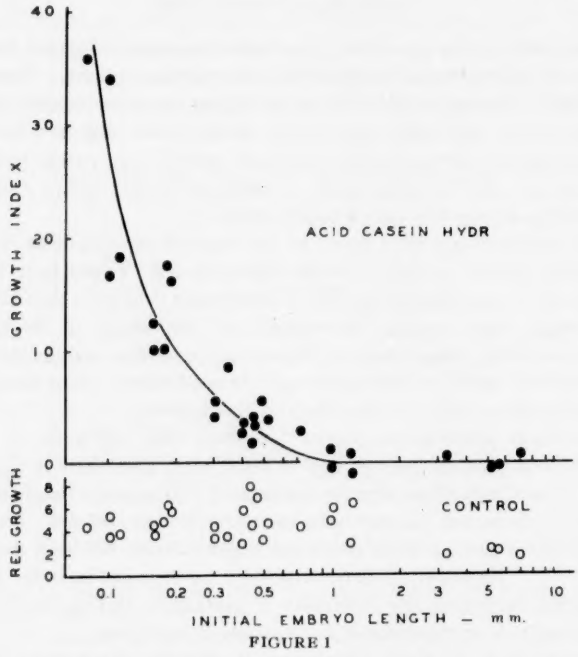

FIGURE 1

Growth of *Datura stramonium* embryos on media without casein hydrolysate (lower half, open circles) and with casein hydrolysate, 400 p.p.m. (upper half, closed circles). Relative growth indicates ratio between final and initial length. Growth index refers to difference between relative growth values of experiment and control.

long, to nearly mature embryos, 7 mm. long, were grown on media containing 400 p.p.m. acid hydrolyzed casein.

It was found that all embryos grew to some extent on control media without amino acids. Their relative growth, i.e., final length divided by initial length, varies between 2 and 8, showing no marked differences between young and nearly mature embryos. This growth is probably supported by accumulated material inside the embryos, which supply becomes

exhausted during the subsequent growth processes. The differences between the relative growth values of the controls and those of simultaneously run experimental series, therefore, express the effect of added amino acids in the medium. These differences have been called *growth indices*. All results have been reported in growth index values unless otherwise stated.

In the lower part of figure 1 the relative growth of the controls has been indicated, whereas in the upper part the relation between the effect of casein hydrolysate (400 p.p.m.) and the stage of development has been given. The influence of the casein hydrolysate has proved to be more or less inversely proportional to the initial stage of development. When the embryos have reached a length of about 1 mm. (young torpedo stage) the presence of casein hydrolysate has no more effect on their elongation during the culture period. The embryos of the control series have become transparent, and may contain anthocyanin or are covered with numerous brown spots. Some are also peculiarly differentiated. Embryos grown on casein hydrolysate are normal in appearance, follow the same stages as in the seed, do not contain anthocyanin, and do not have brown spots.

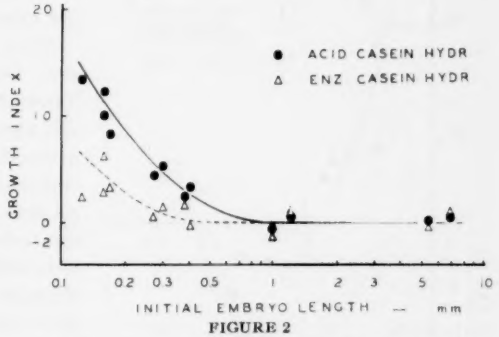

FIGURE 2

Effect of enzymatic and acid casein hydrolysate (both 400 p.p.m.).

Acid vs. Enzymatic Casein Hydrolysate.—Sanders and Burkholder[13] used as an organic nitrogen source acid hydrolyzed casein. However, an enzymatic hydrolysis of casein may be considered more similar to a natural breakdown of endosperm proteins. It is possible that other end products are formed having a specific effect on embryo growth. Melin and Norkrans[6] for example, working with *Lactarius deliciosus*, found that preparations of enzymatic hydrolysate are somewhat more beneficial than acid hydrolyzed preparations; both, however, were inferior to a synthetic mixture of amino acids.

In order to ascertain the differences between enzymatic and acid casein hydrolysates, embryos were grown on media to which 400 p.p.m. of one of the two products was added. Control series without organic nitrogen were run simultaneously. Embryos of nine different stages, from the pro-

embryo stage (0.08 mm.) to nearly mature embryos (~6 mm.), were used for these experiments. The curves in figure 2 show the growth indices of these embryos. As can be seen, acid casein hydrolysate seems to have a better effect on *Datura stramonium* embryos than the hydrolysate obtained by an enzymatic action.

Moreover, the embryos grown on an enzymatic casein hydrolysate are often translucent, especially when excised in a very young stage; their shape is often abnormal and the cotyledons are diverging; also brown spots occur frequently, and in the post-heart stages anthocyanins are commonly present. Excised in the very late stages (bent torpedo to nearly mature embryo), most of them show a normal appearance.

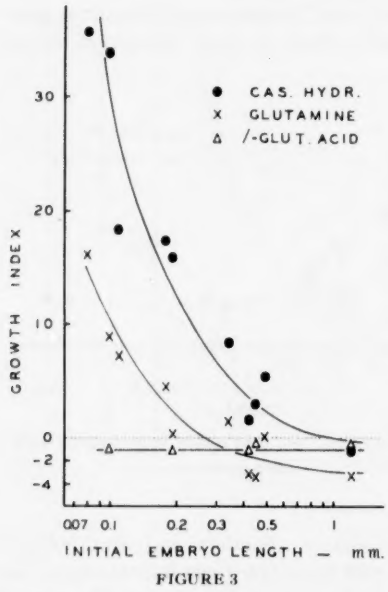

FIGURE 3

Effect of glutamine and *l*-glutamic acid (both 80 p.p.m.) as compared with effect of casein hydrolysate (400 p.p.m.).

These results justify the use of acid hydrolyzed casein for our experiments.

Effect of l- and d-Glutamic Acid and Glutamine.—According to Rijven,[10] glutamine and glutamic acid are able to replace any organic nitrogen source for excised embryos of *Capsella bursa-pastoris*. In an attempt to check this information on *D. stramonium*, embryos were grown in the presence either of glutamine or glutamic acid, both at doses of 80 and 400 p.p.m. The amount of 80 p.p.m. approximately corresponds to the amount of glutamic acid found in 400 p.p.m. casein hydrolysate, according to analyses of Block[3] and Thompson.[15] Two control series, one with 400 p.p.m. casein hydrolysate and one without organic nitrogen, were run simultaneously.

The growth curves obtained are represented in figures 3 and 4. Neither *l*- nor *d*-glutamic acid in low or high concentration increases growth, whereas glutamine shows a favorable effect, especially on very young embryos. This effect ceases to be appreciable on embryos excised at the young heart stage or later.

On glutamic acid all embryos are transparent, brown spotted or show anthocyanins. The cotyledons, if developed are diverging. This toxic

effect of glutamic acid is also observed with embryos excised at the torpedo stage.

On glutamine, the embryos have a healthy appearance: they are white and opaque as are embryos grown on casein hydrolysate. Most embryos, however, are not fully differentiated, though occasionally some embryos excised in the torpedo stage or later form well developed cotyledons.

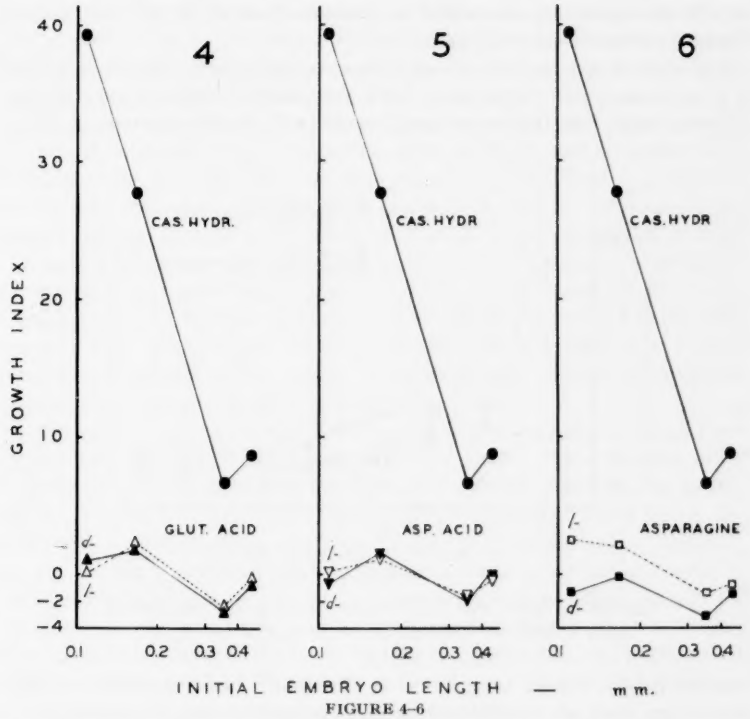

FIGURE 4–6

Effect of *l*- and *d*-glutamic acid, *l*- and *d*-aspartic acid and *l*- and *d*-asparagine as compared with effect of casein hydrolysate (400 p.p.m.). Glutamic acid: 80 p.p.m. Aspartic acid and asparagine: 25 p.p.m.

Nevertheless, the influence of glutamine is weak as compared with the effect of casein hydrolysate. Glutamine in a concentration of 80 p.p.m. gave better results than in a concentration of 400 p.p.m.

The results suggest that *Datura stramonium* embryos utilize glutamine, but, unlike *Capsella bursa-pastoris* embryos, cannot convert it to all nitrogenous compounds necessary for growth and differentiation.

Effect of l- and d-Aspartic Acid and l- and d-Asparagine.—Aspartic acid has been found by Sanders and Burkholder,[13] to have a negligible effect on embryo growth, when supplied as the only nitrogen source. Rijven[10] found identical results for embryos of *Capsella bursa-pastoris*. These results are completely confirmed by our experiments: both *l-* and *d-* aspartic acid are unable to support growth; both cause an alteration of the tissue, which becomes brown spotted and often transparent. These amino acids as well as asparagine were added in concentrations of 25 and 250 p.p.m. Figure 5 represents some of the results.

The effect of asparagine has been represented in figure 6: there is no effect of *d*-asparagine, and *l*-asparagine has a very limited effect on very young embryos only. In the latter case, about half of the embryos show a

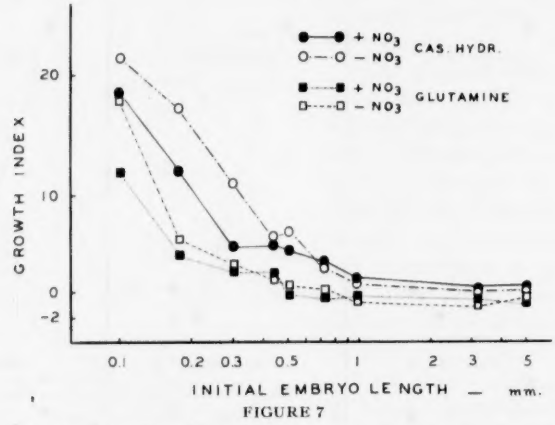

FIGURE 7

Growth on media with and without nitrate in the presence of casein hydrolysate (400 p.p.m.) or glutamine (80 p.p.m.).

healthy tissue, though their shape is abnormal; besides, excised at the heart stage, they are covered with brown spots and contain anthocyanins.

Effect of Nitrate.—Most salt formulae of nutrient media for embryo culture contain nitrates.[8, 12, 16] We do not know, however, whether embryos utilize oxidized nitrogen or whether they depend entirely on reduced nitrogen in the form of amino acids.

With the purpose of obtaining evidence on the nutritive value of nitrate ions, experiments were run with casein hydrolysate or glutamine both with and without nitrate. The original salt mixture contained 0.001 mol $Ca(NO_3)_2 \cdot 4H_2O$ and 0.00084 mol KNO_3. These were replaced by equivalent amounts of phosphate and chloride in order to maintain an equal cation distribution in the medium.

The differences between the control embryos grown on media without organic nitrogen and either with or without nitrate are small and not significant. The trend, nevertheless, is toward less growth on media with nitrate. The phenomenon of growth on media without any nitrogen proves that the embryos are able to use an internal nitrogen supply. It is surprising to note, that in the presence of organic nitrogen, nitrate causes a decrease of growth of very young embryos. The older embryos, showing no marked effect of casein hydrolysate or glutamine, grow equally well on both media. The growth indices on both plus and minus nitrate series in figure 7 make this clear. These experiments show that for young embryos nitrates are not a necessary requirement.

Discussion.—Addition of a mixture of amino acids (casein hydrolysate) to the culture medium has a favorable effect on the growth of *Datura stramonium* embryos. The youngest embryos are most benefited. Glutamine has a beneficial effect, but less than casein hydrolysate. Glutamic acid, asparagine, and aspartic acid have no effect at all. Nitrates inhibit growth.

Casein hydrolysate does not cause an increase in elongation of embryos excised at the torpedo stage or later, but it has a favorable effect on the differentiation. Brown spots or anthocyanins, which appear for example with aspartic acid or asparagine, never occur with casein hydrolysate. They must be considered as the results of an inadequate supply of nutrients necessary for biochemical and internal differentiation.

Dicarboxylic amino acids and their amides have been shown to play an important role in the protein metabolism of plants. Several cases have been described of tissue culture on media with only one amino acid or amide in the medium. Working with barley embryos, Brown[4] found better results with asparagine than with aspartic acid or glutamic acid. Rijven,[10] on the contrary, obtained remarkable slow growth using aspartic acid in cultures of *Capsella bursa-pastoris*, as compared with excellent growth on glutamine or glutamic acid. With orchid cultures, Knudson[5] found negative results with aspartic acid, whereas Spoerl,[14] also with orchid embryos, obtained good growth with aspartic acid and poor growth with glutamic acid. Apparently the reaction of embryos is highly specific.

The results with embryos of *Datura stramonium* indicate that casein hydrolysate is superior to any one of the amino acids used. This confirms the original study by Sanders and Burkholder.[13] Our results also show that glutamine is superior to any one of the other substances used, and only inferior to casein hydrolysate. Apparently *D. stramonium* embryos do not have the synthetic ability of *Capsella bursa-pastoris* embryos. The latter embryos are also able to use glutamic acid. Nevertheless, glutamine seems to play an important function in the metabolism of *Datura stramonium* embryos. Glutamine is not present in acid casein hydrolysate; evidently its function can be taken over by other amino acids.

Though Riker and Gutsche,[11] working with sunflower tissue, found poor growth with *l*-aspartic acid and fair growth with *dl*-aspartic acid, we could not observe any difference between the *l*- and *d*-forms tested, both being ineffective.

The inhibiting effect of nitrate ions is not well understood. Riker and Gutsche[11] observed the reverse: a stimulation of growth by nitrate for Helianthus tissue in the presence of some amino acids. Sanders[12] found that an increase in phosphate resulted in less growth of *D. stramonium* embryos. Therefore, use of phosphate instead of nitrate cannot explain this inhibition. More experimental evidence is required for a satisfactory explanation.

Summary.—The stimulatory effect of casein hydrolysate on the growth of *Datura stramonium* embryos decreases when the stage of development of the embryos advances. With embryos excised at the torpedo stage or later no effect on the elongation can be observed. Enzymatic casein hydrolysate is inferior to acid hydrolyzed casein. Glutamine has a limited effect on growth. Glutamic acid, aspartic acid and asparagine have no effect or are inhibitory: they cause formation of anthocyanins and brown spots. Nitrate ions decrease the effect of casein hydrolysate or glutamine on very young stages.

* This work has been supported in part by a grant from the National Cancer Institute of the U. S. Public Health Service. Contribution from the Department of Botany, Smith College, New Series No. 53.

† Present address: Institut de Botanique Générale, Université, Genève, Switzerland.

‡ The acid and enzymatic casein hydrolysate, *l*- and *d*-asparagine, *l*- and *d*-aspartic acid and glutamine were from the General Biochemicals, Inc., Chagrin Falls, Ohio. *l*-Glutamic acid was a product from the Nutritional Biochemicals Corp., Cleveland, Ohio. *d*-Glutamic acid came from Pfanstiehl Chemical Co., Waukegan, Ill.

[1] Algeus, S., *Physiologia Plantarum*, **4**, 449 (1951).

[2] Almestrand, A., *Ibid.*, **4**, 224 (1951).

[3] Block, R. J., and Bolling, Diana, "The Amino Acid Composition of Proteins and Foods," Charles C Thomas, Springfield, Ill., p. 396 (1945).

[4] Brown, H. T., *Trans. Guiness Res. Lab.*, **1**, 228 (1906).

[5] Knudson, L., *New York Agr. Exptl. Sta. (Cornell)* Rept., p. 111 (1932).

[6] Melin, E., and Norkrans, Birgitta, *Physiologia Plantarum*, **1**, 176 (1948).

[7] Morel, G., *Ann. Epiphities*, **15** (*N. S.*), Sér. Path. Végétale, Mém. **5**(1948).

[8] Randolph, L. F., and Cox, L. G., *Proc. Am. Soc. Hort. Sci.*, **43**, 284 (1943).

[9] Rietsema, J., Satina, S., and Blakeslee, A. F., *Am. J. Bot.*, **40**, 538(1953).

[10] Rijven, A. H. G. C., *Acta Bot. Neerlandica*, **1**, 157 (1952).

[11] Riker, A. J., and Gutsche, Alice E., *Am. J. Bot.*, **35**, 227 (1948).

[12] Sanders, Mary E., *Ibid.*, **37**, 2 (1950).

[13] Sanders, Mary E., and Burkholder, P. R., PROC. NATL. ACAD. SCI., **34**, 516 (1948).

[14] Spoerl, E., *Am. J. Bot.*, **35**, 88 (1948).

[15] Thompson, J. F., and Steward, F. C., *Plant Physiol.*, **26**, 421 (1951).

[16] Tukey, H. B., *Proc. Am. Soc. Hort. Sci.*, **32**, 313 (1934).

THE BEHAVIOR OF MICELLAR ELECTROLYTES IN THE NEIGHBORHOOD OF THE CRITICAL CONCENTRATION

BY CHARLES A. KRAUS

METCALF RESEARCH LABORATORY, BROWN UNIVERSITY

Communicated October 26, 1953

Salts having one ion containing a long hydrocarbon chain exhibit the properties of ordinary electrolytes in aqueous solution at lower concentrations. However, as concentration is increased, a point is reached where a discontinuity occurs in the derivative of the properties with respect to concentration. This concentration is termed the critical concentration of the electrolyte. It is now generally considered that above the critical concentration the long chain ions of the electrolyte associate to form charged aggregates called micelles.

Of the various properties of micellar electrolytes that have been investigated in the critical region, none permits of more precise and convenient measurement than their electrical conductance. At low concentration, the equivalent conductance decreases as a linear function of the square root of concentration in accordance with Onsager's Theory. At the critical concentration, the Λ—C plot changes its direction abruptly. In most cases that have been investigated the conductance curves fall off sharply at the critical point. However, in some instances, the equivalent conductance rises sharply at the critical concentration and passes through a maximum. Such observations have been recorded by Evers, Grieger, and Kraus[1] for solutions of octadecylpyridonium chloride in methanol-water mixtures and by Brown, Grieger, and Kraus[2] for solutions of octadecylpyridonium iodate in water. More recently, McDowell and Kraus[3] have measured the conductance of octadecyltrialkylammonium bromates from the ethyl to the *n*-amyl salt, inclusive. Data for octadecyltrimethylammonium bromate have been reported by Bair and Kraus.[4] The propyl, butyl, and amyl derivatives exhibit conductance maxima.

The data of McDowell and Kraus[3] for solutions of octadecyltriamylammonium bromate are of particular interest. Precise measurements were carried out to concentrations as low as 1.04×10^{-5} N and the critical concentration lies near 1.6×10^{-5} N. With this electrolyte, the equivalent conductance rises from a value of 68.97 at the critical concentration to a maximum of 100.01 at 7.16×10^{-5} N. A plot of Λ *vs.* C is shown as plot 1, figure 1. As may be seen from the figure, the conductance rises sharply at the critical concentration and already shows a value of 73.21 at 1.79×10^{-5} N. The fact that this conductance itself exhibits no discontinuity indicates that not all the salt is present as micellar electrolyte at concentrations just above the critical.

Let us make the simple assumption that the concentration of electrolyte in non-micellar state remains constant at concentrations above the critical and equal to that at the critical. This enables us to compute the equivalent conductance of the micellar electrolyte. By subtracting the critical con-

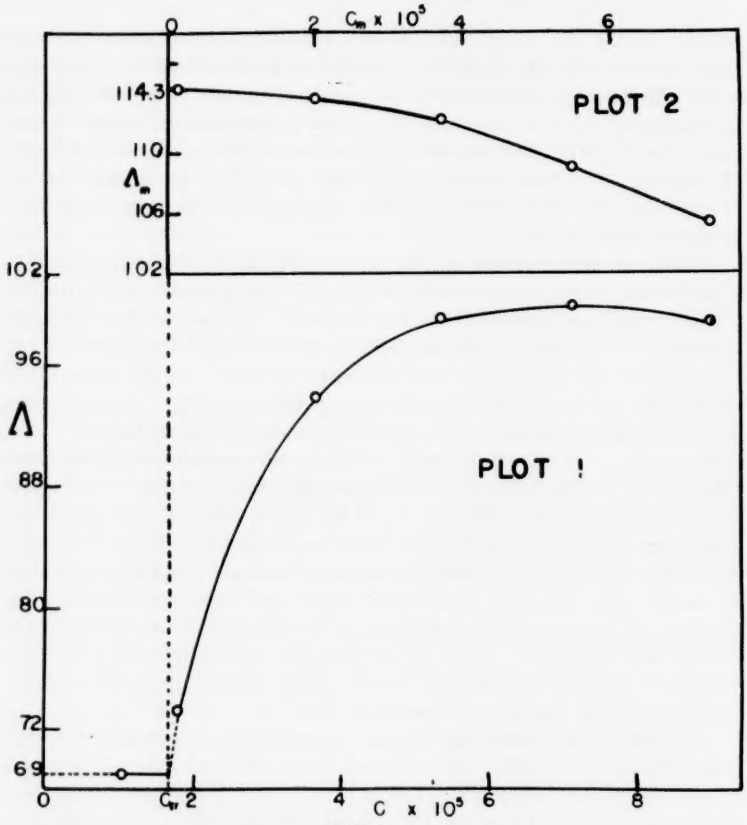

FIGURE 1

centration, C_{cr}, from the total concentration, C, and the specific conductance of the solution at the critical concentration, K_{cr}, from the specific conductance, K, of the solution at concentration C, we have the necessary data for computing the equivalent conductance of the micellar electrolyte. Let us write C_m, K_m, and Λ_m for the concentration, specific conductance and

equivalent conductance, respectively, of the micellar electrolyte. Thus we have:

$$C - C_{cr} = C_m(1), K - K_{cr} = K_m(2)$$

and

$$10^3 K_m/C_m = \Lambda_m(3)$$

The results of this computation are presented in table 1. The number of the experimental observation appears in column 1, the total concentration, C, of electrolyte in column 2, the specific conductance of the solution in column 3 and the equivalent conductance, Λ, of the electrolyte in column 4. In columns 5, 6, and 7 appear, respectively, the concentration, C_m, of the micellar electrolyte, the specific conductance, K_m, due to the micellar electrolyte and the equivalent conductance, Λ_m, of the micellar electrolyte. At the head of the table are given values of C_{cr}, the critical concentration, K_{cr}, the specific conductance of the solution at the critical concentration and Λ_{cr}, the equivalent conductance at that concentration. The specific conductance of the critical solution is obtained by multiplying the critical concentration by 68.97, the equivalent conductance of the solution just below the critical.

TABLE 1

$C_{cr} = 1.625 \times 10^{-5}$ $K_{cr} = 1.1208 \times 10^{-6}$ $\Lambda_{cr} = 68.97$

EXP. NO.	$C \times 10^5$	$K \times 10^6$	Λ_c	$C_m \times 10^5$	$K_m \times 10^6$	Λ_m
1	1.0390	0.7166	68.97	.....	.....	.....
2	1.7926	1.3124	73.21	0.01676	0.1916	114.32
3	3.6726	3.4478	93.88	2.0476	2.3270	113.65
4	5.3702	5.3203	99.07	3.7477	4.2013	112.13
5	7.1585	7.1592	100.01	5.8360	6.0402	109.12
6	9.0232	8.9285	98.95	7.4007	7.8095	105.54

It is obvious that the value of Λ_m computed for the micellar electrolyte will depend on the value chosen for C_{cr}. If the value chosen for C_{cr} is too large, values of Λ_m, as computed, will be too large and, conversely, they will be too small when C_{cr} is too small. However, the effect of an error in C_{cr} will be small unless the concentration C lies near the critical. Thus the value computed for Λ_m at point number 2 is very sensitive to the value chosen for C_m; the value computed for point 3 is relatively insensitive. It is a comparatively simple matter to adjust C_{cr} so that the computed values of Λ_m are a monotone function of concentration and that they approach a definite value of Λ_{0m} at $C = C_{cr}$. To illustrate, if we assume $C_{cr} = 1.61 \times 10^{-5}$, Λ_m at point 2 is 110.6 and at point 3 it is 113.3. If we assume $C_{cr} = 1.625 \times 10^{-5}$, we obtain values of 114.32 and 113.65 for Λ_m at points 2 and 3, respectively. A change of approximately one per cent in the value of

C_{cr} changes the value of Λ_m by 4% at point 2 and 0.3% at point 3. At concentrations above that of point 3, Λ_m is quite insensitive to any error that might be made in the value of C_{cr}.

A plot of Λ_m vs C_m is shown as plot 2 of figure 1. It will be noted that initially Λ_m falls off only slowly with increasing concentration. As may be seen from table 1, in going from point 2 ($C_m = 0.01676 \times 10^{-5}$) to point 3 ($C_m = 2.0476 \times 10^{-5}$), the value of Λ_m decreases from 114.32 to 113.65. In going from point 3 to point 4 ($C_m = 3.7477 \times 10^{-5}$), Λ_m decreases to 112.13. It is of interest to note that the solution of point 2 contains less than 10% of total electrolyte as micelles; at point 6, 80% of the electrolyte exists as micelles.

The consistency of the results obtained over a rather extended concentration range of micellar electrolyte lends support to the assumption made, that the concentration of non-micellar electrolyte remains substantially constant once the critical concentration has been reached. It follows that any electrolyte added at concentrations not too much above that of the critical all goes to form micelles. It also indicates that the state of the micellar ions is but little dependent on concentration in the low concentration region.

When the data for octadecyltributylammonium bromate and octadecyltripropylammonium bromate are analyzed according to the method outlined above the results obtained are similar to those obtained with octadecyltriamylammonium bromate. However, the equivalent conductance of the micellar electrolyte decreases as the substituent alkyl groups on the nitrogen atom become smaller; the decrease is roughly proportional to the decrease in the height of the maxima of the equivalent conductance as we pass from one salt to another.

For the amyl, butyl, and propyl derivatives, the conductance values at the maximum are respectively, 100, 87, and 77; the conductance at the critical concentration being 69.0, 71.3, and 71.5, respectively. The lower micellar conductance of the butyl and propyl derivatives is due to the increasing association of the counter ions with the ions of the micelles as the alkyl groups attached to the charged nitrogen atom become smaller. There is little doubt that if the data for octadecyltriethylammonium bromate could be analyzed, it would be found that the conductance of the micellar electrolyte would be less than that of the simple electrolyte at the critical concentration. Unfortunately, the necessary data at concentrations above the critical are lacking for this salt.

We may briefly discuss the nature of solutions of long chain salts at concentrations below the critical. Salts of quaternary ammonium ions having chains of 14 carbon atoms or less behave like 1–1 electrolytes below the critical concentration. The slopes of the Λ—$\sqrt{C}$ plots correspond to that of a 1–1 salt in accordance with Onsager's Theory. Octadecyl- and hexadec-

yltrimethylammonium salts yield linear Λ—$\sqrt{C}$ plots but their slopes correspond to that of a 2–1 electrolyte.[1] The Λ—$\sqrt{C}$ plot for hexadecyltributylammonium bromate is linear but its slope corresponds to that of a 3–1 electrolyte.[3] To account for the greater slope of the Λ—$\sqrt{C}$ plots for salts having chains of 16 or 18 carbon atoms, we are led to conclude that two or three long chain ions are associated to form what is effectively a doubly or triply charged ion. It is of interest to note that hexadecyltributylammonium bromate forms triply charged ions while the corresponding methyl derivatives form doubly charged ions.[4] The tendency of long chain ions to associate at concentrations below the critical depends not only on the length of the hydrocarbon chain, it also depends on the number of carbon atoms in the other substituent alkyl groups.

The critical concentration depends on the size of the substituent alkyl groups as well as on the number of carbon atoms in the long chain. Thus, the critical concentration of octadecyltrimethylammonium bromate is 2.3×10^{-4}, while that of the corresponding amyl derivative is 1.6×10^{-5}. The critical concentration of hexadecyltributylammonium bromate is 3.1×10^{-4}. The addition of six carbon atoms to the three smaller groups has about the same effect on the critical concentration as has the addition of two carbon atoms to the long chain.

Doubtless the long chain ions arrange themselves in some regular order in the micelles. How large groups like the amyl group fit into any structure is somewhat difficult to visualize. However, if van der Waal's forces are concerned in holding the ions together in the micelles, then they must arrange themselves in such manner that the van der Waal's forces of the smaller groups are also involved.

The counter ions interact to form ion pairs with ions in the micellar structure. This is indicated by the fact that, as the substituent groups of the long chain ions become smaller, the equivalent conductance of the micellar electrolyte decreases. So also bromates and iodates exhibit conductance maxima whereas salts of smaller ions do not. The conductance decreases of the micellar electrolyte with increasing concentration can only be ascribed to the bonding of counter ions by the micellar ions. We may infer that the charges of the micellar ions occupy positions at the outer surface of the micelles. What kind of equilibrium exists between the simple, long chain ions and the micellar ions we do not know. However, the results of the present analysis indicate that the concentration of simple long-chain ions remains substantially constant at concentrations above the critical. This, of course, may no longer be true for high salt concentrations.

[1] Evers, E. C., Grieger, P. F., and Kraus, C. A., *J. Am. Chem. Soc.*, **68**, 1137 (1946).
[2] Brown, G. L., Grieger, P. F., and Kraus, C. A., *Ibid.*, **71**, 95 (1949).
[3] McDowell, M. J., and Kraus, C. A., *Ibid.*, **73**, 2173 (1951).
[4] Bair, E. J., and Kraus, C. A., *Ibid.*, **73**, 1129 (1951).

ON THE EFFECT OF PRETWISTING ON BENDING

By Francis D. Murnaghan

Instituto Tecnológico de Aeronáutica, São José dos Campos, Brasil*

Communicated September 30, 1953

It is known[1] that if a thin-walled beam is twisted before being bent the deflection of the beam is not the sum of the deflections due to torsion and bending separately; but, so far as we know, no satisfactory explanation of this fact of experience has yet been given. We propose to show in the present note that, even in the case of a solid circular beam, in order to obtain the sum of the deflections due to torsion and bending separately there must be superimposed on the twisting and bending moments a transverse loading, i.e., a loading perpendicular to the plane of bending, proportional to the square of the distance from the fixed end of the beam. This is a first-order effect which may be explained by means of the classical infinitesimal theory of elasticity. That it has not been pointed out before, in a subject so long studied, must be attributed to the fact that due attention has not been paid to the commonplace that a strain may well be infinitesimal without the deflections being infinitesimal. Thus, in the infinitesimal bending of a moderately long beam, the deflection near the free end may be so large that it cannot be treated as infinitesimal. When a twisted beam is bent the torsion stresses are changed by the deflection in such a way that they no longer have a zero resultant, this resultant being, in fact, perpendicular to the plane of bending and proportional to the square of the distance from the fixed end. Since the familiar theory of the loaded beam tells us that the deflection of a loaded beam, in which the load is proportional to the square of the distance from the fixed end, is a polynomial function of the sixth degree in this distance, it is evident that even for only moderately long beams the effect of pretwisting may be significant. In presenting the mathematical argument we find it convenient to adopt the method we have used when studying finite deformations but we methodically neglect (since the effect we are discussing is a first-order one) all powers higher than the first, and all products, of the strain components.

Denoting by (a, b, c) the initial coordinates of any point of the beam, whose axis we take as the c-axis, and by $\theta = kc$ the angle of twist, the displacement in simple torsion is furnished by the equations

$$x = (\cos\theta)a + (\sin\theta)b;\ y = (-\sin\theta)a + (\cos\theta)b;\ z = c.$$

Here k, the twist per unit length, is infinitesimal so that we neglect its square; nevertheless, $\theta = kc$ is not infinitesimal when c is sufficiently large. Thus the angle of twist of the end of a sufficiently long beam

may well be many radians without the strain failing to be infinitesimal. In superimposing simple bending upon the twisted beam the coordinates (x', y', z') of the point whose coordinates before the bending were (x, y, z), and before the torsion were (a, b, c), are furnished by the equations

$$x' = x + \frac{1}{2R}(z^2 + \sigma x^2 - \sigma y^2);\ y' = y + \frac{\sigma}{R}xy;\ z' = z - \frac{1}{R}xz$$

where σ is Poisson's ratio and R is the radius of curvature of the axis of the beam at the origin. Upon eliminating (x, y, z) and then dropping the primes we see that the deflection due to superposing simple bending on simple torsion is furnished by the equations

$$x = (\cos\theta)a + (\sin\theta)b + \frac{1}{2R}c^2 + \frac{\sigma}{2R}\{(\cos 2\theta)(a^2 - b^2) + (\sin 2\theta)2ab\}$$

$$y = (-\sin\theta)a + (\cos\theta)b + \frac{\sigma}{2R}\{-(\sin 2\theta)(a^2 - b^2) + (\cos 2\theta)2ab\}$$

$$z = c - \frac{c}{R}\{(\cos\theta)a + (\sin\theta)b\}.$$

The quantities a/R, b/R, c/R are assumed to be infinitesimal but the term $c^2/2R$ which appears in the formula for x may well be so large, even for only moderately long beams, that it cannot be regarded as infinitesimal despite the fact that the strain is infinitesimal; exactly as, in torsion, the product $\theta = kc$ of the infinitesimal k by c is not infinitesimal so, in bending, the product $c^2/2R$ of the infinitesimal c/R by $c/2$ is not infinitesimal. In order to compute the strain matrix η we first calculate the Jacobian matrix J of x, y, z with respect to a, b, c; then η is one-half the result of subtracting the unit matrix from J^*J where J^* denotes the transpose of J. In forming the product J^*J we systematically neglect all squares and products of the infinitesimals $k, a/R, b/R, c/R$. We obtain

$$J = \begin{bmatrix} \cos\theta & \sin\theta & \\ +\frac{\sigma}{R}\{(\cos 2\theta)a + (\sin 2\theta)b\} & -\frac{\sigma}{R}\{(\cos 2\theta)b - (\sin 2\theta)a\} & ky + \frac{c}{R} \\ -\sin\theta & \cos\theta & \\ +\frac{\sigma}{R}\{-(\sin 2\theta)a + (\cos 2\theta)b\} & +\frac{\sigma}{R}\{(\sin 2\theta)b + (\cos 2\theta)a\} & -kx \\ -\frac{c}{R}\cos\theta & -\frac{c}{R}\sin\theta & 1 - \frac{1}{R}\{(\cos\theta)a + (\sin\theta)b\} \end{bmatrix}$$

$$\eta = \begin{bmatrix} \frac{\sigma}{R}\{(\cos\theta)a + (\sin\theta)b\} & 0 & \frac{1}{2}k\left\{b + \frac{c^2}{2R}\sin\theta\right\} \\ 0 & \frac{\sigma}{R}\{(\cos\theta)a + (\sin\theta)b\} & -\frac{1}{2}k\left\{a + \frac{c^2}{2R}\cos\theta\right\} \\ \frac{1}{2}k\left\{b + \frac{c^2}{2R}\sin\theta\right\} & -\frac{1}{2}k\left\{a + \frac{c^2}{2R}\cos\theta\right\} & -\frac{1}{R}\{(\cos\theta)a + (\sin\theta)b\} \end{bmatrix}.$$

Thus the first invariant I_1 of strain, i.e., the sum of the diagonal elements of η, is $\frac{(2\sigma - 1)}{R}\{(\cos\theta)a + (\sin\theta)b\}$ so that

$$\lambda I_1 + 2\mu\eta = \begin{bmatrix} 0 & 0 & \mu k\left\{b + \frac{c^2}{2R}\sin\theta\right\} \\ 0 & 0 & -\mu k\left\{a + \frac{c^2}{2R}\cos\theta\right\} \\ \mu k\left\{b + \frac{c^2}{2R}\sin\theta\right\} & -\mu k\left\{a + \frac{c^2}{2R}\cos\theta\right\} & -\frac{E}{R}\{(\cos\theta)a + (\sin\theta)b\} \end{bmatrix}$$

where $E = \frac{\mu(3\lambda + 2\mu)}{\lambda + \mu}$ is Young's modulus. When we drop first order infinitesimals in J it reduces to a rotation matrix R and the stress matrix is furnished by the formula $T = R(\lambda I_1 + 2\mu\eta)R^*$.

$$R = \begin{bmatrix} \cos\theta & \sin\theta & 0 \\ -\sin\theta & \cos\theta & 0 \\ 0 & 0 & 1 \end{bmatrix}$$

and we obtain

$$T = \begin{bmatrix} 0 & 0 & k\mu\{(\cos\theta)b - (\sin\theta)a\} \\ 0 & 0 & -k\mu\left\{(\sin\theta)b + (\cos\theta)a + \frac{c^2}{2R}\right\} \\ k\mu\{(\cos\theta)b - (\sin\theta)a\} & -k\mu\left\{(\sin\theta)b + (\cos\theta)a + \frac{c^2}{2R}\right\} & -\frac{E}{R}\{(\cos\theta)a + (\sin\theta)b\} \end{bmatrix}.$$

The coordinates of the force per unit area acting on an element perpendicular to the z-axis are furnished by the last column of T. In computing the total force over the end of the beam we may take the coordinates of the element of area to be (0, 0, $dadb$) since they differ from these by infinitesimals and the force per unit area is infinitesimal. Thus the resultant force has a non-zero second coordinate, namely, $-(k\mu c^2 A/2R)$ where A is the cross-sectional area. When this loading is not supplied, the deflection of the beam, under combined twisting and bending, is the sum of three parts: (1) the deflection due to simple torsion; (2) the deflection due to simple bending; (3) the deflection due to a load $k\mu c^2 A/2R$ in the direction of the b-axis, i.e., perpendicular to the plane of bending.

* Present address, 6202 Sycamore Road, Baltimore 12, Md.

[1] den Hartog, J. P., *Advanced Strength of Materials*, McGraw-Hill Book Co., 1952, p. 319.

THE EFFECT OF GENERATION TIME ON THE DELAYED APPEARANCE OF INDUCED MUTANTS IN ESCHERICHIA COLI*

BY EDGAR L. LABRUM†

DEPARTMENT OF GENETICS, CARNEGIE INSTITUTION OF WASHINGTON, COLD SPRING HARBOR, NEW YORK

Communicated by M. Demerec, October 21, 1953

When mutations are induced in *Eshcerichia coli* by radiations or chemical mutagens, a number of cell divisions must occur before the total yield of induced mutations will be manifested. This delay in appearance of induced mutants in *E. coli* has been demonstrated for genetic changes leading to phage-T1 resistance[1, 2] and to streptomycin resistance[3, 4] for reversions to non-deficiency in auxotrophic strains,[5] and for reversions to non-dependence in streptomycin-dependent strains.[6] The delayed effect therefore seems to be a wide-spread phenomenon associated with the various induced-mutation systems in *E. coli* that have so far been studied quantitatively. The investigations of Demerec and Cahn[5] suggested that the pattern of delayed appearance of induced mutants—that is, the number of generations required for total manifestation—is determined by the particular genetic locus involved and is unaffected by the kind of mutagenic agent used. The recent studies of Witkin[2] with ultraviolet-induced mutations to T1 resistance in *E. coli* B/r demonstrated that incubation of the cells at 16°C. after irradiation resulted in a greatly reduced total yield of induced mutants, as compared with the total yield obtained with 37° incubation. The number of generations required for manifestation of all induced mutants was the same, however, at the two temperatures. This finding suggested an intimate relationship between cell division and the delayed appearance of induced mutants.

The work of Novick and Szilard[7] with the chemostat showed that the rate of spontaneous mutation to phage-T5 resistance in the B/1t/f strain of *E. coli* was independent of the rate of cell division. This finding and Witkin's observations led us to investigate the pattern of delayed appearance in bacterial populations maintained at different generation times but at the same temperature after treatment with a mutagenic agent.

In these experiments the division rate of cells was varied by two different methods: the use of chemostats, and the use of two different solid media. The tryptophan-requiring strain B/1t/f of *E. coli*[7] was used throughout the investigation. The mutation system studied was the change from sensitivity to resistance to coliphage T5. Manganous chloride was the mutagen employed in all experiments.

Experiments with the Chemostat.—The chemostats used in these studies

were the same in design as that described by Novick and Szilard.[8] A synthetic lactate medium was used and tryptophan was the controlling growth factor, in a concentration of 1 μg. per ml. for all chemostat experiments. Cultures of B/1t/f were grown in nutrient broth with aeration and treated with the mutagenic chemical manganous chloride. After treatment, the cells were centrifuged and resuspended in liquid lactate medium. This suspension was the inoculum for the chemostats. Each of three chemostats was inoculated with a number of treated cells approximately equal to the

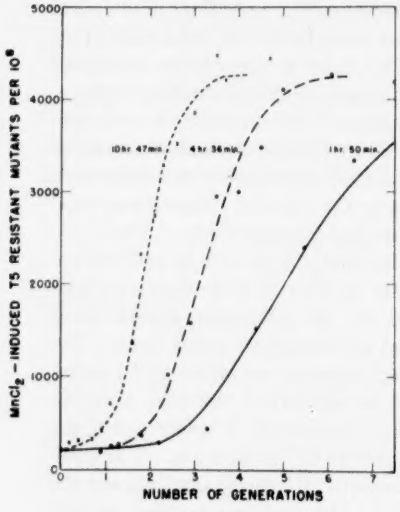

FIGURE 1

Effect of generation time on the rate of delayed appearance of $MnCl_2$-induced T5-resistant mutants, as a function of generations. The generation times of three populations of *E. coli* strain B/1t/f grown in chemostats are indicated on the respective curves.

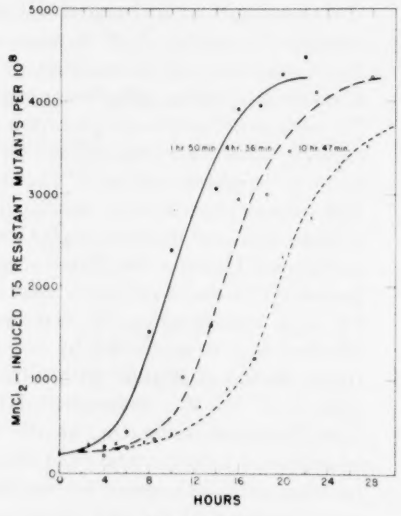

FIGURE 2

Effect of generation time on the rate of delayed appearance of $MnCl_2$-induced T5-resistant mutants, as a function of time. The generation times of three populations of *E. coli* strain B/1t/f grown in chemostats are indicated on the respective curves.

total cell concentration which the chemostat was able to maintain when in operation. Since the cells were in a resting stage at the time of inoculation, they were incubated with aeration in the growth tube of the chemostat for a period equal to the length of the lag phase, which was approximately 10 hours under these conditions. At the end of that time the chemostats were set in operation by starting the flow of medium from the storage tanks into the growth tubes. The rates of flow of the medium were adjusted so that the bacteria in the three populations were dividing at dif-

ferent rates. At frequent intervals samples were taken from each population and analyzed, by the usual plating techniques, for number of viable cells per ml. and for frequency of T5-resistant mutants. Three experiments were performed at different times, with essentially the same results. No correction was necessary for spontaneous mutations, since they did not contribute significantly to the observed increase in mutant frequency during the time required for these experiments.

In figure 1 the results of a typical experiment are presented graphically. The frequencies of $MnCl_2$-induced T5-resistant mutants in each of the three populations are plotted arithmetically as a function of generations. The initial portion of each curve represents a period during which the induced mutants appeared at a low but gradually increasing rate. This was followed by a period during which the bulk of induced mutants appeared at a linear rate until the total yield of mutants was approached. From a comparison of the slopes of the linear portions of the three curves it is evident that the rate of appearance of induced mutants was highest in the population that had the longest generation time (10 hrs. 47 min.) and lowest in the population with the shortest generation time (1 hr. 50 min.).

In figure 2 the data from the same experiment are plotted as a function of time. In this case it can be seen that the rates of appearance of induced mutants are approximately the same throughout the linear portions of the three curves. The fact that the three curves do not coincide is due to differences in length of the initial periods characterized by low rate of appearance.

Experiments with Solid Media.—The phage-spraying technique developed by Demerec[1] has proved to be an invaluable method for the study of delayed appearance of induced mutants in *E. coli*. Therefore experiments were designed with a view to confirming the essential findings of the chemostat studies by use of the spray technique. The same B/1t/f strain was used, and T5-resistant clones were scored.

The method consisted of plating a known number of $MnCl_2$-treated cell onto six plates of a solid medium. After a suitable incubation period, which allowed the cells to accomplish a certain number of divisions, growth was stopped by chilling the plates. Two of the six plates were washed with 10 ml. of saline, and the wash fluid was plated out quantitatively to determine the total number of cells per plate. The other four plates were sprayed with an aerosol of a suspension of phage T5 to determine the number of T5-resistant mutant clones.

The generation time was varied by plating the $MnCl_2$-treated cells onto two different kinds of solid medium. One was nutrient agar supplemented with 1% dextrose; the other was the same synthetic lactate medium used in the chemostat experiments with the addition of 1.5% agar and tryptophan in a concentration of 20 μg. per ml. The generation times of strain B/1t/f

on the two media were 18 minutes and 55 minutes, respectively. The temperature for all incubation periods was 37°C. Curves representing the rate of appearance of spontaneous mutants as a function of generations were determined by the spray techniques for cells dividing on the two different media. These curves were used to correct values obtained by scoring T5-resistant clones on the plates spread with $MnCl_2$-treated bacteria.

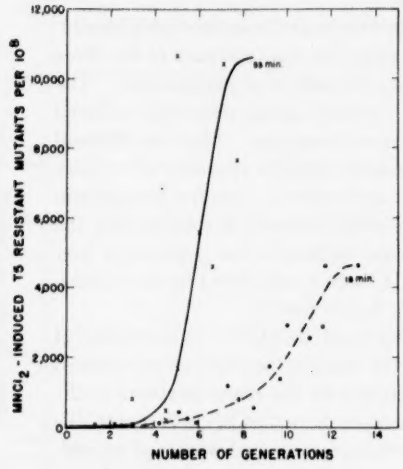

FIGURE 3

Effect of generation time on the rate of delayed appearance of $MnCl_2$-induced T5-resistant mutants, as a function of generations. The solid line represents frequencies of induced mutants among cells of strain B/1t/f of *E. coli* grown on solid synthetic lactate medium; the broken line, frequencies among cells grown on nutrient agar plus 1% dextrose. Generation times of the bacteria on the two media are indicated.

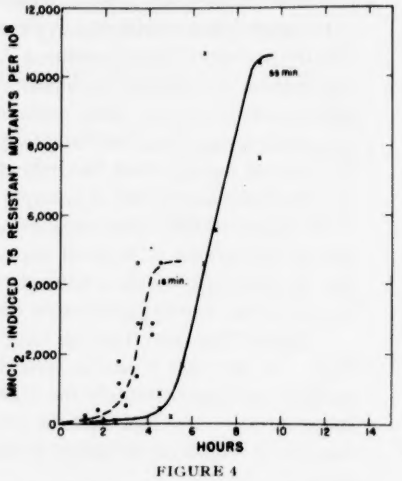

FIGURE 4

Effect of generation time on the rate of delayed appearance of $MnCl_2$-induced T5-resistant mutants, as a function of time. The solid line represents frequencies of induced mutants among cells of strain B/1t/f grown on solid synthetic lactate medium; the broken line, frequencies among cells grown on nutrient agar plus 1% dextrose. Generation times of the bacteria on the two media are indicated.

In figure 3 the frequencies of T5-resistant clones per 10^8 viable bacteria plated are plotted arithmetically as a function of generations. The resulting curves show the same general characteristics as those representing the data of the chemostat experiments (Fig. 1); they demonstrate an initial low rate of appearance of induced mutants, followed by an increased rate that appears to be linear until it approaches total manifestation. The slopes of the linear portions of the curves are not the same, indicating that the rates of appearance of induced mutants per cell per generation were different on the two media.

In figure 4 the same data are plotted as a function of absolute time. The length of the lag phase, which was $1\frac{1}{2}$ hours on nutrient agar plus dextrose and 2 hours on lactate agar, was deducted from all plotted times. The resulting curves are again comparable to those obtained in the chemostat experiments (Fig. 2), in that they show a constant rate of appearance of induced mutants per unit time during the period represented by the linear portions of the curves.

The use of two different media to obtain different generation times introduced into these experiments another variable—namely, nutrition—which there is no reason to suspect was present in the chemostat studies. The relation between pattern of delayed appearance and generation time on the two different media, however, was qualitatively what had been predicted on the basis of the results obtained in the chemostat experiments. The nature of the nutrient medium seemed to have a more pronounced effect on total number of mutants manifested than on rate of appearance of induced mutants.

Investigation of the Delayed Onset of Division.—It has been suggested that irregularity in the time of onset of division of individual bacterial cells may play a role in the delayed appearance of induced mutants.[4, 9] An experiment suggested by Dr. Aaron Novick was performed to gain more information about this point.

$MnCl_2$-treated B/lt/f cells were inoculated into a flask of sterile, liquid lactate medium supplemented with tryptophan (20 μg. per ml.), so that there was approximately 1 cell per 3 ml. of medium. One ml. of the inoculated medium was dispensed into each of 295 glass tubes, which were then incubated for 20 hours. After the incubation period a pour plate with nutrient agar was prepared from the contents of each tube, and the plates were incubated for 48 hours. At the end of that time there were 201 plates without colonies and 94 plates with one or more colonies. Thus it was probable that most of the cultures showing growth had started from a single cell. On the basis of colony counts, the cultures were grouped according to the approximate number of divisions accomplished in each (table 1).

TABLE 1

DISTRIBUTION OF SINGLE-CELL CULTURES ACCORDING TO NUMBER OF DIVISIONS ACCOMPLISHED IN 20 HOURS IN LIQUID LACTATE MEDIUM

Generations	0	1	2	3	4	5	6	7	8	9	10	11	12
No. of cultures	6	3	1	0	2	3	4	7	22	15	18	10	3

Since the lag phase for B/lt/f in liquid lactate had previously been found to be about 10 hours, and the generation time 1 hour, the predicted number of generations after a 20-hour incubation period was ten. The results shown in the table indicate that about 72% of the cultures had passed through eight to twelve generations. In other words, a majority of the

cells had begun to divide at the expected time plus or minus 2 hours. The possible significance of these observations with regard to the delayed appearance of induced mutants will be discussed in the following section.

Conclusions and Discussion.—From the results of this investigation it was concluded that, regardless of the length of the generation time, the pattern of delayed appearance of induced T5-resistant mutants in strain B/lt/f of *E. coli* is characterized by two distinct phases. The first occurs during the early cell divisions, when the rate of appearance of induced mutants is low but increases gradually. It is followed by a second phase, throughout which induced mutants appear at a high linear rate that is constant per unit time. The linear rate per cell per generation increases with increase in the length of the generation time. The data did not show this increase in rate of appearance to be directly proportional to increase in generation time.

The experiments in which $MnCl_2$-treated cells were allowed to divide on two different solid media before application of phage showed that the pattern of delayed appearance can vary greatly in the same mutation system depending on the type of medium used; approximately twelve generations were required to achieve total manifestation of induced mutants on nutrient agar plus 1% dextrose, but only seven generations on lactate agar. This effect must be considered when one compares patterns of delayed appearance obtained by plating cells on a synthetic medium with patterns determined by plating on a complex organic medium, where there may be a two- or threefold difference in generation time.

The experiment in which the extent of irregularity in the time of onset of division was determined for $MnCl_2$-treated cells grown in liquid lactate medium showed that a majority of the cells began to divide within two hours, more or less, of the expected time. The number of divisions accomplished by a majority of the cells therefore extended over a range of four generations. The conditions of this experiment were not strictly comparable with those of either the chemostat studies or the experiments using solid media. Nevertheless, it seems unlikely that irregularity in onset of division is a determining factor in the initial phase of delayed appearance, during which induced mutants appear at a low rate. The second phase, however, during which the bulk of induced mutants is manifested at a linear rate, may possibly be accounted for by the range in number of divisions completed by a majority of cells. Further investigations are necessary to define more clearly the extent to which irregular onset of division is involved in the delayed appearance of induced mutants under specific experimental conditions. In the light of these results it is conceivable that the initial low rate at which induced mutants appear represents a true genetic delay in the manifestation of induced mutations, and that the extent of this delay depends at least partly on cell division and the length of the generation time.

Summary.—The patterns of delayed appearance of $MnCl_2$-induced T5-resistant mutants were determined in strain B/lt/f of *E. coli*, grown with various generation times at a constant temperature. The division rate of cells was varied by growing them in chemostats and also by using the phage-spray technique to detect mutant clones among cells grown on two different solid media. It was concluded that, regardless of generation time, the delayed appearance of induced T5-resistant mutants is characterized by an initial phase, during the early cell divisions, when the mutants appear at a low but gradually increasing rate. This is followed by a second phase, throughout which mutants appear at a high linear rate that is constant per unit time. An investigation of the extent of irregularity in the time of onset of division of individual bacterial cells led to the view that such irregularity is not a determining factor in the initial low rate of appearance of induced mutants, but that it may possibly play a role in the second phase, during which induced mutants appear at a high linear rate.

Acknowledgments.—The author is grateful to Drs. M. Demerec, E. M. Witkin, and A. M. M. Berrie for their continuous interest and many helpful discussions during the course of these investigations.

* This study was supported in part by a grant-in-aid from the American Cancer Society upon recommendation of the Committee on Growth of the National Research Council.

† Present address: The Sloan-Kettering Institute, 444 East 68th Street, New York 21, N. Y.

[1] Demerec, M., PROC. NATL. ACAD. SCI., **32,** 36 (1946).
[2] Witkin, E. M., *Ibid.*, **39,** 427 (1953).
[3] Demerec, M., *Genetics*, **36,** 585 (1951).
[4] Newcombe, H. B., *Ibid.*, **38,** 134 (1953).
[5] Demerec, M., and Cahn, E., *J. Bact.*, **65,** 27 (1953).
[6] Labrum, E. L., PROC. NATL. ACAD. SCI., **39,** 280 (1953).
[7] Novick, A., and Szilard, L., *Ibid.*, **36,** 708 (1950).
[8] Novick, A., and Szilard, L., *Cold Spring Harbor Symp. Quant. Biol.*, **16,** 337 (1951).
[9] Newcombe, H. B., and Scott, G. W., *Genetics*, **34,** 475 (1949).

THE RELATIONSHIP BETWEEN KAPPA AND PARAMECIN IN PARAMECIUM AURELIA*

BY JOHN R. PREER, JR., RICHARD W. SIEGEL, AND PEARL S. STARK

ZOOLOGICAL LABORATORY, UNIVERSITY OF PENNSYLVANIA

Communicated by David R. Goddard, October 2, 1953

Three types of genetic cytoplasmic particles, similar in number per animal and staining reactions, have been described in *Paramecium aurelia*. They are designated by the Greek symbols kappa, mu, and pi, and are characterized as follows.

Kappa particles are distinguished by the fact that animals containing them are "killers," for they produce a toxin called "paramecin." This toxin causes death to "sensitive" paramecia. Both the culture medium and breis from killer animals contain paramecin. Kappa was at first described and studied only by genetic techniques[1, 2] and it was not until later that cytological techniques[3] identified kappa with microscopically visible Feulgen-positive bodies. Each killer strain produces a characteristic paramecin (distinguished by the prelethal responses elicited from sensitives) and mutations of kappa have been recognized by changes in paramecin production.[4] Although much data concerned with the genetic, physiological, and chemical nature of kappa and paramecin are available,[5] the relationship between the two has remained obscure.

Mu particles are characterized by the fact that animals containing them are "mate-killers" and cause the death of their sensitive mates following conjugation.[6] Although mate-killers may produce toxins, these are unlike paramecin in that they are not detectable either in breis of mate-killers or in the culture fluid in which mate-killers have lived.[7]

Pi bodies are distinguished by the fact that they are not associated with any demonstrable lethal effect. They were first found cytologically by Hanson[8] in a strain which had once been a killer, and are probably kappa mutants. Of chief interest here is the fact that neither mu nor pi bodies are associated with paramecin production.

Recent studies[9] with the phase microscope revealed that kappa bodies from any killer paramecium are of two major types: "brights" and "non-brights." Brights contain one or two characteristic refractile regions while non-brights do not. Our first clue as to the identity of paramecin was provided by a comparative study of kappa, mu, and pi bodies. Brights occur only in animals producing paramecin. The present communication presents this and other evidence indicating that brights are the bearers of paramecin activity.

Materials.—The following strains of *P. aurelia* were used. Killer stocks G, H, 36, and 50 belong to variety 2 and have been previously described.[2]

Gm1 is a mutant killer derived from stock G.[2] Killer stocks 47,[10] 51,[10] 116,[11], and 169[11] belong to variety 4.

Stocks 130, 131, and 138 belong to variety 8 and are mate-killers.[11]

Dippell[4] has isolated mutant killers from stock 51 and shown that they contain mutant kappas. We have used two strains, 51ml and 51m5, previously described by her, and two, "derived" 51ml and "derived" 51m5, which she has isolated more recently from other mutants (Dippell, personal communication). When these four strains were tested for killing in this laboratory it was found that three of them (51ml, 51m5, and "derived" 51m5) had lost the ability to kill. However, cytological examination revealed that these contain kappa-like cytoplasmic bodies. These bodies thus appear to be similar to the pi bodies discovered by Hanson. They probably represent kappa mutants, each having arisen independently from the kappa in Dippell's strains after they were first isolated by her as mutant killers.

A strain of *P. caudatum*, stock 79a,[3] was used to test the paramecin activity of stock G.

Methods.—The standard methods described[12] for the study of *P. aurelia* were used. Cytoplasmic particles were observed in unfixed material with the phase-contrast microscope after the paramecia had been crushed.[9] The preparation of stained material will be described below.

To compare the mobility of paramecin with kappa and trichocysts in centrifugal fields, breis of killers were centrifuged. To prepare such breis, stock G killers were filtered through 16 layers of cheesecloth and concentrated by centrifugation. Most of the bacteria in the concentrate were removed by suspending and recentrifuging the cells three times in an excess of 0.25% sterile yeast extract. To permit the digestion of many of the bacteria present in food vacuoles, the paramecia were allowed to remain for one to two hours at 27°C. in the yeast medium. The animals were suspended and concentrated as before, transferred to 10% amphibian Ringer's solution, and homogenized with the aid of a syringe. Centrifuge tubes were made from glass tubing (with an inside diameter of 5 mm.), one end of which was fused. One-ml. samples of the brei containing approximately 5×10^4 broken paramecia were centrifuged in a horizontal centrifuge for ten minutes at various speeds. Then the top 0.9 ml. of each brei, the "supernatants," were carefully removed from the tubes leaving as the "precipitates" the bottom 0.1 ml. The amount of paramecin in the supernates and precipitates was determined by recording the number of affected sensitives in serial dilutions (made in 10% Ringer's). That dilution which affected about 25 of 200 stock 79a sensitives after 24 hours at 27°C. was considered the end-point. From a comparison of the end-points of the supernate and precipitate at a given centrifuge speed, the "per cent down" or the amount of paramecin which moved from the top 0.9 ml. to the bottom

0.1 ml. of the centrifuge tube was calculated. There was no evidence of paramecin inactivation due to centrifugation. As a control, breis from sensitives of stock G (these produce no paramecin) were prepared and centrifuged as described above. No killing activity was detected among the controls.

To determine the mobility of kappa and trichocysts, 0.0025-ml. samples of supernate and precipitate (or suitable dilutions of them) were carefully spread on 1 cm.^{2} areas of glass slides. The preparations were air dried, stained for one minute in 0.25% aqueous gentian violet, and examined under oil immersion. The stained kappa bodies and trichocysts in 10 to 40 microscope fields were counted and the average number per field was used to calculate the per cent down. As before, the centrifugation did not reduce

TABLE 1

THE OCCURRENCE OF "BRIGHTS" AMONG STRAINS OF *P. aurelia* CONTAINING KAPPA, MU, AND PI

VARIETY	STRAIN	RESPONSE OF SENSITIVES	CYTOPLASMIC PARTICLES	
			DESIGNATION	BRIGHTS
2	G	Spinning	Kappa	Present
	Gm1	Paralysis	Kappa	Present
	H	Vacuolization	Kappa	Present
	36	Spinning and vacuolization	Kappa	Present
	50	Spinning and vacuolization	Kappa	Present
4	47	Humping	Kappa	Present
	51	Humping	Kappa	Present
	51m1	None	Pi	Absent
	De 51m1	Spinning	Kappa	Present
	51m5	None	Pi	Absent
	De 51m5	None	Pi	Absent
	116	Humping	Kappa	Present
	169	Humping	Kappa	Present
8	130	Mate-killing	Mu	Absent
	131	Mate-killing	Mu	Absent
	138	Mate-killing	Mu	Absent

the total numbers of particles. Stained samples of control breis (prepared from stock G sensitives) contained trichocysts but did not reveal significant numbers of stained bodies which could be confused with kappa.

Results.—Samples of the stocks described above and their mutants were maintained at 0.2 to 0.5 fission per day at 27°C. for two to eight weeks and then the particles present in each were observed with the phase-contrast microscope. Paramecia from each of the ten killer strains were always found to contain brights, the per cent brights among all particles varying from 4 to 30%. Paramecia from the six strains containing mu or pi bodies have never contained brights. These data are summarized in table 1. Hanson's[8] finding that two pi-bearing cultures of independent origin are free of brights confirms and extends these observations.

These results led to the hypothesis that the particle with paramecin activity is the bright particle. A test of the hypothesis was suggested by the preliminary experiments of the senior author which indicated that the centrifugal mobility of brights was very similar to that of paramecin. Consequently, a careful comparison of the mobility of paramecin, brights, and total stainable bodies was undertaken. Stock G was selected as a representative killer because its brights are easily distinguished from non-brights and from bacteria in stained breis. Killer breis were prepared, centrifuged, and assayed as described above.

The mobility of paramecin is graphically represented in figure 1. The smooth curve was obtained by fitting a curve of the form $Y = 1 - e^{-ax}$ to the data by least squares. This equation has no theoretical significance and was chosen only because it was found empirically to fit the data. The points for the sum of brights and non-brights were found to lie well below the curve for paramecin as can be seen in figure 2. But when the brights alone were scored, it was found that the resulting points (also shown in figure 2) approximated very well the paramecin curve.

An attempt was made to study the sedimentation rates of other particulates present in breis. This was done in the case of trichocysts. Undischarged trichocysts were more mobile and discharged trichocysts were less mobile than paramecin.

Discussion.—The presence of brights in ten strains which produce paramecin and the absence of brights in eight strains which do not produce paramecin, clearly indicates a relationship between brights and paramecin. The extremely good agreement between the data for brights and paramecin in respect to centrifugal mobility leaves little doubt that the bright particle is the particulate in breis which carries paramecin activity.

This conclusion is in agreement with the findings that paramecin and brights both contain desoxyribose nucleic acid[3, 9, 13] and that paramecin particles in breis are never more numerous than brights.[14]

Nanney[15] has studied the relationship between kappa and paramecin using x-radiation, and has reached conclusions compatible with ours. His data indicate that, although the two are not identical, kappa and paramecin activities could be associated with the same particle.

It has been shown that the number of genetic kappa particles is approximately equal to the number of visible cytoplasmic bodies in a killer and these bodies have been established as kappa.[3] The interpretation of these numerical data is not quite so clear when one realizes that the cytologically visible bodies actually are made up of two categories—brights and non-brights. If the agreement in the numbers of kappa particles and visible bodies were sufficiently precise, one would have to conclude that brights and non-brights are both kappa. But since brights are present in rather low frequency, one can only be sure that non-brights represent kappa par-

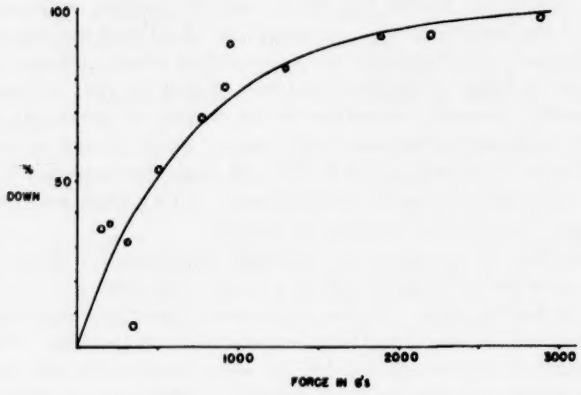

FIGURE 1

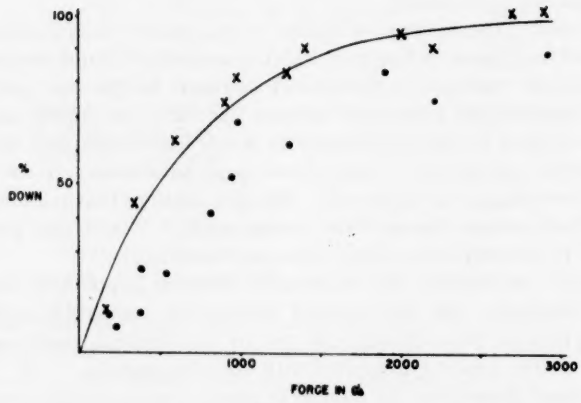

FIGURE 2

Figs. 1 and 2. Comparison of the sedimentation rates of paramecin, kappa, and brights. The per cent particles centrifuged down by different centrifugal forces is plotted.

In figure 1, paramecin is represented by open circles. The smooth curve is of the form $Y = 1 - e^{-ax}$ and was fitted to the points by least squares. In figure 2, kappa (brights plus non-brights) is represented by solid circles and brights are represented by x's. The smooth curve represents paramecin and is the same as the one shown in figure 1.

ticles. If paramecin particles are brights, and since kappa is responsible for the production of paramecin, it follows that non-brights must be responsible for the production of brights.

It is thus clear that mutations of kappa to pi involve a loss of the capacity to *produce* brights. Similarly, mu bodies might represent mutant kappas, although the possibility of an independent origin cannot be excluded.

The question of whether brights are capable of producing new particles has not been answered. Double non-brights have been interpreted as stages in the division of non-brights.[9] If brights can produce new particles then one might expect to find brights which are double in appearance. Actually they are found occasionally, one of the two portions having a refractile area, the other usually without the refractile area.

Attempts to stain the refractile bodies in brights have been unsuccessful and the chemical nature of the structure is unknown. It has been suggested that if kappa is a bacterial symbiont, the refractile bodies may be endospores, but it is noted that bacterial spore stains are negative.[9] Delamater (personal communication) and Sonneborn (unpublished) suggested the possibility that the refractile body may be a virus or viral inclusion body, but there is no pertinent evidence at this time.

Summary.—A small proportion of the cytoplasmic bodies which have been identified with kappa in *P. aurelia* contain one or more refractile regions. Bodies with these regions are called brights. Only those strains which produce the toxin paramecin contain brights. Although animals of other strains unable to produce paramecin may contain kappa-like cytoplasmic bodies, they lack brights. The sedimentation rates of paramecin and brights are indistinguishable, while the sedimentation rate of non-bright kappa is different. It is concluded that brights are the bearers of paramecin activity and that they are produced by non-bright kappas.

* Work aided by grants from Phi Beta Psi Sorority and National Science Foundation.

[1] Sonneborn, T. M., PROC. NATL. ACAD. SCI., **29,** 329–343 (1943).
[2] Preer, J. R., *Genetics,* **33,** 349–404 (1948).
[3] Preer, J. R., *Ibid.,* **35,** 344–362 (1950).
[4] Dippell, R. V., *Heredity,* **4,** 165–187 (1950).
[5] Sonneborn, T. M., *Am. Nat.,* **82,** 26–34 (1948).
[6] Siegel, R. W., *Genetics;* (in press).
[7] Siegel, R. W., *Physiol. Zool.;* (in press).
[8] Hanson, E. D., *Genetics;* (in press).
[9] Preer, J. R., and Stark, P. S., *Exp. Cell Res.* (1953); (in press).
[10] Sonneborn, T. M., and Dippell, R. V., *Biol. Bull.,* **85,** 36–43 (1943).
[11] Levine, M., *Evolution;* (in press).
[12] Sonneborn, T. M., *J. Exptl. Zool.,* **113,** 87–148 (1950).
[13] van Wagtendonk, W. J., *J. Biol. Chem.,* **173,** 691–704 (1948).
[14] Preer, J. R., and Siegel, R. W.; (unpublished).
[15] Nanney, D. L., *Physiol. Zool.;* (in press).

CROSS REACTIVATION OF GENETIC LOCI OF T2 BACTERIOPHAGE AFTER DECAY OF INCORPORATED RADIOACTIVE PHOSPHORUS

By Gunther S. Stent

Virus Laboratory, University of California, Berkeley

Communicated by W. M. Stanley, October 26, 1953

Bacteriophages containing radiophosphorus P^{32} of high specific activity in their desoxyribonucleic acid (DNA) are unstable, i.e., from day to day a progressively decreasing fraction of the initial phage population is still able to form plaques when plated on a sensitive bacterial strain.[1] The cause of death appears to be some direct, short-range effect of the disintegration of a phosphorus atom in the DNA chain, and not the β-radiation attending this radioactive decay.[1, 2] It is the purpose of this communication to show that an appreciable fraction of P^{32} disintegrations destroying the plaque-forming ability of T2 bacteriophage leave the particle still able to donate some but not all of its genetic characters to the progeny of a mixed infection with an undamaged, non-radioactive phage.

Materials and Methods.—Coliphage T2 (wild type), its mutant T2hr_1 (h and r_1 unlinked[3]) and its host *Escherichia coli*, strains B(H) and B(H)/2, obtained from Dr. A. D. Hershey, were employed in this study. When assayed on agar plates seeded with a 1:1 mixture of 24 hr cultures of the two indicator strains, T2h^+r^+ make small, turbid and T2hr large, clear plaques. Their recombinants T2hr^+ and T2h^+r make small, clear and large, turbid plaques, respectively. The genotype spectrum of phages issuing from a mixedly infected bacterium plated before burst can be recognized according to the following schema:

If the bacterium yields the allele combination	h,r or h,h^+r	h,r^+ or h,h^+,r^+	h,r,r^+ or h,h^+,r,r^+	h^+,r	h^+,r^+	h^+,r,r^+
then its plaque type will be	large and clear	small and clear	mottled and clear	large and turbid	small and turbid	mottled and turbid

When our stock of T2 wild type was plated on the mixed indicators, a background of no hr, one h^+r and 10 hr^+ plaques were found among 6000 plaques inspected.

P^{32}-unstable T2 phage was grown according to a modification of the technique of Hershey, Kamen, Kennedy and Gest,[1] to be published in detail elsewhere. Radiophosphorus of high specific activity was obtained from the Isotopes Division, Atomic Energy Research Establishment, Ministry of Supply, Harwell, England.

Phage development in infected bacteria was arrested reversibly by quick-freezing and storage in liquid nitrogen at −196°C. in a glycerol-casamino acid medium devised by Fraser.[4] The fraction of infective centers recovered after thawing is near 0.4 and independent of the length of time of storage.[2]

Experimental: Cross Reactivation of Free Phage.—It was discovered by Luria[5] that bacteriophages whose plaque forming ability, i.e., capacity for independent reproduction, has been destroyed by irradiation with ultraviolet light (UV) can, under certain circumstances, still participate in the reproductive processes occurring within the infected cell. One such phenomenon is *cross reactivation:* if a bacterium is mixedly infected with UV-inactivated and with active phage, differing from each other in their genetic properties, then the markers of the inactive phage appear among the progeny issuing from such a cross. Watson[6] later observed that cross reactivation also occurs with phages inactivated by x-rays. Recently, Doermann[7] has found that only part of the genetic material of X-ray inactivated bacteriophage may participate in cross reactivation and that the ability of different genetic loci of such particles to reappear is eliminated separately by the irradiation.

TABLE 1

CROSS REACTIVATION OF P^{32}-INACTIVATED T2*hr* PHAGE WITH ACTIVE T2h^+r^+

TUBE CONTAINS	TITER OF INFECTED BACTERIA PER ML. YIELDING: EITHER *h* OR *r* OR BOTH	h^+ AND r^+
High P^{32}-T2*hr* + bacteria	1×10^6	0
T2h^+r^+ + bacteria	$<10^5$	8.7×10^7
High P^{32}-T2*hr* + T2h^+r^+ + bacteria	1.2×10^6	5.6×10^7

T2 bacteriophage, inactivated by decay of P^{32} incorporated in its DNA is likewise capable of being cross reactivated. To demonstrate this reactivation, a stock of radioactive T2*hr* was prepared and decay of the free phage was permitted to progress to 0.0005 of its original titer. Bacteria were then mixedly infected at a multiplicity of two each with this inactivated stock of T2*hr* and a non-radioactive stock of T2h^+r^+ and plated before burst on mixed bacterial indicators B + B/2. The different plaque types formed by the infected bacteria were scored separately, according to the schema outlined above, to determine the titer of infective centers liberating any of the alleles of the inactivated T2*hr* stock. In two control tubes bacteria were infected under otherwise identical conditions with either only the inactivated T2*hr* or only the active T2h^+r^+ stock.

The result of this experiment is presented in table 1, where the number of bacteria yielding in mixed infection with T2h^+r^+ one or both of the marker loci of the inactive T2*hr* have been listed and compared with the number of bacteria yielding T2*hr* in the absence of the non-radioactive T2h^+r^+. It

is seen that the number of bacteria yielding some of the loci of the P^{32}-inactivated parent in the cross is more than ten times greater than that of bacteria infected with survivors of the radioactive decay. This tenfold excess, then, is the manifestation of cross reactivation.

Cross Reactivation of Adsorbed Phage.—It has been shown[2] that if a bacterium is singly infected with P^{32}-unstable phage, the inactivation due to radioactive decay of the infective center proceeds, during the early stages of the latent period, at nearly the same rate as the loss of titer of the free phage. We have now studied cross reactivation of P^{32}-unstable T2 whose radioactive decay had taken place only after adsorption to a bacterium also infected with stable phage. The advantage of this method over cross reactivation after P^{32} decay of free phage is that aliquots of the same population of infected cells may be examined at different stages of decay. Decay of adsorbed phage can, furthermore, proceed in a dilute suspension, eliminating irradiation effects on the phage found upon storage of undiluted highly radioactive lysates.

A suspension of bacteria in broth, containing $M/100$ KCN, was infected at a multiplicity of one each with a non-radioactive stock of T2h^+r^+ and with a one-day old stock of T2*hr*, containing P^{32} at a specific activity of 120 millicuries/mg. and referred to hereafter as "high-P^{32}-T2*hr*." The presence of KCN permits adsorption but arrests further phage development.[8] After elimination of unadsorbed phage by centrifugation, the infected bacteria were frozen and stored at $-196°$C. Aliquots were then thawed from day to day, plated on the mixed indicators B + B/2 before and after burst, and the different plaque types scored separately.

The results of this experiment are presented in figure 1. The logarithm of titer has been plotted against $1-e^{-\lambda t}$, λ being the fractional rate of decay of P^{32} per day, $t-1$ the number of days elapsed between freezing and thawing, and hence $1-e^{-\lambda t}$ being the fraction of P^{32} atoms having decayed by the t-th day. (Such a plot gives a straight line P^{32} mortality curve of free phage if the loss of plaque forming ability is due to the decay of a single phosphorus atom.[1]) It is seen that on the day on which the cross was made, there were 10^7 bacteria per ml. yielding only the *hr* parent, 10^7 per ml yielding only the h^+r^+ parent, and 10^7 per ml. yielding both parents and their recombinants together. In addition, we find two classes of infected bacteria in which only one of the marker loci of the high-P^{32}-T2*hr* parent appear, in addition to those of the stable parent T2h^+r^+: 3×10^6 bacteria per ml. yield h,h^+,r^+ and 10^5 bacteria per ml. yield h^+,r,r^+. The over-all yield after burst contains 55% h^+r^+, 31% *hr* and about 7% each of the two recombinants h^+r and hr^+. (The fraction of recombinants is rather low for two unlinked markers like h and r_{11}, due to the fact that at the multiplicity of infection employed here only 0.46 of all infected bacteria were infected with both parents.)

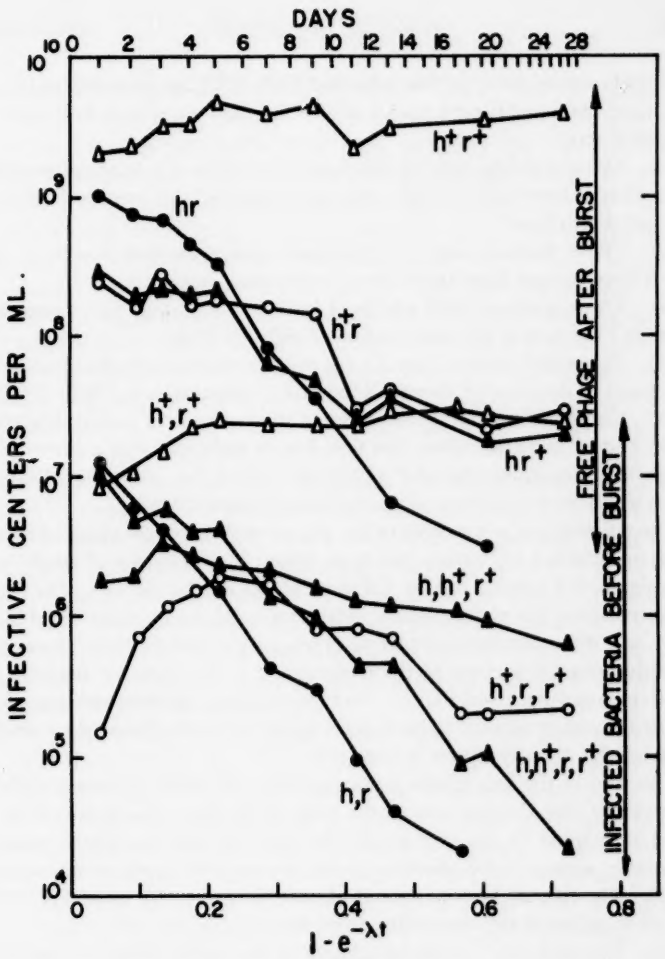

FIGURE 1

DECAY OF HIGH-P^{32}-T2*hr* IN MIXED INFECTION WITH T2h^+r^+

SYMBOL	PLAQUE TYPE	ALLELES LIBERATED BY INFECTED BACTERIUM PLATED BEFORE BURST	PHAGE TYPE PLATED AFTER BURST
●	Large, clear	*h,r*	*hr*
▲	Small, clear	h,h^+,r^+	hr^+
○	Large, turbid or mottled, turbid	h^+,r,r^+	h^+r
△	Small, turbid	h^+,r^+	h^+r^+
◬	Mottled, clear	h,h^+,r,r^+	...

As radioactive decay of the adsorbed high P^{32}-T2*hr* proceeds in the frozen state, the five different classes of infected cells are seen to behave in the following way:

(1) Those yielding only *hr* disappear rapidly at a rate equal to the inactivation of free high P^{32}-T2*hr*, the latter having been measured in a control not shown here.[2]

(2) Those yielding only h^+r^+ increase during the first five days, after which they remain constant at about twice their initial titer.

(3) Those yielding both alleles of both loci h,h^+ and r,r^+ decrease at about 0.7 the rate of the inactivation of high P^{32}-T2*hr*.

(4) Those yielding only the *h* locus of the radioactive parent in addition to h^+ and r^+ decrease at about 0.2 the rate of inactivation of high P^{32}-T2*hr*.

(5) Those yielding only the *r* locus of the radioactive parent in addition to h^+ and r^+ increase during the first five to eight days by a factor of 10, reaching a maximum titer of 2×10^6/ml. After this point they disappear again at about 0.4 the rate of inactivation of high P^{32}-T2*hr*.

The reliability of our scoring of the genotype spectrum of phages liberated from an infected bacterium has been tested by a number of single burst experiments[3, 9] carried out at different stages of the decay. The actual composition of the phage yield of individual cells can be determined in this way, and it was found that plaque type analysis before burst gives a reasonably accurate picture of the distribution of the infected bacteria into the five classes discussed above. An exception was the class yielding h,h^+,r^+ whose frequency seemed to have been somewhat overestimated by analysis before burst at early stages of the decay.

The titer of the four-phage genotypes liberated after burst and their average burst size, defined here as the ratio of the titer of a genotype in the yield after burst to the titer of all those infected bacteria which yield this genotype, appear to be affected by the radioactive decay in this manner:

(1) The titer of *hr* decreases at almost the same rate as high P^{32}-T2*hr*, the average burst size decreasing from 50 to 25.

(2) The titer of h^+r^+ rises by a factor of two and remains constant thereafter, the average burst size having increased from 100 to 200.

(3) The titer of the recombinant hr^+ decreases at about 0.4 the rate of high P^{32}-T2*hr*, the burst size remaining nearly constant between 20 to 30.

(4) The titer of the recombinant h^+r decreases at about 0.4 the rate of high P^{32}-T2*hr* the average burst size increasing from 30 to 100.

Survival of Individual Loci.—These observations demonstrate some quantitative aspects of cross reactivation of P^{32}-inactivated T2. The fact that the class of bacteria yielding both alleles of both loci decreases at only 0.7 the rate of free high-P^{32}-T2*hr* means that 0.3 of those "lethal" P^{32} hits which destroy the ability of the particle to propagate itself independently leave it still able to donate both *h* and r_1 to the progeny of a mixed infection. The

appearance of the class yielding the alleles h,h^+ and r^+ but not r must be due to the fact that some "lethal" hits in the high-P^{32} DNA still leave the h locus free to participate in the cross while excluding the r_1 locus. Since this class disappears at only 0.2 the rate of inactivation of high-P^{32}-T2hr, 0.8 of the "lethal" hits still permit the participation of the h locus. Similarly, the waxing and waning of the class yielding r,r^+,h^+ but not h reflects the possibility of survival of the r_1 locus with exclusion of h. The disappearance of this class at 0.4 the rate of high-P^{32}-T2hr death means that 0.6 of the lethal hits still permit the participation of the r_1 locus. Finally, the increase of the class yielding only h^+r^+ indicates that once both h and r loci have been prevented by P^{32} decay from participation in a mixed infected bacterium originally belonging to the class yielding both alleles and both loci, viable phages bearing the alleles of only the stable parent may still issue from the cell.

From these numerical relations it appears that the elimination of h and r_1 loci by P^{32} decay are independent events since the probability of 0.7 that a lethal hit destroys the ability of the particle to donate both loci is near the sum of the probabilities of eliminating either one, i.e., $0.2 + 0.4$. Secondly, the higher the maximum titer to which the two classes of bacteria yielding only one of the alleles of the high-P^{32}-T2hr rise during decay, the smaller can be the probability that a lethal hit eliminates both h and r_1 at the same time. A calculation shows that the actual maxima observed require this probability to be small.

The interpretation of the average burst sizes of the four genotypes after burst is complicated by the fact that more than one class of infected bacteria contributes to the yield of each type. Nevertheless, on the first day of the experiment, when little decay has as yet taken place, most of the phages which possess one or both of the alleles of the high-P^{32}-T2hr parent originate from bacteria still infected with active T2hr, whereas at late stages of the radioactive decay, the vast majority of such genotypes issue from cells in which the loci of the high-P^{32}-T2hr have survived only through cross reactivation. Hence the fact that the average burst sizes of these genotypes remain fairly constant indicates that a locus, once reactivated in this fashion, is not at a very serious disadvantage in the competition of intracellular growth between the two parental phages.

Discussion.—In order to account for the phenomenon of multiplicity reactivation, Luria[5, 10] proposed a theory which envisions the elimination of radiation-induced lethal genetic factors through recombination. In the hope of supporting this theory, Luria and Dulbecco observed in unpublished cross-reactivation experiments that UV irradiation may eliminate separately genetic markers of T2 phage. A low yield of the surviving marker loci, however, did not permit them to distinguish between (a) direct genetic damage with subsequent reactivation by recombination or (b) physiologi-

cal, i.e. non-genetic, damage and reactivation with subsequent random loss of part of the genetic material. Dulbecco[11] has shown more recently that the details of Luria's theory lead to consequences which do not fit all the observed facts of multiplicity reactivation of UV-inactivated phage. The nature of cross reactivation of x-ray inactivated phage found by Doermann[7] and of P^{32}-inactivated phage reported here indicates, however, that a process of reactivation by genetic recombination might well exist. For the appearance and slow decay of the two classes of infected bacteria producing in relatively high yield only one of the marker loci of high-P^{32}-T2*hr* suggests that in these cells only a part of the genetic apparatus and not the entire P^{32}-inactivated phage was "reactivated." Hence the surviving loci would appear in infective progeny through recombination with phage deriving from the active partner of the cross.

If we now consider the fate of a locus which has not survived radioactive decay, two possibilities suggest themselves for its elimination. On one hand, the "lethal" P^{32} disintegrations may have actually destroyed the locus itself or a section of the linkage group of which this locus forms a part, in which case the fraction of all "lethal" P^{32} disintegrations eliminating a particular locus, such as the factor 0.4 for r_1, represents a fraction of the total phage DNA "sensitive" for this locus. On the other hand, the locus itself may have remained intact after P^{32} decay and the fraction of all disintegrations eliminating the locus represent the probability that it is not separated by recombination from a randomly located P^{32} damage. The operational distinction between these alternatives resides in whether or not the probability of elimination of a locus depends on the conditions of cross reactivation, such as multiplicity of infection of the active partner, latent period, and other factors influencing the recombination process.

A theory of recombination in bacteriophage has recently been proposed in which the intracellular or vegetative phages are thought to engage in genetic exchange through random matings in a "mating pool."[12] Some multiplication precedes mating, indeed the beginning of mating appears to await the "filling" of the mating pool by a sufficient number of replicates of the parental vegetative phages. If cross reactivation is considered in terms of this theory, it seems as if the surviving loci of the P^{32}-inactivated phage commence their multiplication already before recombination with the undamaged partner, for the relatively high burst size of the "reactivated" loci indicates that multiplication of their alleles in the active parent did not begin much sooner than their own. In an experiment not presented here in detail we found, furthermore, that among the first phages matured intracellularly at the conclusion of the eclipse period, the "reactivated" loci are already present in approximately their final proportion. If loci surviving the P^{32} decay, however, commence their multiplication before recombination with the active partner, then it would appear that

the elimination of loci is mainly due to their destruction and not their failure to be recombined away from damaged sites. For if an eliminated locus such as r_1 had undergone any appreciable multiplication in a mixedly infected bacterium, it seems unlikely that there could be a probability as high as 0.4 that not one of the r_1 duplicates succeeded in any of the numerous matings to be recombined into an entirely healthy vegetative phage. Experiments on the cross reactivation of linked markers[7] should assist in the understanding of these questions.

Acknowledgment.—The author is greatly indebted to Dr. A. H. Doermann for communication and discussion of some of his results prior to their publication.

[1] Hershey, A. D., Kamen, M. D., Kennedy, J. W., and Gest, H., *J. Gen. Phys.*, **34**, 305 (1951).
[2] Stent, Gunther S., *Cold Spring Harbor Symp. Quant. Biol.*, **17**, in press (1953).
[3] Hershey, A. D., and Rotman, R., *Genetics*, **34**, 44 (1949).
[4] Fraser, Dean, *J. Biochem;* (in press).
[5] Luria, S. E., PROC. NATL. ACAD. SCI., **33**, 253 (1947).
[6] Watson, J. D., *J. Bact.*, **60**, 697 (1950).
[7] Doermann, A. H.; (personal communication).
[8] Benzer, S., and Jacob, F., *Ann. Inst. Pasteur*, **84**, 186 (1953).
[9] Delbrück, M., *J. Bact.*, **50**, 131 (1945).
[10] Luria, S. E., and Dulbecco, R., *Genetics*, **34**, 93 (1949).
[11] Dulbecco, R., *J. Bact.*, **63**, 199 (1952).
[12] Visconti, N., and Delbrück, M., *Genetics*, **38**, 5 (1953).

---

*EFFECT OF X-RAYS ON CHROMATID ABERRATIONS IN AIR AND IN NITROGEN**

BY C. P. SWANSON† AND DREW SCHWARTZ

BIOLOGY DIVISION, OAK RIDGE NATIONAL LABORATORY, OAK RIDGE, TENNESSEE

Communicated by M. M. Rhoades, October 5, 1953

Since the discovery by Thoday and Read[1] that the frequency of x-ray-induced chromosomal aberrations is drastically lowered by exposure during radiation in atmospheres of reduced oxygen tension, a considerable volume of work has been devoted to the study of the mechanisms involved. To account for the chromosomal effects observed, two hypotheses have been advanced. Giles and coworkers[2–5] have considered that the action of oxygen is such as to govern the frequency of primary breaks (differential breakage hypothesis), this in turn determining the frequency of those aberrations arising from the illegitimate reunion of these broken ends. Their case

rests essentially on two pieces of evidence. The first is that, other things being equal, the oxygen tension during irradiation is the only important variable in determining the final frequency of aberrations, and that altered oxygen tensions after exposure to x-rays are without effect.[3] This argument is based on the generally accepted assumptions that the reunion of broken ends follows breakage, and that completion of the processes of reunion takes a certain amount of time after the cessation of radiation. It would therefore appear that the reunion processes cannot be modified by varying the oxygen tension during the postirradiation period. The second piece of evidence stems from experiments carried out to determine the relative time for illegitimate reunion of breaks produced in high and in low oxygen tensions. By using varying intensities of radiation these workers propose to show that the time for reunion was approximately the same regardless of the atmosphere to which the cells were exposed during irradiation.[5]

The second hypothesis relating to the mechanism of action of reduced oxygen tensions on the production of x-ray-induced aberrations has been advanced by Schwartz.[6] A comparison of types of endosperm mutants in maize induced by x-rays in air and in nitrogen has led to the interpretation that rejoining was higher in the nitrogen series. Thus, with the *a-sh* genes studied, there was a more marked protection of the nitrogen on endosperm mosaics (resulting from terminal losses of chromatin followed by the breakage-fusion-bridge cycle) than on whole losses (arising partially at least from interstitial deletions). If the effect of nitrogen was to reduce the initial frequency of breaks, the reduction factor should be approximately the same for the two types, instead, the reduction factor of whole as opposed to mosaic endosperm losses was 2.7 as opposed to 9.9. The differential reunion hypothesis, as this has been termed, is further supported by studies dealing with the production by x-rays of dominant lethals in Drosophila in air and nitrogen. Utilizing the calculations of Lea and Catcheside,[7] and of Haldane and Lea[8], which give values to the parameters α and q (α = average numbers of breaks/sperm/1000 r; q = probability that a break will rejoin at time of fertilization) which best describe the experimental dominant-lethal curves of Catcheside and Lea[9] and of Demerec and Fano,[10] Baker and Von Halle[11] have shown that, although a reduction in dominant lethals was obtained when irradiation was carried out in nitrogen as opposed to air, the degree of reduction was not compatible with that expected on the differential breakage hypothesis.

Of more immediate interest to the present studies, however, are the observations of Riley, *et al.*,[5] in which chromatid rather than chromosomal aberrations were used in Tradescantia. Chromatid aberrations include those which result from breakage alone (chromatid deletions) as well as those arising out of breakage followed by illegitimate reunion (isochromatid deletions[12] and exchanges). If it is assumed that the effect of a reduced oxygen

tension is to lower the initial frequency of breaks, than it follows that a similar decrease will be found for all types of aberrations, and, in particular, for those aberrations which have a near-linear relation to dose; namely, the chromatid and isochromatid deletions. Instead it was found that the chromatid deletions were much less affected by the reduced oxygen tension than were the isochromatid deletions and the exchanges; in other words, there was a considerably greater effect on those aberrations which involved illegitimate reunion than on those involving breakage only. This evidence then strongly suggests that the recovery process is involved, and that the breakage hypothesis does not account satisfactorily for the observed facts. Riley, *et al.*,[5] in fact, point this out, but they minimize the significance of their data in the light of their much more extensive (but to us, less critical) evidence from the chromosomal studies. What should be emphasized is the fact that support for the breakage hypothesis is drawn wholly from those aberrations (isochromatid deletions, chromatid and chromosomal exchanges) which arise from breakage *followed by illegitimate reunion*, and that those aberrations (chromatid deletions) stemming from breakage only, and which should provide a critical test of the hypothesis, have not been utilized to the extent warranted in considering the mechanism of action of oxygen in the production of aberrations.

Because of what we consider to be a marked discrepancy between observed fact and formulated hypothesis in the chromatid study of Riley, *et al.*, and because we feel that these chromatid data actually favor the reunion hypothesis to a far greater degree than they do the breakage hypothesis, we have undertaken to reinvestigate in a more detailed fashion the effect of oxygen upon the frequency of x-ray-induced chromatid aberrations in Tradescantia. Two different studies were carried out, exposures being made in air and in nitrogen. The first was to determine the frequency of chromatid aberrations as a function of the stage of division, with the x-ray dosage and intensity being held constant. This study also permitted us to approach the question of whether a differential mitotic delay took place in air as opposed to nitrogen, and whether such differential behavior, if present, might help to explain the reduction in aberrations found when x-irradiation was carried out in nitrogen. Giles[4] has pointed out that timing variations in the cycle of division could hardly account for the reductions observed in chromosomal aberrations when exposures were made in nitrogen, but this is not necessarily a valid deduction when one considers that the chromatid aberrations are formed during a relatively short period of time, and that during this time the sensitivity of the chromosomes to breakage by x-rays varies rather widely. The need for considering the question of a possible mitotic delay was also made more pertinent by the observations of Gaulden[13] on the living neuroblast cells of the grasshopper embryo. These cells recover from a mitotic delay imposed by x-radiation more

quickly when exposures are made in nitrogen than when they are made in air.

The second study was concerned with the establishment of x-ray dosage curves at various prophase stages of the mitotic cycle. From such curves it should be possible to determine the air/nitrogen ratios for the different types of aberrations. The ratio of one type of aberration to another changes with the stage of the division cycle, yet under the breakage hypothesis one should expect to find a constant air/nitrogen ratio regardless of the time of irradiation or of sensitivity of the chromosomes to breakage. Failure to find such a constancy would cast serious doubt on the validity of this hypothesis; there is, however, no *a priori* reason for demanding a similar constancy of air/nitrogen ratios under the reunion hypothesis.

Material and Methods.—Except where noted, all x-ray exposures were made at 100 kvp and 15 ma, and at an intensity of 50 r/minute. In addition to the inherent filtration of the beryllium window of the x-ray tube, the radiation was filtered through 1 mm. of aluminum, plus 5 mm. of lucite in the top of the exposure chamber. Inflorescences of *Tradescantia paludosa* were used for all of the experiments described herein. During exposure, the inflorescences were kept in a lucite chamber through which compressed air or nitrogen was flushed at atmospheric pressure. Whenever exposure was made in an atmosphere of nitrogen, the gas was allowed to flow through the chamber for 7 minutes prior to as well as during x-irradiation, and then removed immediately afterward. Acetocarmine smears were made and only metaphase chromosomes were scored for the determination of aberration frequencies.

Experimental Results.—The initial experiments, the data from which are reproduced graphically in figure 1, were carried out in early February when the course of mitosis in the microspores proceeds at a much slower tempo than in the warmer months of spring and summer. As a consequence it was possible to deal exclusively with chromatid aberrations from 8 to 48 hours after irradiation. From 48 to 63 hours after irradiation an admixture of chromatid and chromosomal aberrations was found, with the latter generally predominating. At that time of year, and with the dosage of 150 r employed, the air series could not be scored earlier than 12 hours after radiation because of the induced stickiness of the chromosomes. In the nitrogen series, however, it was possible to score the 8-hour period, and later experiments indicated that under the conditions of our experiment, 150 r in nitrogen induced no stickiness at any time. The dotted portion of the nitrogen curves indicates the frequency of aberrations from 0 to 8 hours after radiation as determined in another experiment, but at a somewhat later period in the spring.

Disregarding the earlier periods after irradiation, about which we could obtain no information in the air series, the data reveal a continual drop in

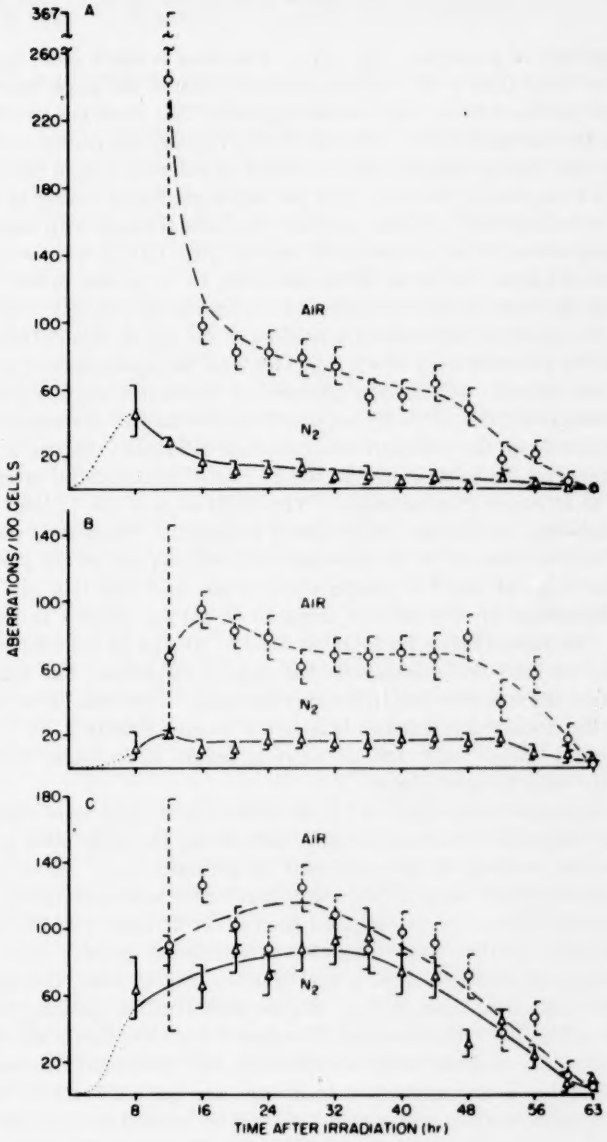

FIGURE 1

Effect of x-rays on chromatid aberrations in air and in nitrogen as a function of time after radiation. *A*. Chromatid exchanges. *B*. Isochromatid deletions. *C*. Chromatid deletions.

the frequency of exchanges (Fig. 1A). This drop is much more apparent in the air series than in the nitrogen series because of the larger number of exchanges in the former, but it is also apparent that there is a parallel decline in the nitrogen series. Because of the exponential rise of exchanges with dosage, the air/nitrogen ratios cannot be calculated from these data. There is a suggestion, however, that the ratios are higher earlier in the division cycle than they are later, and that the ratios change with time.

A comparison of the isochromatid curves (Fig. 1B) shows a somewhat different situation. After an initial rise in the 12- to 16-hour period—a rise which on the basis of other evidence we consider to be a reality—there is a fall in the air series, followed by a leveling of the curve, this in turn being followed by a further drop which coincides with the appearance of chromosomal aberrations. When such mixtures of chromatid and chromosomal aberrations occur it is virtually impossible to distinguish the isochromatid aberrations from the terminal chromosomal deletions. In the nitrogen series, however, there is an almost steady rate of isochromatid production from 8 to 52 hours after radiation. The slight drop at the 12-hour period is an exception, and we are not certain of its reality. These data therefore show that the value of the air/nitrogen ratio will depend on the particular prophase stage at which a comparison is made, and that it is not a constant dependent on the relative amounts of oxygen present in the cells only. The highest ratios are found at the 16-, 20- and 24-hour stages (presumably late and mid-prophase at the time of radiation), but that after this period the ratios remain reasonably constant. Over the 12- to 52-hour period, the average air/nitrogen ratio is 4.3 (range: 8.63 to 2.30), a figure considerably higher than the 2.6 oxygen/helium ratio found by Riley, *et al.*,[5] for their 24-hour period.

The chromatid curve (Fig. 1C) in air shows a great deal more variability than its companion curve in nitrogen, and we can therefore place less reliance on the meaning of any particular air/nitrogen ratio. However, the ratios are in general considerably lower than for the isochromatid deletions, thus confirming over a more extended range of the division cycle the findings of Riley, *et al.*, for their 24-hour period. From the 12- to the 52-hour period the average air/nitrogen ratio is 1.34 (range: 2.43 to 0.86), this agreeing quite well with their figure of 1.4. We are thus forced to consider that any hypothesis dealing with the action of oxygen in the induction of aberrations must take into account that isochromatid and chromatid deletions, although having a similar relation to dosage, are quite differently affected when exposure is made in nitrogen. As will be pointed out in more detail later, the breakage hypothesis cannot adequately explain this seeming discrepancy.

The aberration data just discussed also permit us to determine whether or not recovery from the mitotic delay induced by the radiation occurs more

rapidly in cells exposed in air than in nitrogen, and whether such differences in recovery rate, if present, have any effect in altering the air/nitrogen ratios. Figure 1A shows that such a delay occurs, and that recovery is more rapid in the nitrogen series, i.e., the abrupt drop in exchanges in the air series occurs between the 12- and 16-hour periods, while in the nitrogen series the corresponding drop takes place earlier, between 8- and 12-hour periods. This lag of approximately 4 hours in the division cycle in the air series is also evident, although to a less obvious degree, at the time when the chromatid aberrations are giving way to the chromosomal types. There is also a sharp drop in total chromatid aberration frequency in the air series between the 56- to 60-hour period, while in the nitrogen series it takes place in the 52- to 56-hour period. There is of course no guarantee that a delay induced in cells in the later stages of prophase will be similarly expressed in cells irradiated much earlier in the division cycle; in fact, a uniform delay throughout the division cycle is not to be expected since it has long been known that the cells vary in their sensitivity to radiation during the mitotic cycle. Of more immediate importance is that, even though a delay seems to be more pronounced in the air than in the nitrogen series, the differential recovery from the mitotic delay does little more than change the air/nitrogen ratios slightly. It does not alter the fact that each aberration type has its own peculiar response to radiation in air and in nitrogen.

There is a further need for a more accurate determination of the air/nitrogen ratios, and this can be better ascertained from dosage curves than from single doses given at various stages in the division cycle. From such studies one can determine with certainty whether the air/nitrogen ratios actually change with time, as these studies suggest, or whether the ratios are constant values, as the breakage hypothesis demands. With this in mind, three dosage curves were obtained at the 8-, 12- and 24-hour periods. Initially, the 12- and 24-hour periods were selected as periods of quite different sensitivity to radiation, and the 8-hour period was added when it was found that, in April, when these experiments were carried out and when the rate of cell division was more rapid than it was earlier, stickiness was not of such long duration. (We have since learned that the duration of the "sticky" period induced by a given dose of x-rays is governed by the rapidity of the division cycle, i.e., the more rapid the mitotic change, the more rapid is the recovery from stickiness.) The results of these studies are given in table 1.

Agreement with the data in figure 1 is indicated by the fact that the chromosomes are increasingly sensitive as the division cycle approaches metaphase. Thus the 8-hour period shows a greater frequency of aberrations for any given dose than the 12-hour period, and with the latter correspondingly more sensitive than the 24-hour period. As regards the air/nitrogen ratios, those for the chromatid deletions are approximately 1 for

all three periods, indicating once again that this type of aberration is relatively unaffected by the atmosphere in which the cells are irradiated. The customary air/nitrogen ratios, however, are found for the isochromatid deletions and the chromatid exchanges. On the other hand, the ratios are not constant for these types of aberrations but, rather, appear to be dependent upon the mitotic stage being irradiated. The more sensitive the chromosomes are to breakage in air, the greater the air/nitrogen ratio. Thus, for the 8-, 12- and 24-hour periods, the average isochromatid ratios are 2.8, 2.6, and 2.3 respectively, while those for exchanges are 2.9, 2.4, and 2.0. The isochromatid ratios are significantly different from each other at the 1% level; those for the exchanges are not, although the reality of the differences is suggested by the fact that they parallel exactly the ratios for the isochromatid delations.

TABLE 1

EFFECT OF X-RAYS ON CHROMATID ABERRATIONS IN AIR AND IN NITROGEN AT DIFFERENT INTERVALS AFTER RADIATION. AIR/NITROGEN RATIOS COMPUTED FROM CURVES RATHER THAN FROM ABSOLUTE ABERRATION DATA

TIME AFTER RADIATION (HR)	DOSE (R)	ABERRATIONS/100 CELLS: AIR				NITROGEN				AVERAGE AIR/NITROGEN RATIOS		
		CELLS SCORED	CD.	ISO.	EXCH.	CELLS SCORED	CD.	ISO.	EXCH.	CD.	ISO.	EXCH.
8	25	300	29.3	9.6	6.6	...	...	..	..	1.1	2.8	2.9
	50	200	63.5	21.0	26.0	...	...	..	..			
	100	100	125.0	47.0	89.0	100	116.0	16.0	11.0			
	225	...	...	..	..	50	216.0	36.0	62.0			
12	25	300	27.0	9.0	3.6	...	...	..	..	1.1	2.6	2.4
	50	300	46.0	25.7	9.7	...	...	..	..			
	100	300	79.0	44.7	31.0	300	73.7	17.7	8.0			
	150	200	119.0	67.5	66.5	...	...	..	..			
	225	...	...	..	..	200	138.5	37.5	28.0			
	350	...	...	..	..	100	199.0	62.0	66.0			
24	25	200	14.0	6.5	3.5	...	...	..	..	1.0	2.3	2.0
	50	200	29.5	15.0	8.5	300	25.7	7.7	2.3			
	100	250	55.6	30.8	17.2	200	56.5	14.5	8.0			
	150	200	81.5	51.5	45.5	...	...	..	..			
	225	...	...	..	..	200	116.5	30.0	28.0			
	350	...	...	..	..	200	163.0	55.0	57.0			

Discussion.—The data derived from the experiments reported do not support the differential breakage hypothesis advanced by Giles and his coworkers. In addition to those previously cited by Schwartz[6] and Baker and Von Halle,[11] the critical pieces of evidence which weigh against the hypothesis are several. First, over the entire range of the division cycle when only chromatid aberrations are found, the reduction in the number of chromatid deletions brought about by exposure of cells to x-rays in nitrogen is considerably less than that found for isochromatid deletions. Both types show a near-linear relation to dosage, and consequently should show similar reductions. Their failure to do so was recognized by Riley, *et al.*,[5] but they chose rather to place greater reliance on the earlier chromosomal stud-

ies of Giles and Riley,[3] and to consider that the daily variations in induced chromatid aberration frequencies and the difficulties of accurate scoring of these aberrations introduce doubt as to the validity of the chromatid findings. We believe these arguments are without foundation, particularly since we have been able to confirm repeatedly their chromatid data in all respects. The second piece of evidence not in line with the breakage hypothesis stems from the dosage studies. The chromatid deletions again do not show the amount of reduction, relative to that found for the isochromatid deletions. Important also, is the fluctuation of the air/nitrogen ratios for both isochromatid deletions and exchanges with the stage of the division cycle at which radiation is given. These findings are inexplicable on the assumption that the oxygen tension governs the rate of primary breakage but not the recovery processes. In this connection it should be pointed out that, in general, our air/nitrogen ratios for chromatid deletions are lower and for isochromatid deletions higher than those found by Riley, *et al.* This we now know to be a function of the wave-length of x-ray used. These data will, however, be presented in another report.

It remains to consider whether these data fit into the differential reunion hypothesis of Schwartz.[6] This hypothesis states, in its simplest form, that the degree of reunion of broken ends is greater for irradiations made in nitrogen than in air. This would suggest that all three types of aberrations would be decreased when exposures are made in nitrogen; that they are differentially affected is indicated by the data. One must therefore assume that if there is decrease in chromatid deletions comparable in magnitude to the decreases found for isochromatid deletions and exchanges than there is a compensatory increase in their number such as to restore the original number induced. Such a compensatory increase can be derived from the partial restitution of those breaks which would have gone into the formation of isochromatid deletions and exchanges. An alternative assumption would be that the chromatid deletions form a group of single breaks which are qualitatively different from other breaks in that they are irretrievably broken, i.e., they can neither restitute or rejoin with other broken ends and can therefore be considered "healed." On the basis of wave-length experiments, the details of which will be reported in another publication, we have been able to show that under certain conditions, the frequency of chromatid deletions induced in nitrogen is actually much higher than that induced in air; we, therefore, believe that the former mechanism is operating.

Two additional comments may be made. The first is that the intensity studies of Riley, *et al.*, mentioned earlier and cited by them as support for the breakage hypothesis, actually yield evidence which can provide support for either hypothesis depending upon the initial assumptions made. The dosages and intensities used were such that those in nitrogen were about 2.7 times greater than those in air, yet the decrease in exchanges with a de-

crease in intensity is identical in both situations. The design of the experiment was, of course, based on the assumption that the rate of breakage would be approximately the same despite the difference in dose and intensity, and that a similar rate of decline in exchanges indicates a similar rate of restitution. In the light of the evidence presented here, this experiment can be reinterpreted to mean that the breaks produced in nitrogen were not 2.7 times more frequent per unit of time than those produced in air, but that restitution was approximately 2.7 times more rapid in nitrogen than in air. This suggestion, however, is in need of further testing before being accepted at face value.

The last comment relates to the biochemical interpretation of the oxygen effect.[4] Since there remains a residue of aberrations even after irradiation in an oxygen-free atmosphere, Giles has suggested that there are two categories of breaks, those caused by ionization within the structure of the chromosome (direct effect of x-rays) and those caused by the products of irradiated water (indirect effects of x-rays). Several convincing arguments were presented for assuming that hydrogen peroxide is the agent responsible for indirect breakage. These, however, have a bearing on the problem of breakage if, *and only if*, the breakage hypothesis is correct. Since the present evidence, as well as that presented by Schwartz[6] and Baker and Von Halle,[11] indicates otherwise, the role of hydrogen peroxide in breakage is suspect. Whether other products of irradiated water are important in this respect remains to be proved.

* Work performed under Contract No. W-7405-eng-26 for the Atomic Energy Commission.

† On leave from The Johns Hopkins University for academic year 1952–53.

[1] Thoday, J. M., and Read, John, *Nature*, **160**, 608 (1947); **163**, 133–134 (1949).

[2] Giles, N. H., Jr., and Beatty, A. V., *Science*, **112**, 643–645 (1950).

[3] Giles, N. H., Jr., and Riley, H. P., these PROCEEDINGS, **35**, 640–646 (1949); **36**, 337–344 (1950).

[4] Giles, N. H., Jr., *Symposium on Radiobiology*, John Wiley & Sons, Inc., 1952, pp. 267–284.

[5] Riley, H. P., Giles, N. H., Jr., and Beatty, A. V., *Am. J. Botany*, **39**, 592–597 (1952).

[6] Schwartz, D., these PROCEEDINGS, **38**, 490–494 (1952).

[7] Lea, D. E., and Catcheside, D. G., *J. Genetics*, **47**, 10–24 (1945).

[8] Haldane, J. B. S., and Lea, D. E., *Ibid.*, **48**, 1–10 (1947).

[9] Catcheside, D. G., and Lea, D. E., *Ibid.*, **47**, 1–9 (1945).

[10] Demerec, M., and Fano, U., *Ibid.*, **29**, 348–360 (1944).

[11] Baker, W. K., and Von Halle, E. S., these PROCEEDINGS, **39**, 152–161 (1953).

[12] Isochromatid deletions have been included in the illegitimate reunion category since Catcheside and Lea[14] have shown that sister-strand fusion occurs in at least 95% of these aberrations.

[13] Gaulden, M. E., Nix, M., and Moshman, J., *J. Cellular Comp. Physiol.*, **41**, 451–470 (1953).

[14] Catcheside, D. G., and Lea, D. E., *J. Genetics*, **45**, 186–196 (1943).

SPIRAL AND OTHER ASYMPTOTIC PATHS, AND PATHS OF COMPLETE INDETERMINATION, OF ANALYTIC AND MEROMORPHIC FUNCTIONS*

BY F. BAGEMIHL AND W. SEIDEL

THE INSTITUTE FOR ADVANCED STUDY AND THE UNIVERSITY OF ROCHESTER

Communicated by J. L. Walsh, October 9, 1953

If A and B are point sets in the extended complex plane, we shall denote by $d(A, B)$ the distance between A and B, measured on the Riemann sphere. Let G be a region not containing the point at infinity, whose boundary consists of a finite number of mutually exclusive circles K_j $(j = 1, 2, \ldots, \nu)$, some or all of which may degenerate to single points. By a *boundary path*, abbreviated *b-path*, we shall mean a simple continuous curve, $z = z(t) \in G$, $0 \leq t < 1$, which converges to one of the components of the boundary of G, i.e., for some j, as $t \to 1$, $d(z(t), K_j) \to 0$. If, furthermore, the last limit is approached monotonically, the b-path will be termed a *monotonic b-path*. Let $f(z)$ be meromorphic in G. A b-path which is mapped by $f(z)$ on a set which is everywhere dense in the complex plane will be called a *path of complete indetermination of* $f(z)$. A b path along which $f(z)$ approaches a definite limit, finite or infinite, is an *asymptotic path* of $f(z)$, and the limit is an *asymptotic value* of $f(z)$.

In 1918, Gross[1] obtained an example of a meromorphic function in $|z| < +\infty$ for which every b-path is a path of complete indetermination. Such functions also exist[2] in $|z| < 1$. The condition in these examples that $f(z)$ be meromorphic is essential, as every regular function in $|z| < R \leq +\infty$ possesses at least one asymptotic value.[3] In 1934, Valiron[4] obtained an example of a regular, unbounded function in $|z| < 1$, which remains bounded on certain spiral b-paths, and tends to infinity along certain other spiral b-paths.

In this paper we shall establish, among other results, the existence in a region G of the above form whose boundary components do not degenerate to points, of a non-constant regular function possessing prescribed asymptotic values, finite or infinite, along enumerably many prescribed spiral monotonic b-paths (cf. Corollary 1). It will also be shown that the example due to Gross can be extended to finitely connected regions (cf. the "Remark" following the proof of Theorem 1). In fact, there exist meromorphic functions in G which exhibit these two phenomena simultaneously, relative to different components of the boundary (cf. Theorem 1). We shall also obtain several sufficient conditions for a meromorphic function to have certain paths of complete indetermination.[5]

THEOREM 1. *Let λ, μ, and ν be non-negative integers with $1 \leq \nu = \lambda + \mu$, and G be a region not containing the point at infinity, whose boundary consists*

of ν mutually exclusive circles $K_1, K_2, \ldots, K_\nu$, some or all of which may degenerate to single points. If $\lambda > 0$, let $S_0, S_1, \ldots, S_n, \ldots$ be an arbitrary enumerable set of mutually exclusive b-paths in G, each of which converges monotonically[6] to one of the circles $K_1, K_2, \ldots, K_\lambda$, and $w_0, w_1, \ldots, w_n, \ldots$ be a sequence of complex numbers, some or all of which may be infinite. Then there exists a single-valued non-constant function $f(z)$ in G, regular if $\lambda = \nu = 1$, or if $\mu = 0$ and no K_j $(j = 1, 2, \ldots, \nu)$ is degenerate, but meromorphic otherwise, such that, if $\lambda > 0$, $f(z)$ possesses the asymptotic value w_n along S_n for every n, and, if $\mu > 0$, every b-path converging to any one of the circles $K_{\lambda+1}, K_{\lambda+2}, \ldots, K_{\lambda+\mu}$ is a path of complete indetermination of $f(z)$.

Proof:[7] For every integer j satisfying $1 \leq j \leq \nu$, let C_n^j $(n = 0, 1, 2, \ldots)$ be circles in G which are concentric with K_j, such that $d(C_n^j, K_j)$ tends monotonically to 0 as $n \to \infty$, and have the property that C_0^j and the region bounded by C_0^j and K_j does not contain any point of C_0^k $(k = 1, 2, \ldots, \nu;\ k \neq j)$. We denote by D_n $(n = 0, 1, 2, \ldots)$ the bounded, closed set consisting of the circles C_n^j $(j = 1, 2, \ldots, \nu)$ and the region bounded by these circles. There is clearly no loss of generality in assuming that, in case $\lambda > 0$, the initial point of every S_n lies between the circles C_0^j and C_1^j, where S_n converges to K_j, so that $S_n \cdot C_0^j = 0$ for every n and j; and that, if $\mu = 0$, not all the numbers w_n are the same (for otherwise we could consider an additional b-path with a different assigned asymptotic value; as will be seen from the proof, this assumption is made merely to ensure that the function $f(z)$ finally obtained in this case is not identically constant).

Let $C_k = C_k^1 + C_k^2 + \ldots + C_k^\nu$ $(k = 0, 1, 2, \ldots)$. In case $\lambda > 0$, denote for every n by A_{nk} the set of $z \in S_n$ in[8] $\overline{D_k - D_{k-1}}$ $(k = n+1, n+2, n+3, \ldots)$; let a_{nk} be the point $A_{nk} \cdot C_k$ $(n = 0, 1, 2, \ldots;\ k = n+1, n+2, n+3, \ldots)$, and a_{nn} be the point $A_{n,n+1} \cdot C_n$ $(n = 1, 2, 3, \ldots)$. If $\mu > 0$, let T_n^j be a circle concentric with K_j and lying between C_{n-1}^j and C_n^j $(j = \lambda+1, \lambda+2, \ldots, \lambda+\mu;\ n = 1, 2, 3, \ldots)$, and set $T_n = T_n^{\lambda+1} + T_n^{\lambda+2} + \ldots + T_n^{\lambda+\mu}$ $(n = 1, 2, 3, \ldots)$. Put $F_n = D_n + A_{0,n+1} + A_{1,n+1} + \ldots + A_{n,n+1} + T_{n+1} + A_{n+1,n+2}$ $(n = 0, 1, 2, \ldots)$; here and in what follows, any expression which, because of the vanishing of λ or μ for the region G under consideration, is not well-defined, is simply to be ignored. Let $H = \sum_{n \geq 0} (\overline{F_n - D_n})$.

In case $\lambda > 0$, we set $\omega_n(z) \equiv w_n$ for $z \in S_n$ if w_n is finite, but, if $w_n = \infty$, $\omega_n(z)$ denotes a real, continuous function of $z \in S_n$ which tends to $+\infty$ as z approaches the boundary of G along S_n. In case $\mu > 0$, we denote by $\{\tau_n\}$ a sequence of complex numbers which is everywhere dense in the complex plane.

We now define, by induction on n, a function $\varphi_n(z)$ on F_n, and a function $Q_n(z)$ which is a polynomial or a rational function according as $\lambda = \nu = 1$ or not, as follows:

$$\varphi_0(z) = \begin{cases} 0, & z \in D_0 \\ \omega_0(z), & z \in A_{01} \\ \omega_1(z), & z \in A_{12} \\ \tau_1, & z \in T_1 \end{cases}$$

The set F_0 is evidently closed and bounded, and its boundary consists of a finite number of Jordan curves and, in case $\lambda > 0$, Jordan arcs, no two of which have more than a finite number of points in common (in fact, at this stage of the induction, no two have any points in common). Furthermore, $\varphi_0(z)$ is continuous on F_0 and regular at all interior points of F_0. Consequently,[9] there exists a $Q_0(z)$ (cf. the preceding paragraph), having no poles on $F_0 \cup H$, or in G in case $\mu = 0$ and no K_j ($j = 1, 2, \ldots, \nu$) is degenerate, satisfying the conditions

$$\begin{aligned} &|Q_0(z) - \varphi_0(z)| < 1, && z \in F_0; \\ &Q_0(a_{j1}) = \omega_j(a_{j1}), && (j = 0, 1). \end{aligned}$$

Suppose, now, that $n > 0$ and that we have defined $\varphi_{n-1}(z)$ on F_{n-1}, and $Q_0(z), Q_1(z), \ldots, Q_{n-1}(z)$ so that $Q_0(z) + Q_1(z) + \ldots + Q_{n-1}(z)$ has no poles on H, and

$$Q_{n-1}(a_{jn}) = \omega_j(a_{jn}) - [Q_0(a_{jn}) + Q_1(a_{jn}) + \ldots + Q_{n-2}(a_{jn})], \quad (j = 0, 1, \ldots, n), \quad (1)$$

where the expression in brackets is missing for $n = 1$. We define $\varphi_n(z)$ on F_n as follows:

$$\varphi_n(z) = \begin{cases} 0, & z \in D_n \quad (2) \\ \omega_j(z) - [Q_0(z) + Q_1(z) + \ldots + Q_{n-1}(z)], & z \in A_{j,n+1}, (j = 0, 1, \ldots, n) \quad (3) \\ \omega_{n+1}(z) - [Q_0(z) + Q_1(z) + \ldots + Q_{n-1}(z)], & z \in A_{n+1,n+2} \\ \tau_{n+1} - [Q_0(z) + Q_1(z) + \ldots + Q_{n-1}(z)], & z \in T_{n+1}. \quad (4) \end{cases}$$

Clearly $\varphi_n(z)$ is regular at all interior points of F_n, and, in view of (1), $\varphi_n(z)$ is continuous on F_n. Consequently, as before, there is a $Q_n(z)$, having no poles on $F_n \cup H$, or in G in case $\mu = 0$ and no K_j ($j = 1, 2, \ldots, \nu$) is degenerate, satisfying

$$|Q_n(z) - \varphi_n(z)| < 2^{-n}, \quad z \in F_n; \quad (5)$$

$$Q_n(a_{j,n+1}) = \omega_j(a_{j,n+1}) - [Q_0(a_{j,n+1}) + Q_1(a_{j,n+1}) + \ldots + Q_{n-1}(a_{j,n+1})], \quad (j = 0, 1, \ldots, n+1).$$

This completes the induction.

If $z \epsilon D_n$, then, because of (2) and (5), $|Q_{n+k}(z)| < 2^{-(n+k)}$ ($k = 0, 1, 2, \ldots$), and, since $Q_n(z)$ is regular on D_n, $\sum_{k=0}^{\infty} Q_{n+k}(z)$ is a regular function in the interior of D_n, so that $f(z) = \sum_{n=0}^{\infty} Q_n(z)$ is a meromorphic function in the interior of D_n. Every point of G, however, is interior to some D_n; $f(z)$, therefore, is meromorphic throughout G. (In case $\lambda = \nu = 1$, every $Q_n(z)$ is a polynomial, and $f(z)$ is actually regular throughout G. If $\mu = 0$ and no K_j ($j = 1, 2, \ldots, \nu$) is degenerate, every $Q_n(z)$ is regular in G, and hence $f(z)$ is regular there.) We shall show that $f(z)$ satisfies the conclusions of Theorem 1.

Let n be arbitrary, and $z \epsilon A_{nk}$ ($k > n$). According to (5), (3), and (2),

$$|f(z) - \omega_n(z)| \leq |Q_0(z) + Q_1(z) + \ldots + Q_{k-1}(z) - \omega_n(z)| + |Q_k(z)| + |Q_{k+1}(z)| + \ldots < 2^{-(k-1)} + \sum_{j=k}^{\infty} 2^{-j}.$$

Hence,

$$\lim_{k \to \infty} \max_{z \epsilon A_{nk}} |f(z) - \omega_n(z)| = 0,$$

which shows that $f(z)$ possesses the prescribed asymptotic value w_n on S_n. A similar argument, referring to (5), (4), and (2), yields the relation

$$\lim_{k \to \infty} \max_{z \epsilon T_k} |f(z) - \tau_k| = 0,$$

which implies that every b-path converging to any one of the circles $K_{\lambda+1}, K_{\lambda+2}, \ldots, K_{\lambda+\mu}$ is a path of complete indetermination of $f(z)$. Since at least one of the numbers λ, μ is positive, and not all numbers of the sequence $\{w_n\}$ are the same, $f(z)$ is not identically constant. This completes the proof of Theorem 1.

Remark: In case $\mu = \nu = 1$ and K_1 is the point at infinity, Theorem 1 yields a function having the property of the function constructed by Gross mentioned above, and if $\mu = \nu > 1$, yields similar examples for ν-tuply connected regions.

We note several corollaries of Theorem 1 which may be obtained by specifying $\{S_n\}$ or $\{w_n\}$ more precisely. For simplicity they will be stated for a simply connected region, but the extension to a ν-tuply ($\nu > 1$) connected region G for which no K_j ($j = 1, 2, \ldots, \nu$) degenerates to a single point is immediate.

COROLLARY 1. *Let $\{S_n\}$ be a sequence of mutually exclusive spiral monotonic b-paths in $|z| < R \leq +\infty$. Let $\{w_n\}$ be any sequence of complex numbers, some or all of which may be infinite. Then there exists a non-*

constant $f(z)$, regular in $|z| < R$, which, for every n, possesses the asymptotic value w_n on S_n.

If we choose the numbers of $\{w_n\}$ in Corollary 1 to be everywhere dense in the complex plane, and modify $\{S_n\}$ so that, for every n, arg z is unbounded from below and from above as z describes S_n, we obtain

COROLLARY 2. *There exists a function $f(z)$, regular in $|z| < R \leq +\infty$, such that every b-path on which* arg z *is bounded from below or from above is a path of complete indetermination of $f(z)$.*[10]

COROLLARY 3. *There exists a function $f(z)$, regular in $|z| < R \leq +\infty$, such that every b-path on which* arg z *does not tend to a finite limit is a path of complete indetermination of $f(z)$.*

To construct such an $f(z)$, we note first that the set of all pairs p of rational numbers (θ, θ') satisfying $-\pi < \theta < \theta' \leq +\pi$ is enumerable and may therefore be written as a sequence $\{p_n\}$ $(n = 0, 1, 2, \ldots)$. For every n, let $\varphi_{n0}, \varphi_{n1}, \ldots, \varphi_{nk}, \ldots$ be an enumerable set of real numbers such that, if the two numbers constituting p_n are denoted by θ_n and θ_n', then $\theta_n < \varphi_{nk} < \theta_n'$ $(k = 0, 1, 2, \ldots)$; as is easily seen, we may further specify that $\varphi_{mj} \neq \varphi_{nk}$ if $m \neq n$. Let the sequence $\{w_k\}$ of complex numbers be everywhere dense in the complex plane. Define S_{nk} to be the set of $z = \rho e^{i\varphi}$ with $0 \leq \rho < R$ and $\varphi = \varphi_{nk}$ $(k, n = 0, 1, 2, \ldots)$. According to Theorem 1, there exists an $f(z)$, regular in $|z| < R$, which tends to w_k as $|z| \to R$ along S_{nk}, for every n and k. The truth of the corollary is immediately evident now if we observe that every b-path on which arg z does not tend to a finite limit must, for some n, intersect every S_{nk} $(k = 0, 1, 2, \ldots)$ infinitely often.

The next theorem gives a simple sufficient condition on the zeros (or, more generally, the a-points) of a meromorphic function $f(z)$ in order that certain b-paths be paths of complete indetermination of $f(z)$. For some of the terminology in the statement and proof of the theorem, the reader is referred to an earlier paper of the present authors.[11]

THEOREM 2. *Let $f(z)$ be a non-constant meromorphic function in $|z| < 1$, and A be a fixed arc $\lambda <$ arg $z < \mu$, $0 < \mu - \lambda \leq 2\pi$, $|z| = 1$. For every pair of numbers α, β satisfying $\lambda < \alpha < \beta < \mu$, denote by $S_{\alpha\beta}$ the open sector $\alpha <$ arg $z < \beta$, $0 < |z| < 1$. Suppose that $f(z)$ has the infinitely many zeros z_n $(n = 0, 1, 2, \ldots)$ in $|z| < 1$, and that*

$$\sum_{z_n \in S_{\alpha\beta}} (1 - |z_n|) = \infty \tag{6}$$

for every $S_{\alpha\beta}$. Then there exists a residual subset of the radii terminating in the points of A, each of which is a path of complete indetermination of $f(z)$.

Proof: According to an earlier result of the present authors,[12] it is sufficient to show that the cluster set of $w = f(z)$ at every point of A is the whole w-plane.

Suppose that this is not the case. Then there exists an $S_{\alpha\beta}$ in which $f(z)$ omits all the values of a finite disk $|w - a| < r$. The function $g(z) = 1/(f(z) - a)$ is therefore regular and bounded in $S_{\alpha\beta}$. Let $\beta - \alpha = 2\gamma$, and denote by S_γ an open sector of $|z| < 1$ defined by $0 < |z| < 1$, $-\gamma < \arg z < \gamma$. We shall assume that $S_{\alpha\beta} = S_\gamma$; it will be seen from the proof that this entails no loss of generality. Map S_γ conformally on the unit circle $|\omega| < 1$ by means of the function[13]

$$\omega = \omega(z) = \frac{2z^{\pi/2\gamma} - 1}{2z^{\pi/2\gamma} + 1} \cdot \frac{2 + z^{\pi/2\gamma}}{2 - z^{\pi/2\gamma}}.$$

If we set $z_n = \rho_n e^{i\varphi_n} \in S_\gamma$ and $\omega_n = \omega(z_n)$, an elementary calculation shows that

$$1 - |\omega_n|^2 > c_1 \rho_n^{\pi/2\gamma} (1 - \rho_n^{\pi/\gamma}) \cos \frac{\pi\varphi_n}{2\gamma}, \tag{7}$$

where c_1 is a positive absolute constant. In particular, if $z_n \in S_{\gamma/2} \subset S_\gamma$, then $\cos \frac{\pi\varphi_n}{2\gamma} > \frac{\sqrt{2}}{2}$, and (7) can be replaced by

$$1 - |\omega_n| > c_2(1 - \rho_n^{\pi/\gamma}), \tag{8}$$

where c_2 is a positive absolute constant. Now $1 - |z_n| \leq 1 - |z_n|^{\pi/\gamma} < c_2^{-1}(1 - |\omega_n|)$, and hence, in view of (8),

$$\sum_{z_n \in S_\gamma} (1 - |\omega_n|) \geq \sum_{z_n \in S_{\gamma/2}} (1 - |\omega_n|) = \infty. \tag{9}$$

If we set $h(\omega) = g(z(\omega))$, where $z(\omega)$ denotes the inverse function of $\omega(z)$, then evidently $h(\omega)$ is regular and bounded in $|\omega| < 1$, and $(h\omega_n) = -1/a$. According to (9) and Blaschke's theorem,[14] this implies that $h(\omega)$ is identically equal to $-1/a$, which contradicts the hypothesis that $f(z)$ is not identically constant. Thus, the cluster set of $f(z)$ at every point of A must be the whole w-plane, and this completes the proof of the theorem.

It is not difficult to see that the sufficient condition (6) for the conclusion of Theorem 2 is not necessary. Let $\Omega(z)$ be a function[15] which is regular, non-constant, and different from zero in $|z| < 1$, and which tends to zero along almost every radius in $|z| < 1$. Furthermore, let $\{z_n\}$ be an at most enumerable set of points in $|z| < 1$ such that $\sum(1 - |z_n|)$ converges, and denote by $B(z)$ the (finite or infinite) Blaschke product having these zeros. Then[16] both $\Omega(z)$ and $\Omega(z) \cdot B(z)$ satisfy the conclusion of Theorem 2, but (6) does not hold.

It is easily seen that an analogous argument[17] proves

THEOREM 3. *Let $0 \leq R \leq +\infty$, and $f(z)$ be a non-constant meromorphic function in $|z| < R$. Let $\zeta_0 = Re^{i\theta_0}$ if $R < +\infty$, $\zeta_0 = \infty$ if $R = +\infty$, and suppose that $f(z)$ has infinitely many zeros z_n $(n = 0, 1, 2, \ldots)$ tending*

to ζ_0, such that, if $R < +\infty$, $\sum_{z_n \in S} |z_n - \zeta_0|^{\alpha} = \infty$, and if $R = +\infty$, $\sum_{z_n \in S} |z_n|^{-\alpha} = \infty$, for every $\alpha > 1$ and every Stolz angle S with vertex ζ_0. Then there exists a residual set of rectilinear segments terminating in ζ_0, each of which is a path of complete indetermination of $f(z)$.[18]

A sufficient condition of a different type for the existence of paths of complete indetermination is furnished by

THEOREM 4. *Let $f(z)$ be meromorphic in $|z| < 1$, and suppose that as $z \to e^{i\theta_0}$ along each member of a set of rectilinear segments in $|z| < 1$ which are everywhere dense in $|z| < 1$ and which terminate in $e^{i\theta_0}$, $f(z)$ tends to a limit, finite or infinite, but that $f(z)$ does not tend to a limit uniformly in any Stolz angle with vertex $e^{i\theta_0}$. Then there exists a residual set of segments terminating in $e^{i\theta_0}$, each of which is a path of complete indetermination of $f(z)$.*

Proof: Let $\{D_n\}$ be the sequence of open disks in the w-plane having rational radii and centers of the form $\alpha + \beta i$, where α and β are real and rational. For every n, denote by E_n the set of segments in $|z| < 1$ which terminate in $e^{i\theta_0}$ and on each of which $w = f(z)$ omits every value in D_n. The set E_n cannot be dense in any Stolz angle with vertex $e^{i\theta_0}$. For if it were dense in some Stolz angle Γ, then $f(z)$, by continuity, would omit every value in D_n throughout Γ. The function $g(z) = 1/(f(z) - a)$, where a denotes the center of D_n, would then be regular and bounded in Γ. By hypothesis, Γ contains at least one segment along which $f(z)$ tends to some value c, and hence along which $g(z)$ tends to the value $1/(c - a)$. According to Lindelöf's theorem, this would imply that $g(z)$ tends uniformly to $1/(c - a)$, and hence $f(z)$ tends uniformly to c, in every Stolz angle with vertex $e^{i\theta_0}$, contrary to assumption. Thus the complement of $\cup E_n$ is a residual set of segments each of which possesses the property asserted in the theorem.

* Presented to the American Mathematical Society, October 24, 1953.

[1] Gross, W., "Über die Singularitäten analytischer Funktionen," *Monatsh. Math. Phys.*, **29**, 3–47 (1918), p. 14.

[2] Cf. Kierst, S., and Szpilrajn, E., "Sur certaines singularités des fonctions analytiques uniformes," *Fund. Math.*, **21**, 276–294 (1933).

[3] *Ibid.*, p. 291.

[4] Valiron, G., "Sur les singularités des fonctions holomorphes dans un cercle," *C. R. Acad. Sci. Paris*, **198**, 2065–2067 (1934). Other examples of functions regular in $|z| < 1$ which tend to infinity along spiral b-paths were recently obtained by P. Erdös and the present authors, "Sur quelques propriétés frontières des fonctions holomorphes définies par certains produits dans le cercle-unité," *Ann. École Norm. Sup.* (to appear).

[5] For other sufficient conditions, see F. Bagemihl and W. Seidel, "A General Principle Involving Baire Category, with Applications to Function Theory and Other Fields," these PROCEEDINGS, **39**, 1068-1075 (1953).

[6] As will be seen from the proof, this condition is needlessly restrictive, but is introduced for the sake of simplicity.

[7] Certain features of the proof were suggested to us by an example given by L.

Bieberbach, *Lehrbuch der Funktionentheorie*, vol. II, 2nd ed., Leipzig and Berlin, 1931, pp. 152–155.

[8] As usual, $\bar{M}$ denotes the closure of M.

[9] Walsh, J. L., *Interpolation and Approximation by Rational Functions in the Complex Domain, Am. Math. Soc. Colloquium Publications*, vol. XX, New York, 1935, pp. 47, 260, 310, 313.

[10] For a related result, *cf.* Kierst and Szpilrajn, *loc. cit.*, p. 291.

[11] Bagemihl, F., and Seidel, W., *loc. cit.*

[12] *Ibid.*, Theorem 6.

[13] Cf. Bierberbach, *loc. cit.*, p. 35.

[14] *Ibid.*, p. 111.

[15] Cf. Lusin, N., and Priwaloff, J., "Sur l'unicité et la multiplicité des fonctions analytiques," *Ann. Sci. École Norm. Sup.*, (3), **42**, 143–191 (1925), p. 185.

[16] Cf. Bagemihl, F., and Seidel, W., *loc. cit.*, Theorem 7(b).

[17] Referring this time to Bagemihl, F., and Seidel, W., *ibid.*, Theorem 9 instead of Theorem 6.

[18] It is actually sufficient to assume merely that, for every Stolz angle S with vertex ζ_0, there exists a Stolz angle S_1 with vertex ζ_0 but otherwise wholly contained in the interior of S, such that $\sum |z_n - \zeta_0|^{\pi/\alpha(S)} = \infty$, $\sum |z_n|^{-\pi/\alpha(S)} = \infty$, respectively, where $\alpha(S)$ denotes the angular opening of S and the summation is extended over all $z_n \in S_1$. The proof relies on another extension of Blaschke's theorem; cf. Tsuji, M., "On Blaschke's Theorem," *Jap. J. Math.*, **3**, 65–68 (1926).

*THE GLOBAL BEHAVIOR OF DIFFERENTIAL EQUATIONS ON N-DIMENSIONAL MANIFOLDS**

By Felix Haas

Department of Mathematics, Princeton University

Communicated by S. Lefschetz, October 1, 1953

The study of differential equations in-the-large goes back to Poincaré. Poincaré and Bendixson proved the classical theorem in the field for characteristics remaining in a bounded domain of the plane. The theorem states that if such a characteristic does not have any singular points in its ω-limit set then this ω-limit set consists of exactly one closed curve characteristic (*limit cycle* of Poincaré). Until fairly recently not much was known about the structure of the limit set on manifolds. Denjoy[1] proved in the case of the two-dimensional torus that under certain analytic conditions the limit set is either a closed curve or the whole torus. In a previous communication this author proved that the limit set cannot be dense on a two-dimensional orientable closed manifold unless the manifold is the torus.[2,3] In fact, it was possible to give a number of sufficient conditions for the Poincaré-Bendixson Theorem to hold on closed, orientable two-dimensional manifolds different from the torus.[4]

In this communication the study of the global behavior of differential

equations on n-dimensional manifolds is initiated. Little is known in the field beyond the case when the manifold has Euler characteristic zero and the vector field is free of singular points.[6, 7] In this paper information will be given about manifolds with or without Euler characteristic zero carrying vector fields with or without singular points.

Definition: M_n will denote a compact n-dimensional twice-differentiable manifold. V will be a vector field on M_n with the following properties: (1) V is continuous, (2) V is sufficiently regular for the differential equation defined by V to satisfy a Lipschitz Condition, (3) the singular points of V form a compact set.

The pair (M_n, V) satisfying these conditions will be said to satisfy H_1.

Definition: Let C^+ be a positive semicharacteristic of (M_n, V) and let $\bar{C}$ be the set of ω-limit points of C^+.

If either the Euler characteristic of M_n is different from zero or V has singular points the following theorem rules out the behavior discussed by Denjoy for the case of a torus.

THEOREM 1. *Let (M_n, V) satisfy H_1. Suppose, in addition, that M_n is connected and there exists C^+ such that $\bar{C}$ is free of singular points. Then $\bar{C}$ is nowhere dense on M_n unless M_n has Euler characteristic zero and V is free of singular points. In this special case $\bar{C}$ is the whole manifold M_n.*

Theorem 1 is almost a direct consequence of Theorem 2.

THEOREM 2. *Let (M_n, V) satisfy H_1. Suppose there exists C^+ such that $\bar{C}$ is free of singular points and such that $\bar{C}$ contains an open set G. Then if E^+ is a characteristic of $\bar{C}$ and q is a point of E^+ there exists a point q' which follows q on E^+ and which is an interior point of G.*

It is to be noted that Theorems 1 and 2 give no information about odd-dimensional manifolds carrying a vector field free of singular points, since the Euler characteristic of a compact odd-dimensional manifold is always zero. However, the following theorem sheds light on this case.

THEOREM 3. *Let (M_n, V) satisfy H_1. Let M_n be the product of an $(n-1)$-dimensional manifold, M_{n-1}, with a circle S^1, $M_n = M_{n-1} \times S^1$. Let θ be the polar coordinate induced on M_n by S^1. Then if $d\theta/dt > 0$ for all points of M_n the differential equation defined by V admits periodic solutions unless the Euler characteristic of M_{n-1} is zero.*

Sketch of proof of Theorem 2: The theorem is proved in two steps. It is shown that if $\bar{C}$ contains a single boundary point then B contains an open set D which is part of a minimal set (in the sense of Birkhoff). If $\bar{C}$ has no boundary points or if $\bar{C}$ contains an open set contained in a minimal set the theorem follows.

Sketch of proof of Theorem 1: It follows from Theorem 2 that $\bar{C}$ is open in M_n. It is well known that $\bar{C}$ is closed in M_n. Hence, $\bar{C}$ is a component of M_n. The rest of the proof follows trivially.

Sketch of proof of Theorem 3: If we let $(M_{n-1} \times 0)$ be the product of

M_{n-1} with the point $\theta = 0$ on S^1 and $(M_{n-1} \times 2\pi)$ be the product of M_{n-1} with the point $\theta = 2\pi$ of S^1 then $(M_{n-1} \times 0) = (M_{n-1} \times 2\pi) = W^{n-1}$. $d\theta/dt > 0$ implies that each characteristic starting on W^{n-1} returns to W^{n-1}. We may thus define a map of W^{n-1} onto itself, which we shall denote by ϕ, in the following way. If p belongs to W^{n-1} then ϕp is the point at which the characteristic through p returns to W^{n-1}. ϕ is obviously a homeomorphism. We claim ϕ is homotopic to the identity map. For, consider the map ψ of $(W^{n-1} \times I)$ onto W^{n-1} defined as follows: Let $\sigma(p, x)$ be the point on the characteristic $p\phi p$ of our differential equation which has angular coordinate $\theta = (2\pi)x$. (Since $d\theta/dt > 0$ this is unique.) Then let $\psi(p, x)$ be the point with the same first $n - 1$ coordinates as $\sigma(p, x)$ but with the last coordinate equal to zero. Then

(i) ψ: $W^{n-1} \times 0$ is the identity.

(ii) ψ: $W^{n-1} \times 1$ is the map ϕ.

(iii) ψ is obviously a homotopy.

Hence, the map ϕ is homotopic to the identity. The Lefschetz number of ϕ therefore equals the Euler characteristic of W^{n-1} which is the same as the Euler characteristic of M_{n-1}.

By hypothesis M_n is compact, and this implies that M_{n-1} is compact. Hence, since the Lefschetz number of ϕ equals the Euler characteristic of M_{n-1} ϕ has fixed points unless the Euler characteristic of M_{n-1} is zero. The fixed points of ϕ correspond to periodic solutions. This proves the theorem.

The case when the Euler characteristic of M_{n-1} equals zero is then a special case. Different techniques, more like those used by Denjoy in his work on differential equations on the torus, are needed to describe ϕ. It is hoped that this case, as well as more detailed proofs of Theorems 1, 2, and 3 will be included in a subsequent paper.

* Work sponsored by the Office of Naval Research under contract N6ORI-105 at Princeton University.

[1] Denjoy, A., "Sur les courbes definies par les equations differentielles a la surface du tore," *J. Math. Pures et Appl.*, **11** (9), 333–375 (1932).

[2] Haas, F., "On the Global Behavior of Differential Equations on Two-Dimensional Manifolds," *Proc. Am. Math. Soc.*, **4** (4), 630–636 (1953).

[3] Haas, F., "A Theorem About Characteristics of Differential Equations on Closed Manifolds," PROC. NATL. ACAD. SCI., **38** (12), 1044–1047 (1952).

[4] Haas, F., "Poincaré-Bendixson Type Theorems for Differential Equations Defined on Two-Dimensional Manifolds Different from the Torus," *Ann. Math.* (to appear).

[5] Lefschetz, S., *Algebraic Topology*, A.M.S. Colloquium publication, vol. **xxvii**.

[6] Reeb, G., "Sur les solutions périodiques de systemes différentiels perturbés," *Canadian J. Math.*, **3** (3), 339–362 (1951).

[7] Seifert, H., "Closed Integral Curves in 3-Space and Isotopic Two-Dimensional Deformations," *Proc. Am. Math. Soc.*, **1** (6), 287–308 (1950).

[8] Siegel, C. L., "Note on Differential Equations on the Torus," *Ann. Math.*, **46** (3), 423–428 (1945).

CONJUGATE NETS, CONFORMAL STRUCTURE, AND INTERIOR TRANSFORMATIONS ON OPEN RIEMANN SURFACES*

BY JAMES JENKINS AND MARSTON MORSE

JOHNS HOPKINS UNIVERSITY AND INSTITUTE FOR ADVANCED STUDY

Communicated October 7, 1953

§1. Let Q be an open, orientable, connected, locally euclidean surface. Families of curves F and G are defined on Q with singularities at a countable, closed, discrete set ω of singular points, and are conditioned as in reference 1. The families of curves, obtained from curves of F and G by suitable continuation as simple curves through the singular points, are denoted by F^* and G^* respectively.

A pair $[F, G]$ of admissible families is called a *conjugate net* on Q, if for any sufficiently small neighborhood H of a point q of Q the curves in $F|H$ and $G|H$ are level curves on H of $\Re f_H$ and $\Im f_H$, respectively, where $w = f_H(p)|(p \in H)$ defines an interior map (sense preserving by our definition) of H into the w-plane. If Q has a conformal structure and if f_H is analytic, $[F, G]$ is termed *isothermal* on Q. If $[F, G]$ is a conjugate net on Q and if $[F, G]$ becomes isothermal for some conformal structure on Q, then $[F, G]$ is said to be *isothermally realizable*. Not every conjugate net $[F, G]$ on Q is isothermally realizable, as we show by example in the detailed treatment. We seek necessary and sufficient conditions on $[F, G]$ of a top (topological) nature, that $[F, G]$ be isothermally realizable.

Suppose that a conjugate net $[F, G]$ gives the non-singular level loci, respectively, of $\Re f$ and $\Im f$, where $w = f(p)|(p \in Q)$ is an interior map of Q into the w-plane. We say then that $[F, G]$ *contours* f. If Q is top equivalent to a finite z-plane, $[F, G]$ always contours some single-valued, interior map, f, of Q into the w-plane.[2] Let M be the universal covering surface of Q and Γ its cover group. If Γ is not trivial a conjugate net $[F, G]$ on Q contours an interior map of Q only exceptionally. As an example let Q be a surface Σ^* formed from a z-sphere Σ by deleting a north pole $N: z = \infty$, and a south pole $S: z = 0$. The family $[F_0, G_0]$ on Σ^* in which F_0 is the family of meridians and G_0 the family of parallels of constant latitude, contours no interior map of Σ^* into the w-plane. However $\log z$, which is single-valued on M, is contoured by $[F_0, G_0]$. This suggests the introduction of a basic class of interior maps λ of M into the w-plane as follows.

Class A. Class A shall consist of all interior maps $w = \lambda(p)|(p \in M)$ of M into the w-plane such that for each top map, $g \in \Gamma$, of M onto M,

$$\lambda g(p) = a_g \lambda(p) + b_g + ib_g' \qquad (p \in M, a_g \neq 0) \qquad (1.1)$$

where a_g, b_g, and b_g' are real constants uniquely determined by g and λ.

The significance of Class A is shown by the following fundamental theorems.

THEOREM 1.1. *A necessary and sufficient condition that a conjugate net* $[F, G]$ *on* Q *be isothermally realizable is that there exist an interior map,* $\lambda \epsilon A$, *contoured on* Q *by* $[F, G]$.

THEOREM 1.2. *Each interior map,* $\lambda \epsilon A$, *defines in a canonical way a conformal structure on* Q, *and each conformal structure on* Q *can be canonically defined by suitable choice of* $\lambda \epsilon A$.

Without going into details here we can say that the conformal structure on Q, canonically defined by $\lambda \epsilon A$, is one in which the preferred representations of Q in some neighborhood of a non-singular point p_0 of Q have the form $p = \lambda^{-1}(w)$, $p \epsilon Q$, so that the plane variable w is the local conformal parameter in a sufficiently small neighborhood of the point $w_0 = \lambda(p_0)$. With this understood we list four basic problems.

(i). Given a curve family F, admissible on Q, when does there exist a family G such that $[F, G]$ is a conjugate net on Q? [Cf. ref. 2.] (ii). Under what top conditions on a conjugate net $[F, G]$ on Q does $[F, G]$ contour an interior map $\lambda \epsilon A$? (iii). If $[F, G]$ contours $\lambda \epsilon A$ how are the coefficients a_ϱ, b_ϱ, b_ϱ' in (1.1) limited by the top characteristics of $[F, G]$. When does $[a_\varrho, b_\varrho, b_\varrho'] = [1, 0, 0]$? (iv). If $[F, G]$ contours $\lambda \epsilon A$, and λ canonically defines a conformal structure on Q, how do the resulting numerical conformal invariants of Q (when they exist) depend on the top characteristics of $[F, G]$?

Σ^*. We are able to answer these questions relatively completely in the logically basic case where Γ is generated by one element g. Suppose for the moment that Q admits some conformal structure. Let M^g be formed from M by identifying points p and $g(p)$ in M. The resulting surface M^g is top equivalent to the above punctured sphere Σ^*. The universal covering surface of M_ϱ is again M. We are then led[3] to study the problem in which $Q = \Sigma^*$. However many of our theorems apply to the general Q.

THEOREM 1.3. *A* $\lambda \epsilon A$ *is analytic on* M_λ *(defined as* M *conformally structured by* λ*) and the conjugate net* $[F, G]$ *on* Q *which projects into a net* $[F_M, G_M]$ *which contours* λ *is isothermal on* Q_λ *(*Q *conformally structured by* λ*).*

Transverse curve families. At this point we suppose that Q is separable and hence metrizable. Let R be an open subset of Q and let F and G be curve families admissible over R. We say that G is *transverse* to F over R if each element in G is an F-transversal [cf. ref. 3, §2]. We show that if G is transverse to F over R, F is transverse to G over R, and that F and G are mutually conjugate as defined above. The problem of conjugacy thus reduces to the problem of transversality.

§2. *F Admissible on* Σ^*.—To give solutions of the problems posed in §1 it is necessary to describe the curves in a family F admissible on Σ^*. Various definitions are needed.[3] Recall that elements in F^* are open

arcs or top circles on $\Sigma^* = \Sigma - N - S$. A sensed Jordan curve whose carrier is an element in F^* is called an *inner cycle*. An open arc in F^* with unique limiting end points at N and S is called an *F^*-meridian*. A simple, sensed, open curve, carried by an element in F^* with unique negative and positive limit points coinciding in $N[S]$, is called an *N-loop* [*S-loop*]. A countable sequence of disjoint N-loops, closed by N, bounding a region containing S, taken in their circular order about N, and consistently sensed, make up a continuous, sensed, closed curve which is locally simple except at N, and is termed an *N-cycle*. An S-cycle is similarly defined. N and S-cycles together with inner cycles are called *F^*-cycles*.

The first basic division of families F into classes is into families F which include a meridian and those which do not. A necessary and sufficient condition that F contain no meridian is that F contain a 1-parameter continuous family of non-singular elements in F which are all asymptotic in one sense to a common F^*-cycle φ or are all inner cycles. F may contain families of both of these types. The family of asymptotes may be asymptotic in the other sense to a different F^*-cycle but never to φ.

Regions. The family F defines certain fundamental regions (open connected sets) on Σ^*. Among the most important are the following. (1) A *meridional* region R is one in which points on non-singular F-meridians are everywhere dense. A meridional region is either doubly connected or simply connected. When doubly connected it is unique. When simply connected the boundary of R in Σ^* consists of two meridians and at most a countable set of disjoint N or S-loops. There is no singular point in a meridional region. (2) An *N-loop* [*S-loop*] *interior* is that region on Σ^* bounded by the loop which does not contain $S[N]$. If φ_n, $n = 1, \ldots$, is a sequence of non-singular N-loops with interiors $I\varphi_n$ such that $I\varphi_1 \subset I\varphi_2 \subset \ldots$, then Union $I\varphi_n$ is called an N-element. A maximal N-element is called an *N-primitive*. *S-primitives* are similarly defined. These primitives are fundamental.

Two primitives which intersect are identical. The number of primitives with diameters exceeding a positive constant is finite. Every loop is in the closure of a primitive. If there exists an F-meridian, Σ^* is the union of the closures on Σ^* of a finite set of meridional regions, and a finite or countably infinite set of primitives, all regions being disjoint. If F has a meridian but no meridional regions, we say that F gives *loop coverage* of Σ^*.

The index $\nu(F)$. A non-singular arc on Σ^* is termed m-transverse if the union of m consecutive transverse arcs. A non-singular top circle on Σ^* is termed m-transverse ($m > 1$) if the union of m consecutive transverse arcs, and 1-transverse if every open subarc is a transversal. An m-transverse top circle on Σ^*, separating N from S, for which m is a minimum is called an *F-guide*. The minimum m will be denoted by

$\nu(F)$. A point P of junction of two successive transverse arcs in an F-guide is called a *reversing point.* At P g reverses its sense of crossing of elements of F. By definition an F-guide is non-singular. An F-guide always exists with $\nu(F)$ finite. If F has a meridian, a necessary and sufficient condition that $\nu(F) = 0$ is that there exist a doubly connected meridional region R. The F-guide then lies in R. If F has no meridian $\nu(F) = 0$ or 2, and is 0 if and only if there are asymptotes in F. Each reversing point of an F-guide g lies in a primitive. There is one and only one reversing point in each primitive met by g.

The index $\mu(F)$. In the absence of meridional regions we set $\mu(F) = 0$. If there is just one meridional region set $\mu(F) = 1$. To proceed recall that an F-guide g meets each simply connected, meridional region R in an open arc without reversing point. The integer $\mu(F)$ counts these meridional regions R, counting as one any maximal sequence s of disjoint meridional regions successively met by g with an even number of reversing points between successive regions of s.

Kaplan[6] has studied non-singular families in the plane and on Σ^*. Our results confirm his in the non-singular case. However the introduction of the F-guide, $\nu(F)$, $\mu(F)$, primitives, and the existence of a restricted G (§3) transverse to a restricted F, are new concepts first published here.

§3. *Restricted Families* F.—In general a family F, admissible on Σ^*, does not contour a PH (pseudoharmonic) function on Σ^*. The true situation is revealed only by studying the covering surface M of Σ^*, and on M the curve family F_M which projects into F on Σ^*. Let p be a point in M with latitude α and longitude Θ, and let $p^{(n)} \in M$ be the point on M with latitude α and longitude $\Theta + 2n\pi$, $n = 0, \pm 1, \pm 2, \ldots$. Since M is simply connected there exists a function u which is PH over M and contoured by F_M.[1] We term such a u F_M*-admissible* on M, and say that u is *invariant* under a transformation $T(a, b)$ if for each $p \in M$

$$u(p^{(1)}) = a\,u(p) + b, \qquad (a \neq 0) \tag{3.1}$$

where a and b are real constants. Condition (3.1) is obtained from (1.1) for the case of Σ^* on taking $g \in \Gamma$ as the transformation which carries p into $p^{(1)}$, and replacing λ in (1.1) by the real part u of λ. There are two basic theorems.

THEOREM 3.1. *If there is at least one meridian in* F^* *and if there exists a function* u *which is* F_M*-admissible over* M *and invariant under a transformation* $T(a, b)$:

(i) *then* $a > 0$ *or* $a < 0$ *according as* $\nu(F)$ *is even or odd,*

(ii) *the conditions* $\mu(F) = 1$ *and* $a = 1$ *imply* $b \neq 0$,

(iii) *the conditions* $\mu(F) = 0$ *and* $a = 1$ *imply* $b = 0$.

Conversely if $T(a, b)$ *satisfies these necessary conditions but is otherwise arbitrary there exists a function* u *which is* F_M*-admissible over* M, *and invariant under* $T(a, b)$.

An inner cycle φ will be said to be *positively sensed* if the longitude of a point of φ which traces φ in its positive sense becomes infinite as φ is traversed arbitrarily many times. An N-cycle or S-cycle ψ will be said to be positively sensed if there exists a top circle on Σ^* separating N from S, positively sensed after the manner of φ, and within an arbitrarily small Fréchet distance of ψ.

The two open arcs into which a non-cyclic element in F^* is divided by a point p will be called F^*-*rays*, and given the senses by virtue of which p is an initial limiting point. An F^*-ray which is asymptotic to a positively [negatively] sensed F^*-cycle will be said to be of *asymptotic type* $+$ [$-$]. Let e represent $+$ or $-$. An element in F^* in which both F^*-rays are of type e will be said to be of *type* $[e, e]$, otherwise of type $[e, -e]$ or $[-e, e]$.

THEOREM 3.2. *In the case in which there is no meridian in F^* let u be a function which is F_M-admissible over M and invariant under $T(a, b)$. If there exist asymptotic F^*-rays then $a > 0$ and $a \neq 1$, each asymptotic F^*-ray is of type $+$ or $-$ according as $a > 1$ or $a < 1$, and inner F^*-cycles are isolated. If there are no asymptotic F^*-rays $a = 1$ and $b = 0$.*

Conversely corresponding to any family F and transformation $T(a, b)$ satisfying these conditions there exists a function u, F_M-admissible over M and invariant under $T(a, b)$.

Restricted F. We term a family F defined over Σ^* a restricted curve family if there exists a transformation $T(a, b)|a \neq 0$ and a function u, F_M-admissible over M and invariant under $T(a, b)$. When F has a meridian F is always restricted in accordance with Theorem 3.1. When F has no meridian it follows from Theorem 3.2 that F is restricted if and only if there are no asymptotic F^*-rays, or if asymptotic F^*-rays are all of one asymptotic type e and inner F^*-cycles are isolated. Families F exist in profusion which are not restricted. When F has no meridian and is restricted, the asymptotic limit cycles are isolated in Σ^*. The following is a difficult but basic theorem.

THEOREM 3.3. *Corresponding to an arbitrary restricted family F defined over Σ^* there exists at least one restricted curve family G transverse to F over Σ^*.*

Examples show that not every G transverse to a restricted F is restricted.

§4. *Interior Transformations.*—We return to the fundamental problem of the existence and nature of interior transformations λ, defined over the covering surface M of Σ^* and in Class A, as conditioned by (1.1). That is, λ is here to satisfy a relation of the form

$$\lambda(p^{(1)}) = a\lambda(p) + b + ib', \qquad (a \neq 0) \tag{4.1}$$

with a, b, b' real. We say then that λ is *invariant under* $T(a, b, b')$. There then exists a pair $[F, G]$ of restricted and mutually transverse curve families such that λ is contoured by $[F_M, G_M]$. We say then that $[F, G]$ is

associated with $T(a, b, b')$. We are concerned with the syntheses of λ, starting with a restricted F, seeking a restricted transverse G with a freedom to be determined, and finally a λ contoured by $[F, G]$ and invariant under $T(a, b, b')$, again with a freedom to be determined.

An interior transformation λ, defined on M, with $\lambda = u + iv$, is invariant under $T(a, b, b')$ if and only if u is invariant under $T(a, b)$ and v is invariant under $T(a, b')$. Thus we return to the results of §§2 and 3 and introduce appropriate notation as follows. We say that a class of restricted curve families F and a class K of transformations $T(a, b)$ are *associated* if corresponding to *each* $F \in H$ and *each* $T(a, b) \in K$ there exists a function u, F_M-admissible on M and invariant under $T(a, b)$. It is natural to distinguish the following seven classes H_i, $i = 1, \ldots, 7$, of restricted curve families and associated classes K_i of transformations $T(a, b)$. Here Π denotes the open half (a, b)-plane in which $a > 0$.

H_1: $\nu(F)$ even, positive $\mu(F) > 1$.
K_1: (a, b) arbitrary in Π.
H_2: $\nu(F)$ even, positive, loop coverage.
K_2: (a, b) arbitrary in Π, excluding every point but $(1, 0)$ on the line $a = 1$.
H_3: $\nu(F)$ even, $\geqq 0$, $\mu(F) = 1$.
K_3: (a, b) arbitrary in Π, excluding the point $(1, 0)$.
H_4: asymptotic F^*-rays of type $+$ exist.
K_4: $1 < a < \infty$, b arbitrary.
H_5: asymptotic F^*-rays of type $-$ exist.
K_5: $0 < a < 1$, b arbitrary.
H_6: no meridian or asymptotic F^*-ray exists.
K_6: $(a, b) = (1, 0)$.
H_7: $\nu(F)$ odd.
K_7: (a, b) arbitrary in the half plane $a < 0$.

No two classes K_i are identical. Each restricted curve family F is in a unique class H_i, $i = 1, \ldots, 7$. Each curve family $F \in H_i$ is associated with each $T(a, b)$ in K_i and with no other transformations. Given K_i, H_i is the maximal class of curve families for which this is true.

Let H_{ij} denote the class of restricted pairs $[F, G]$ with $F \in H_i$, $G \in H_j$. We term H_{ji} *conjugate* to H_{ij}. With H_{ij} we shall correlate the class T_{ij} of transformations $T(a, b, b')$ defined as follows. Let A_i be the set of points (a, b, b') in which (a, b) ranges over the values for which $T(a, b) \in K_i$ and b' is arbitrary. Similarly let A_i' be the set of points (a, b, b') for which (a, b) ranges over the values for which $T(a, b') \in K_i$ and b is arbitrary. Let $A_{ij} = A_i \cap A_j'$ and let T_{ij} be the set of transformations $T(a, b, b')$ in which (a, b, b') ranges over A_{ij}. The fact that for each $[F, G]$ in H_{43} or in H_{53}, $\nu(F) = \nu(G) = 0$, while for $[F, G]$ in H_{63}, $\nu(F) = 2$ and $\nu(G) = 0$, we indicate by writing

$$H_{43} = H_{43}^{\omega 0}, \qquad H_{53} = H_{53}^{00}, \qquad H_{63} = H_{63}^{20}$$

with similar meanings attached to H_{34}^{00}, H_{35}^{00}, H_{36}^{02}.

THEOREM 4.1. *The non-empty classes H_{ij} of restricted pairs $[F, G]$ are as follows: H_{ii}, $i = 7, 1, 2, 3, 4, 5$, H_{ij}, $i, j = 1, 2, 3$, H_{43}^{00}, H_{53}^{00}, H_{63}^{20} and their conjugate classes. For these classes each pair $[F, G]$ in H_{ij} is associated with each transformation $T(a, b, b')$ in T_{ij}. These classes H_{ij} are disjoint and include all restricted pairs $[F, G]$. The classes T_{ij} include each transformation associated with a pair in H_{ij}.*

COROLLARY 4.1. *To each restricted curve family F defined over Σ^* there correspond restricted curve families G transverse to F. For each such pair $[F, G]$ there exists an interior map λ of M into a complex plane such that λ is contoured by $[F_M, G_M]$ and invariant under some transformation $T(a, b, b')$. Thus every restricted pair $[F, G]$ is isothermally realizable.*

We turn now to a transformation λ which, like an integral, has an *additive module* $b + ib'$. Introduce three classes of values of a real variable b. In B_1, b is arbitrary, in B_2, $b = 0$, and in B_3, $b \neq 0$.

COROLLARY 4.2. (i) *In Corollary 4.1 the map λ can be chosen so that*

$$\lambda(p^{(1)}) = \lambda(p) + b + ib', \qquad (p \in M)$$

for some choice of (b, b') if and only if F or G includes a meridian, neither F nor G includes an asymptotic ray and $\nu(F)$ and $\nu(G)$ are even. (ii) *A map contoured by $[F, G]$ has a module $b + ib'$ if and only if $[F, G]$ is in a class entered in the following table in some* ith *row and* jth *column with $b \in B_i$ and $b' \in B_j$.*

b \ b'	B_1	B_2	B_3
B_1	H_{11}	H_{12}	H_{13}
B_2	H_{21}	H_{22}	$H_{23} \cup H_{63}^{20}$
B_3	H_{31}	$H_{32} \cup H_{36}^{02}$	H_{33}

The problem of the existence of an interior map, *single-valued* on Σ^* and contoured by $[F, G]$, is solved by the following.

COROLLARY 4.3. *There exists an interior map f of Σ^* into the complex plane contoured by a restricted transverse pair $[F, G]$ if and only if F and G contain meridians, both $\nu(F)$ and $\nu(G)$ are even and positive, and neither $\mu(F)$ nor $\mu(G) = 1$.*

With the aid of other numerical invariants of F and G, in particular of our F and G-*characteristic sequences* of pluses and minuses, it is possible to reveal a more intimate pattern of topological conditions of F on G and G on F, when F and G are restricted and mutually transverse. There is also the interesting use of *extremal length* to qualify our mappings. These matters will be reported on later.

* This note is an abstract of results to appear in the *Acta Mathematica 1954*, or in the *Report*[5] *of the Michigan Conference of June 1953*. These papers, together with three earlier papers of this series and papers by Kaplan[6] are listed below:

[1] "Topological Methods on Riemann Surfaces. Pseudoharmonic Function," Contributions to the Theory of Riemann Surfaces, *Ann. Math. Studies*, No. 30, 111–139 (1953).

[2] "The Existence of Pseudoconjugates on Riemann Surfaces," *Fund. Math.*, **39**, 269–287 (1952).

[3] "Curve Families F* Locally the Level Curves of a Pseudoharmonic Function," *Acta Mathematica* (1954).

[4] "Contour Equivalent Pseudoharmonic Functions and Pseudoconjugates," *Am. J. Math.*, **75**, 23–51 (1952).

[5] "Conjugate Nets on an Open Riemann Surface," Report of the Michigan Conference of June 1953; (to be published).

[6] Kaplan, "Regular Curve Families Filling the Plane," *Duke Math. J.*, **I**, 7, 154–185 (1940); **II**, 8, 11–45 (1941). "The Structure of a Curve-Family on a Surface in the Neighborhood of an Isolated Singularity," *Am. J. Math.*, **64**, 1–35 (1942).

*ON A DIFFERENTIAL-GEOMETRIC METHOD IN THE THEORY OF ANALYTIC STACKS**

By K. Kodaira

Department of Mathematics, Princeton University

Communicated by S. Lefschetz, September 9, 1953

1. Introduction.—Let V be a compact Kähler variety of complex dimension n and let F be a complex line bundle[1] over V whose structure group is the multiplicative group of complex numbers. Moreover let $\Omega^p(F)$ be the stack (faisceau) over V of germs of holomorphic p-forms with coefficients in F and let $H^q(V;\ \Omega^p(F))$ be the qth cohomology group of V with coefficients in $\Omega^p(F)$. It is important for applications to determine the circumstances under which the cohomology group $H^q(V;\ \Omega^p(F))$ vanishes. In the present note we shall prove by a differential-geometric method due to Bochner[2] some sufficient conditions for the vanishing of $H^q(V;\ \Omega^p(F))$ in terms of the characteristic class of the bundle F.

2. Harmonic Forms with Coefficients in Complex Line Bundles.[3]—We denote by $ds^2 = 2\sum g_{\alpha\beta^*}(dz^\alpha d\bar{z}^\beta)$ the Kähler metric on V. Take a sufficiently fine finite covering $\mathfrak{U} = \{U_j\}$ of V. Then the bundle F is determined by the system $\{f_{jk}\}$ of non-vanishing holomorphic functions f_{jk} defined, respectively, in $U_j \cap U_k$ and satisfying $f_{jk}f_{kl}f_{lj} = 1$ in $U_j \cap U_k \cap U_l$. Clearly there exists a system $\{a_j\}$ of real positive functions a_j of class C^∞ defined, respectively, in U_j satisfying

$$\frac{a_j}{a_k} = |f_{jk}|^2, \qquad \text{in } U_j \cap U_k. \tag{1}$$

A form φ with coefficients in F is, by definition, a system $\{\varphi_j\}$ of exterior differential forms φ_j defined, respectively, in U_j such that

$$\varphi_j = f_{jk} \cdot \varphi_k, \qquad \text{in } U_j \cap U_k.$$

For a form $\varphi = \{\varphi_j\}$ with coefficients in F, $\bar{\partial}\varphi = \{(\bar{\partial}\varphi)_j\}$ and $\delta\varphi = \{(\delta\varphi)_j\}$ are defined, respectively, by

$$(\bar{\partial}\varphi)_j = \bar{\partial}\varphi_j, \qquad (\delta\varphi)_j = -*a_j\partial\left(\frac{1}{a_j}*\varphi_j\right),$$

provided that φ is differentiable, where $*\varphi_j$ denotes the dual form of φ_j with respect to the preassigned Kähler metric ds^2 on V. The form φ is called *harmonic* if $\bar{\partial}\varphi = 0$ and $\delta\varphi = 0$.

Let $\Omega^p(F)$ be the stack (faisceau) over V of germs of holomorphic p-forms with coefficients in F. Then, as was shown by the author,[4] *the cohomology group $H^q(V; \Omega^p(F))$ of V with coefficients in $\Omega^p(F)$ is isomorphic to the space $H^{p,q}(F)$ consisting of all harmonic forms of type (p, q) with coefficients in F:*

$$H^q(V; \Omega^p(F)) \cong H^{p,q}(F). \tag{2}$$

As one readily infers, the mapping

$$\varphi = \{\varphi_j\} \to \varphi^\dagger = \{\varphi_j^\dagger\}, \quad \varphi_j^\dagger = \frac{1}{a_j}*\bar{\varphi}_j$$

maps $H^{p,q}(F)$ isomorphically onto $H^{n-p,n-q}(-F)$, where $-F$ denotes the complex line bundle defined by the system $\{f_{jk}^{-1}\}$. Combining this with (2), we obtain therefore the isomorphism[5]

$$H^q(V; \Omega^p(F)) \cong H^{n-q}(V; \Omega^{n-p}(-F)). \tag{3}$$

3. *An Inequality.*—The equations $\bar{\partial}\varphi = 0$, $\delta\varphi = 0$ for $\varphi = \{\varphi_j\}$,

$$\varphi_j = (1/p!q!)\sum \varphi_{j\tau_1\cdots\tau_p\alpha_1^*\cdots\alpha_q^*}\, dz^{\tau_1}\cdots dz^{\tau_p} d\bar{z}^{\alpha_1}\cdots d\bar{z}^{\alpha_q},$$

can be written explicitly in the forms

$$\sum_{m=0}^{q} (-1)^m \nabla_{\alpha_m^*}\varphi_{j\tau_1\cdots\tau_p\alpha_0^*\cdots\alpha_{m-1}^*\,\alpha_{m+1}^*\cdots\alpha_q^*} = 0, \tag{4}_1$$

$$\sum g^{\lambda\mu^*}(\nabla_\lambda + \rho_{j\lambda})\varphi_{j\tau_1\cdots\tau_p\mu^*\alpha_1^*\cdots\alpha_q^*} = 0, \tag{4}_2$$

where ∇_λ, ∇_{α^*} denote the covariant differentiations with respect to the local coordinates z^λ, $\bar{z}^\alpha$ and where

$$\rho_{j\lambda} = -\partial_\lambda \log a_j, \qquad \partial_\lambda = \frac{\partial}{\partial z^\lambda}.$$

Let $R^\sigma{}_{\tau\alpha^*\beta} = \bar{\partial}_\alpha(\sum g^{\sigma\nu^*}\partial_\beta g_{\tau\nu^*})$ be the curvature tensor and let $R_{\alpha^*\beta} = \sum_\tau R^\tau{}_{\tau\alpha^*\beta}$ be the Ricci tensor.[6] Moreover we set

$$X_{\lambda\alpha^*} = -\partial_\alpha \rho_{j\lambda} = \partial_\lambda \bar{\partial}_\alpha \log a_j. \tag{5}$$

Then, by a simple computation, we infer from (4) that, for any harmonic form $\varphi = \{\varphi_j\} \in H^{p,q}(F)$, the following relation holds:

$$\sum g^{\lambda\mu^*}(\nabla_\lambda + \rho_{j\lambda})\nabla_{\mu^*}\varphi_{j\tau_1\cdots\tau_p\alpha_1^*\cdots\alpha_q^*} = \sum_m \sum_h \sum R^{\sigma}{}_{\tau_h\alpha_m^*}{}^{\mu^*} \times$$

$$\varphi_{j\tau_1\cdots(\sigma)_h\cdots\tau_p\alpha_1^*\cdots(\mu^*)_m\cdots\alpha_q^*} + \sum_m \sum [X^{\mu^*}{}_{\alpha_m^*} - R^{\mu^*}{}_{\alpha_m^*}] \times$$

$$\varphi_{j\tau_1\cdots\tau_p\alpha_1^*\cdots(\mu^*)_m\cdots\alpha_q^*}, \tag{6}$$

where $X^{\mu^*}{}_{\alpha^*} = \sum g^{\lambda\mu^*}X_{\lambda\alpha^*}$, $R^{\mu^*}{}_{\alpha^*} = \sum g^{\lambda\mu^*}\bar{R}_{\lambda^*\alpha}$ and where $(\sigma)_h$ or $(\mu^*)_m$ indicates that τ_h or α_m^* is to be replaced by σ or μ^* respectively. We note here that $\partial\bar{\partial}\log a_j = \partial\bar{\partial}\log a_k$ in $U_j \cap U_k$, so

$$\sum X_{\lambda\alpha^*}dz^\lambda d\bar{z}^\alpha = \partial\bar{\partial}\log a_j \tag{7}$$

is a well defined 2-form on the whole of V. Now we set

$$\xi_{\mu^*} = \frac{1}{a_j}\sum \nabla_{\mu^*}\varphi_{j\tau_1\cdots\tau_p\alpha_1^*\cdots\alpha_q^*}\bar{\varphi}_j^{\tau_1\cdots\tau_p\alpha_1^*\cdots\alpha_q^*}$$

where

$$\bar{\varphi}_j^{\tau_1\cdots\tau_p\alpha_1^*\cdots\alpha_q^*} = \sum g^{\tau_1\sigma_1^*}\cdots g^{\tau_p\sigma_p^*}g^{\beta_1\alpha_1^*}\cdots g^{\beta_q\alpha_q^*}\overline{\varphi_{j\sigma_1\cdots\sigma_p\beta_1^*\cdots\beta_q^*}}.$$

Then $\xi = \sum \xi_{\tau^*}d\bar{z}^\tau$ is a well defined 1-form on V and

$$-\delta\xi = \sum g^{\lambda\mu^*}\nabla_\lambda\xi_{\mu^*}$$

$$= \# + \frac{1}{a_j}\sum g^{\lambda\mu^*}(\nabla_\lambda + \rho_{j\lambda})\nabla_{\mu^*}\varphi_{j\tau_1\cdots\tau_p\alpha_1^*\cdots\alpha_q^*}\bar{\varphi}_j^{\tau_1\cdots\tau_p\alpha_1^*\cdots\alpha_q^*} \tag{8}$$

where

$$\# = \frac{1}{a_j}\sum g^{\lambda\mu^*}\nabla_{\mu^*}\varphi_{j\tau_1\cdots\tau_p\alpha_1^*\cdots\alpha_q^*}\overline{\nabla_{\lambda^*}\varphi_j^{\tau_1\cdots\tau_p\alpha_1^*\cdots\alpha_q^*}} \geqq 0.$$

Denoting by g the determinant $g = |g_{\alpha\beta^*}|$, we have $\int_V \delta\xi \cdot g dV = 0$, where $dV = (i)^n dz^1 d\bar{z}^1 \cdots dz^n d\bar{z}^n$. Combining (6) with (8), we obtain therefore the inequality

$$0 \geqq \int_V \Big\{ q\sum(\delta^\sigma{}_\tau[X^{\beta^*}{}_{\alpha^*} - R^{\beta^*}{}_{\alpha^*}] + pR^\sigma{}_{\tau\alpha^*}{}^{\beta^*})\cdot$$

$$\frac{1}{a_j}\varphi_{j\sigma\tau_2\cdots\tau_p\beta^*\alpha_2^*\cdots\alpha_q^*}\bar{\varphi}_j^{\tau\tau_2\cdots\tau_p\alpha^*\alpha_2^*\cdots\alpha_q^*}\Big\} g dV. \tag{9}$$

By a (p, q)-form we shall mean a $(p + q)$-form of type (p, q). A real (1,1)-form ψ on V can be written in the form $\psi = i\sum \psi_{\alpha\beta^*}(z, \bar{z})dz^\alpha d\bar{z}^\beta$, where $\psi_{\alpha\beta^*} = \psi_{\alpha\beta^*}(z, \bar{z})$ satisfy $\bar{\psi}_{\alpha\beta^*} = \psi_{\beta\alpha^*}$. *We say that such a form* ψ

is positive and write $\psi > 0$ *if the Hermitian form* $\sum \psi_{\alpha\beta^*}(z, \bar{z})\bar{u}^\alpha u^\beta$ *in* n *variables* $u^1, u^2, \ldots, u^n$ *is positive definite at each point* z *on* V.

Now, let $c(F)$ be the characteristic class of the principal bundle associated with F.

LEMMA. *Let* $\{a_j\}$ *be a system of functions satisfying* (1). *Then the real* d*-closed* (1,1)*-form* $\gamma = (i/2\pi)\partial\bar{\partial} \log a_j$ *belongs*[7] *to the characteristic class* $c(F)$ *of the bundle* F. *Conversely, given a* d*-closed real* (1,1)*-form* γ *of class* C^∞ *belonging to the characteristic class* $c(F)$, *there exists a system* $\{a_j\}$ *of positive functions* a_j *of class* C^∞ *satisfying* (1) *such that* $(i/2\pi)\partial\bar{\partial} \log a_j = \gamma$.

Proof: Let π be the canonical projection of F onto V and let ζ_j be the linear coordinate on the fibre $\pi^{-1}(z)$, $z \in U_j$, such that $\zeta_j = f_{jk}(z)\zeta_k$ for $z \in U_j \cap U_k$. The principal bundle F^* associated with F is obtained from F by removing the origin $\zeta_j = 0$ of each fibre $\pi^{-1}(z)$. Now

$$\Phi = \frac{1}{2\pi i}(d \log \zeta_j - \partial \log a_j)$$

is a well defined 1-form of class C^∞ on the principal bundle F^* and

$$-d\Phi = \frac{i}{2\pi}\partial\bar{\partial} \log a_j,$$

while the restriction of Φ to the fibre $\pi^{-1}(z)^* = \pi^{-1}(z) - (0)$ of F^* equals the d-closed 1-form $(1/2\pi i)d \log \zeta_j$ which represents the basic cohomology class of $\pi^{-1}(z)^*$. This shows that $\gamma = (i/2\pi)\partial\bar{\partial} \log a_j$ belongs to the characteristic class $c(F)$ of F^*.

To prove that every γ belonging to $c(F)$ can be written in the form $\gamma = (i/2\pi)\partial\bar{\partial} \log a_j$, we take a system $\{a_j'\}$ satisfying (1) and consider the difference $\gamma_0 = \gamma - (i/2\pi)\partial\bar{\partial} \log a_j'$. Obviously the harmonic part $H\gamma_0$ of γ_0 vanishes and consequently $\gamma_0 = \Delta G\gamma_0 = 2\partial\bar{\partial}G\gamma_0$, where G denotes the Green's operator. Using the formula[8] $\Lambda\partial - \partial\Lambda = -i\bar{\partial}$, we get therefore $\gamma_0 = i2\partial\bar{\partial}\Lambda G\gamma_0$. Now $r = 2\Lambda G\gamma_0$ is a real scalar function of class C^∞ defined on the whole of V and, hence, setting $a_j = a_j' \cdot e^{z+\bar{r}}$ we obtain a system $\{a_j\}$ of positive functions a_j of class C^∞ satisfying (1) and also $(i/2\pi)\partial\bar{\partial} \log a_j = \gamma$.

Now, letting $\gamma = (i/2\pi)\sum X_{\alpha\beta^*}dz^\alpha d\bar{z}^\beta$ be an arbitrary real (1,1)-form, we introduce the Hermitian form

$$\Theta^{p,q}(\gamma, u; z) = \sum (\delta^\sigma{}_\tau[X^{\beta^*}{}_{\alpha^*} - R^{\beta^*}{}_{\alpha^*}] + pR^\sigma{}_{\tau\alpha^*}{}^{\beta^*}) \times u_{\sigma\tau_2\ldots\tau_p\beta^*\alpha_2^*\ldots\alpha_q^*}\bar{u}^{\tau\tau_2\ldots\tau_p\alpha^*\alpha_2^*\ldots\alpha_q^*}$$

in a skew-symmetric tensor $u_{\tau_1\tau_2\ldots\tau_p\alpha_1^*\ldots\alpha_q^*}$ at each point z on V, provided that $q \geqq 1$. Then the inequality (9) can be written in the following form:

$$\int_V \frac{g}{a_j}\Theta^{p,q}(\gamma, \varphi_j; z)dV \leqq 0, \qquad \text{for } q \geqq 1. \tag{10}$$

With the help of the above lemma, we derive from (10) the following theorem:

THEOREM 1. *If the characteristic class $c(F)$ of F contains a real d-closed $(1,1)$-form $\gamma = (i/2\pi)\sum X_{\alpha\beta^*}dz^\alpha d\bar{z}^\beta$ which is sufficiently large with respect to the order $>$ in the sense that the Hermitian form $\Theta^{p,q}(\gamma, u; z)$ is positive definite at each point z on V, then the cohomology groups $H^q(V, \Omega^p(F))$ and $H^{n-q}(V, \Omega^{n-p}(-F))$ both vanish, provided that $1 \leqq q \leqq n$.*

Proof: In view of (2) and (3), it is sufficient to show that $H^{p,q}(F) = 0$. By virtue of the above lemma, we may choose the system $\{a_j\}$ satisfying (1) such that $(i/2\pi)\partial\bar{\partial} \log a_j = \gamma$. Then the inequality (10) holds for any $\varphi = \{\varphi_j\} \in H^{p,q}(F)$, while, by hypothesis, $\Theta^{p,q}(\gamma, \varphi_j; z) > 0$ unless $\varphi_j = 0$. This proves that $H^{p,q}(F) = 0$, q. e. d.

In the case where $p = n$, we have

$$\Theta^{n,q}(\gamma, u; z) = n! \sum X^{\beta^*}{}_{\alpha^*} u_{12\ldots n\beta^*\alpha_2^*\ldots\alpha_q^*}\bar{u}^{12\ldots n\alpha^*\alpha_2^*\ldots\alpha_q^*}.$$

Hence $\Theta^{n,q}(\gamma, u; z)$ is positive definite if and only if $\gamma > 0$. As a corollary to the above theorem, we therefore obtain the following:

THEOREM 2. *If $c(F)$ contains a real d-closed $(1,1)$-form $\gamma > 0$, then the cohomology groups $H^q(V, \Omega^n(F))$ and $H^{n-q}(V, \Omega^0(-F))$ both vanish for $1 \leqq q \leqq n$.*

By the *canonical bundle* over V we shall mean the complex line bundle K defined by the system $\{J_{jk}\}$ of Jacobians

$$J_{jk} = \frac{\partial(z_k^1, \ldots, z_k^n)}{\partial(z_j^1, \ldots, z_j^n)},$$

where $(z_j^1, \ldots, z_j^n)$ is the local coordinates in U_j. We note that $-c(K)$ equals the first Chern class of the variety V. Since the isomorphism

$$\Omega^0(F) \cong \Omega^n(F - K)$$

holds in an obvious manner, we get from the above theorem the following:

THEOREM 3. *If $c(F) - c(K)$ contains a real d-closed $(1,1)$-form $\gamma > 0$, then the cohomology group $H^q(V, \Omega^0(F))$ vanishes for $1 \leqq q \leqq n$.*

* This work was supported by a research project at Princeton University sponsored by the Office of Ordnance Research, U. S. Army.

[1] By a complex line bundle over V will be meant an analytic fibre bundle over V whose fibre is the complex number field C and whose structure group is the mutiplicative group C^* of complex numbers acting on C. Cf. Kodaira, K., and Spencer, D. C., "Groups of Complex Line Bundles Over Compact Kähler Varieties," these PROCEEDINGS, **39**, 868–872 (1953).

[2] Bochner, S., "Curvature and Betti Numbers" (I) and (II), *Ann. Math.*, **49**, 379–390 (1948); **50**, 77–93 (1949).

[3] See Kodaira, K., "On Cohomology Groups of Compact Analytic Varieties with Coefficients in Some Analytic Faisceaux," these PROCEEDINGS, **39**, 865–868 (1953).

[4] Kodaira, *loc. cit.*

[5] This result reduces to a special case of Serre's duality theorem.

[6] See Garabedian, P. R., and Spencer, D. C., "A Complex Tensor Calculus for Kähler Manifolds," *Acta Math.*, **89**, 279–331 (1953).

[7] In view of de Rham's theorem, any cohomology class may be regarded as a class of d-closed forms. By a d-closed form we shall mean a form which is closed under d.

[8] Garabedian and Spencer, *loc. cit.*, p. 290.

ON A THEOREM OF LEFSCHETZ AND THE LEMMA OF ENRIQUES-SEVERI-ZARISKI*

BY K. KODAIRA AND D. C. SPENCER

DEPARTMENT OF MATHEMATICS, PRINCETON UNIVERSITY

Communicated by S. Lefschetz, October 8, 1953

1. *Introduction.*—The present note is mainly concerned with a generalization of a theorem of Lefschetz which establishes a relation between the cohomology groups of an algebraic variety and those of its general hyperplane sections. We generalize the theorem to the case of cohomology groups of Kähler varieties with coefficients in some analytic stacks. Our generalization includes the lemma of Enriques-Severi-Zariski as a special case.

2. *Some Exact Sequences of Stacks.*—Let V be a compact Kähler variety of complex dimension n and let S be a non-singular analytic subvariety of V of complex dimension $n-1$. Take a sufficiently fine finite covering $\{U_j\}$ of V. Then, in each U_j, the subvariety S is defined by a holomorphic equation $s_j = 0$. We associate with S the complex line bundle[1] $\{S\}$ determined by the system $\{s_{jk}\}$ of non-vanishing holomorphic functions $s_{jk} = s_j/s_k$ defined, respectively, in $U_j \cap U_k$. We note that the characteristic class[2] $c(\{S\})$ of $\{S\}$ is the dual of the homology class of the cycle S. For simplicity's sake, we set $c(S) = c(\{S\})$. Now, let F be an arbitrary complex line bundle over V and let $\Omega^p(F)$ be the stack over V of the germs of holomorphic p-forms with coefficients in F. Take a point $\mathfrak{p} \in S \cap U_j$ and choose a system of local coordinates $(z_j^1, \ldots, z_j^n)$ in U_j such that $s_j(z) = z_j^1$. Then each germ $\eta_j \in \Omega^p(F)_\mathfrak{p}$ can be written in the form

$$\eta_j = \sum_{1<\alpha_1<\ldots<\alpha_p} \eta_{j\alpha_1\ldots\alpha_p}\, dz_j^{\alpha_1} \ldots dz_j^{\alpha_p} + \sum_{1<\alpha_2<\ldots<\alpha_p} \eta_{j1\alpha_2\ldots\alpha_p}\, dz_j^1\, dz_j^{\alpha_2} \ldots dz_j^{\alpha_p},$$

where $\Omega^p(F)_\mathfrak{p}$ is the fiber of $\Omega^p(F)$ over the point $\mathfrak{p}$. With the help of this expression, we associate with η_j two germs η_j', η_j'' of holomorphic forms on S defined, respectively, by

$$\eta_j' = \sum_{1<\alpha_1<\ldots<\alpha_p} (\eta_{j\alpha_1\ldots\alpha_p})_S\, dz_j^{\alpha_1} \ldots dz_j^{\alpha_p},$$

$$\eta_j'' = \sum_{1<\alpha_2<\ldots<\alpha_p} (\eta_{j1\alpha_2\ldots\alpha_p})_S\, dz_j^{\alpha_2} \ldots dz_j^{\alpha_p},$$

where $(\quad)_S$ denotes restriction to S. Let $\{f_{jk}\}$ be the system of non-vanishing holomorphic functions defining the bundle F. Assuming that $\mathfrak{p} \in U_j \cap U_k$, we infer readily from the relation $\eta_j = f_{jk}\eta_k$ that

$$\eta_j' = (f_{jk})_S \cdot \eta_k' \tag{1}$$

and that

$$\eta_j'' = (f_{jk}S_{jk}^{-1})_S \cdot \eta_k'' + \sum_{\alpha>1} \left(f_{jk}\frac{\partial z_k^\alpha}{\partial z_j^1}\right)_S \eta_{k\alpha}' \tag{2}$$

where

$$\eta_{k\alpha}' = \sum_{1<\alpha_1<\ldots<\alpha_p} (\eta_{k\alpha\alpha_1\ldots\alpha_p})_S \, dz_k^{\alpha_1} \ldots dz_k^{\alpha_p}.$$

The equality (1) shows that $\eta_j' \in \Omega^p(F_S)_\mathfrak{p}$ and that $r' : \eta_j \to \eta_j'$ is a homomorphic mapping of the stack $\Omega^p(F)$ *onto* $\Omega^p(F_S)$, where F_S denotes the restriction of F to S. Letting $\Omega''^p(F)$ be the kernel of this homomorphism r', we obtain therefore the *exact sequence*

$$0 \longrightarrow \Omega''^p(F) \xrightarrow{i} \Omega^p(F) \xrightarrow{r'} \Omega^p(F_S) \longrightarrow 0. \tag{3}$$

Now, it follows from (2) that, if $\eta_j' = 0$, the relation

$$\eta_j'' = (f_{jk}S_{jk}^{-1})_S \cdot \eta_k''$$

holds. This shows that $\eta_j'' \in \Omega^{p-1}(F_S - \{S\}_S)$ for any $\eta_j \in \Omega''^p(F)$. Moreover $r'' : \eta_j \to \eta_j''$ is a homomorphic mapping of $\Omega''^p(F)$ *onto* $\Omega^{p-1}(F_S - \{S\}_S)$. As one readily infers, $\zeta_j = s_j^{-1} \cdot \eta_j$ is holomorphic if and only if η_j'' vanishes, while $i : \zeta_j \to \eta_j = s_j\zeta_j$ is an isomorphic mapping of $\Omega^p(F - \{S\})$ *into* $\Omega''^p(F)$. Thus we see that *the sequence*

$$0 \longrightarrow \Omega^p(F - \{S\}) \xrightarrow{i} \Omega''^p(F) \xrightarrow{r''} \Omega^{p-1}(F_S - \{S\}_S) \longrightarrow 0 \tag{4}$$

is exact. From (3) and (4) we obtain the corresponding *exact cohomology sequences:*

$$\ldots \xrightarrow{i^*} H^{q-1}(V, \Omega^p(F)) \xrightarrow{r'^*} H^{q-1}(S, \Omega^p(F_S)) \xrightarrow{\delta^*} H^q(V, \Omega''^p(F)) \longrightarrow \ldots \tag{5}$$

and

$$\ldots \xrightarrow{i^*} H^{q-1}(V, \Omega''^p(F)) \xrightarrow{r''^*} H^{q-1}(S, \Omega^{p-1}(F_S - \{S\}_S)) \xrightarrow{\delta^*} H^q(V, \Omega^p(F - \{S\})) \longrightarrow \ldots. \tag{6}$$

We note that $\Omega''^0(F) \cong \Omega^0(F - \{S\})$. Thus, in the extremum case $p = 0$, the above sequences (5), (6) reduce to a single exact sequence

$$\cdots \xrightarrow{i^*} H^{q-1}(V, \Omega^0(F)) \xrightarrow{r'^*} H^{q-1}(S, \Omega^0(F_S)) \xrightarrow{\delta^*} H^q(V, \Omega^0(F - \{S\})) \longrightarrow \cdots. \quad (7)$$

3. Generalization of a Theorem of Lefschetz.—We say that a complex line bundle F is *ample* if the characteristic class $c(F)$ of F contains a real d-closed $(1, 1)$-form[3] $\gamma > 0$.

THEOREM 1. *Assume the bundle $\{S\}$ to be sufficiently ample compared with F in the sense that each cohomology class $c(m\{S\} - F)$, $m = 1, 2, \ldots, n$, contains, respectively, a real d-closed $(1, 1)$-form $\gamma_m > 0$ for which $\Theta^{p,q}(\gamma_m, u, z)$, $1 \leqq p, q, \leqq n$, are positive definite at each point z on V, where $\Theta^{p,q}(\gamma, u, z)$ are the Hermitian forms in u introduced in the previous note.[4] Then the restriction map*

$$r'^*: H^q(V, \Omega^p(F)) \to H^q(S, \Omega^p(F_S))$$

is an isomorphism into or onto according as $p + q = n - 1$ or $p + q < n - 1$.

Proof: Set $F_m = F - m\{S\}$. Then, by virtue of Theorem 1 of the previous note,[5] the cohomology group $H^q(V, \Omega^p(F_m))$ vanishes for $q \leqq n - 1$, $1 \leqq m \leqq n$. Hence, replacing F by F_m, we infer from (5) the isomorphism

$$H^q(S, \Omega^p(F_{mS})) \cong H^{q+1}(V, \Omega''^p(F_m)), \quad \text{for } q \leqq n - 2, \quad 1 \leqq m \leqq n, \quad (8)$$

where F_{mS} denotes the restriction $(F_m)_S$ of F_m to S. Similarly, setting $F = F_{m-1}$ in (6), we get

$$H^q(V, \Omega''^p(F_{m-1})) \cong H^q(S, \Omega^{p-1}(F_{mS})), \quad \text{for } q \leqq n - 2, \quad 1 \leqq m \leqq n, \quad (9)$$

provided that $p \geqq 1$ (we assume always $p \leqq n - 1$). Combining (8) with (9), we obtain

$$H^q(V, \Omega''^p(F)) \cong H^{p+q}(V, \Omega''^0(F_p)), \quad \text{for } p + q \leqq n - 1, \quad p \geqq 1, \quad (10)$$

while we have $\Omega''^0(F_p) \cong \Omega^0(F_{p+1})$. By Theorem 1 of the previous note,[6] we have

$$H^q(V, \Omega''^p(F)) \cong H^{p+q}(V, \Omega^0(F_{p+1})) = 0, \quad \text{for } p + q \leqq n - 1. \quad (11)$$

This clearly holds also in the case $p = 0$. Now, combining (5) with (11), we infer readily that $r'^*: H^q(V, \Omega^p(F)) \to H^q(S, \Omega^p(F_S))$ is an isomorphism into or onto according as $p + q = n - 1$ or $p + q < n - 1$, q. e. d.

The above theorem may be regarded as a generalization of a theorem of Lefschetz concerning the homology of hyperplane sections of algebraic

varieties. In fact, letting C be the field of complex numbers, we have the commutative diagram[7]

$$\begin{array}{ccc} H^s(V, C) \cong & \sum_{p+q=s} & H^q(V, \Omega^p) \\ \Big\downarrow r^* & & \Big\downarrow r'^* \\ H^s(S, C) \cong & \sum_{p+q=s} & H^q(S, \Omega_S^p), \end{array}$$

where $\Omega^p = \Omega^p(0)$ is the stack over V of germs of holomorphic p-forms (without coefficients in a bundle), $\Omega_S^p = \Omega^p(0_S)$ the corresponding stack over S and where r^* is the canonical restriction map. We therefore infer from Theorem 1 the following:

THEOREM 2.[8] *If the bundle $\{S\}$ is sufficiently ample in the sense that the cohomology class $c(S)$ contains a real d-closed $(1, 1)$-form $\gamma > 0$ for which the Hermitian forms $\Theta^{p,q}(\gamma, u, z)$, $1 \leqq p, q \leqq n$, are positive definite at each point z on V, then the restriction map $r^*: H^s(V, C) \to H^s(S, C)$ is an isomorphism into or onto according as $s = n - 1$ or $s < n - 1$.*

4. The Lemma of Enriques-Severi-Zariski.[9]—The lemma of Enriques-Severi-Zariski may be formulated as follows: *Let V be a non-singular algebraic variety imbedded in a projective space and let S_h be the section of V cut out by a general hypersurface of order h. Given a divisor D on V, there exists an integer $h_0(D)$, depending on D, such that the isomorphism*

$$H^0(V, \Omega^0(\{D\})) \overset{r'^*}{\cong} H^0(S_h, \Omega^0(\{D\}_{S_h})) \tag{12}$$

holds for all $h \geqq h_0(D)$. It is clear that this lemma reduces to a special case of our Theorem 1 above. In fact, since the cohomology class $c(S_h)$ contains the real d-closed $(1, 1)$-form $h \cdot \omega$, $\omega = i \sum g_{\alpha\bar{\beta}} dz^\alpha d\bar{z}^\beta > 0$ being the fundamental form associated with the "standard" Kähler metric on V, we can find an integer $h_0 = h_0(D)$ such that $\{S_h\}$ is sufficiently ample compared with $\{D\}$ in the sense of the hypothesis of Theorem 1 for all $h \geqq h_0(D)$.

5. Characteristic Deficiencies.—In analogy with the case of algebraic varieties,[10] we define the *deficiency* $\operatorname{def}(F/S)$ of the bundle F over S by

$$\operatorname{def}(F/S) = \dim H^0(S, \Omega^0(F_S)) - \dim r'^* H^0(V, \Omega^0(F)).$$

The deficiency $\operatorname{def}(\{S\}/S)$ of $\{S\}$ over S may be called the *characteristic deficiency* of S, since $\operatorname{def}(\{S\}/S)$ is equal to the deficiency of the characteristic system on S of the complete linear system $|S|$.

THEOREM 3.[11] *The characteristic deficiency $\operatorname{def}(\{S\}/S)$ of a non-singular prime divisor S on V is never greater than the number g_1 of the linearly independent simple differentials of the first kind attached to V, and the equality*

def$(\{S\}/S) = g_1$ *holds if the bundle* $\{S\}$ *is sufficiently ample in the sense that the cohomology class* $c(S) + c_1$ *contains a real d-closed* $(1, 1)$*-form* $\gamma > 0$*, where* c_1 *is the first Chern class of* V.

Proof: Setting $F = \{S\}$ in (7), we get the exact sequence

$$\ldots \to H^0(V, \Omega^0(\{S\})) \xrightarrow{r'^*} H^0(S, \Omega^0(\{S\}_S)) \xrightarrow{\delta^*} H^1(V, \Omega^0) \to H^1(V, \Omega^0(\{S\})) \to \ldots. \quad (13)$$

By a result of Dolbeault,[12] dim $H^1(V, \Omega^0) = g_1$, while Theorem 3 of the previous note asserts that $H^1(V, \Omega^0(\{S\}))$ vanishes if $c(S) + c_1$ contains $\gamma > 0$. Hence, from (13), we conclude our theorem.

6. *Remarks.*—The Euler characteristic $\chi_V(\mathfrak{F})$ of V with coefficients in a stack $\mathfrak{F}$ over V is defined by

$$\chi_V(\mathfrak{F}) = \sum(-1)^q \dim H^q(V, \mathfrak{F})$$

provided that each cohomology group $H^q(V, \mathfrak{F})$ has a finite dimension. Setting

$$\chi_V^p(F) = \chi_V(\Omega^p(F)),$$

we infer from (5) and (6) the equalities

$$\chi_V^p(F) = \chi_V(\Omega''^p(F)) + \chi_S^p(F_S),$$

$$\chi_V(\Omega''^p(F)) = \chi_V^p(F - \{S\}) + \chi_S^{p-1}(F_S - \{S\}_S),$$

and consequently

$$\chi_V^p(F) = \chi_V^p(F - \{S\}) + \chi_S^p(F_S) + \chi_S^{p-1}(F_S - \{S\}_S). \quad (14)$$

In this connection we add here a remark on our note concerning arithmetic genera of algebraic varieties.[13] Since, as (2) shows, η_j'' is not invariantly defined unless $\eta_j' = 0$, the mapping $\eta_j \to \eta_j' + \eta_j''$ does *not* give the isomorphism

$$\Omega^p(F)/\Omega^p(F - \{S\}) \cong \Omega^p(F_S) + \Omega^{p-1}(F_S - \{S\}_S)$$

except for the case $p = 0$ or $p = n$. Thus the formula (13) in our note[14] cannot be justified, whereas the formula (16) of fundamental importance, which we derived from (13), still holds, since (16) reduces to a special case of our equality (14) above. A similar remark applies to the note.[15]

* This work was supported by a research project at Princeton University sponsored by the Office of Ordnance Research, U. S. Army.

[1] For the relation between divisors and complex line bundles, see K. Kodaira and D. C. Spencer, "Divisor Class Groups on Algebraic Varieties," these PROCEEDINGS **39**, 872–877 (1953).

[2] See Kodaira and Spencer, *loc. cit.*

[3] By a d-closed (p, q)-form we shall mean a $(p + q)$-form of type (p, q) which is closed under d. Cf. Kodaira, K., "On a Differential-Geometric Method in the Theory of Analytic Stacks," these PROCEEDINGS, **39**, 1268–1273 (1953).

[4] Kodaira, *loc. cit.*

[5] Kodaira, *loc. cit.*

[6] Kodaira, *loc. cit.*

[7] This follows from a result of Dolbeault, P., "Sur la cohomologie des variété analytiques complexes," *Compt. rend., Paris*, **236**, 175–177 (1953).

[8] Lefschetz, S., *L'Analysis situs et la géometrie algébrique*, Gauthier-Villars, Paris, 1924, pp. 88–91.

[9] Zariski, O., "Complete Linear Systems on Normal Varieties and a Generalization of a Lemma of Enriques-Severi," *Ann. Math.*, **55**, 552–592 (1952).

[10] See, for example, Zariski, O., *loc. cit.*

[11] This theorem may be regarded as a generalization of a "fundamental" theorem for algebraic surfaces to the effect that an algebraic surface of irregularity q possesses exactly q independent simple differentials of the first kind. See Zariski, *Algebraic Surfaces*, Springer, Berlin, 1935, p. 123.

[12] Dolbeault, *loc. cit.*

[13] Kodaira, K., and Spencer, D. C., these PROCEEDINGS, **39**, 641–649 (1953).

[14] Kodaira and Spencer, *loc. cit.* in ref. 14, p. 645.

[15] Spencer, D. C., "Cohomology and the Riemann-Roch Theorem," these PROCEEDINGS, **39**, 660–669 (1953).

ON A NEW PROBLEM CONCERNING TRINOMIAL CONGRUENCES INVOLVING RATIONAL INTEGERS

BY ERNA H. PEARSON AND H. S. VANDIVER

ATLANTA, GEORGIA; AND DEPARTMENT OF MATHEMATICS, UNIVERSITY OF TEXAS

Communicated October 5, 1953

As a background for the study of the topic mentioned in the title, we first consider more general problems. Let

$$c_1 x_1^{m_1} + \ldots + c_s x_s^{m_s} = c, \qquad (1)$$

where the c's are given elements in a finite field of order p^n, p prime, none zero, the m's divide $p^n - 1$ with the x's to be determined in this field, none zero. For $c \neq 0$ and $s = 1$ it is known that there exist fields of this type where the equation has no solutions. On the other hand,[1] if $s \geqq 2$ with $c \neq 0$ and $s > 2$ for $c = 0$, we know that the equation always has at least k solutions in non-zero x's, for k any given positive integer, provided p^n exceeds a certain limit. The passage from the case $s = 1$, $c \neq 0$ to the case $s = 2$, $c \neq 0$ is a fundamental one.

Consideration of the first case for various values of p involves the use of congruences with respect to a prime ideal in an algebraic field and leads into the theory of class fields and laws of reciprocity. In the second case, however, different types of developments have arisen, particularly having

to do with the exponential sums connected with that part of the theory of cyclotomic fields which is generally called cyclotomy[1] or the theory of the division of the circle. Also, we are thus led into the theory of the zeta function for function fields. Another way of showing the difference is to note that if we illustrate the first case by using a congruence of the form (with ω not an n-th power in K)

$$x^n \equiv \omega \pmod{\mathfrak{p}},$$

where $\omega \not\equiv 0 \pmod{\mathfrak{p}}$ and where ω is an integer in the algebraic field K defined by $\alpha = e^{2i\pi/n}$, $\mathfrak{p}$ is a prime ideal in K, this gives

$$(x - \sqrt[n]{\omega})(x - \alpha\sqrt[n]{\omega}) \ldots (x - \alpha^{n-1}\sqrt[n]{\omega}) \equiv 0 \pmod{\mathfrak{p}},$$

if we introduce the Kummer field defined by K and $\sqrt[n]{\omega}$. We may naturally expect then that the theory of Kummer fields in this development would be a convenient tool to apply to our problem. However, if we illustrate the second case by means of the trinomial congruence

$$\omega_1 x_1^{m_1} + \omega_2 x_2^{m_2} + \omega_3 \equiv 0 \pmod{\mathfrak{p}},$$

where the ω's are integers in K with $\omega_1\omega_2\omega_3 \not\equiv 0 \pmod{\mathfrak{p}}$, in general the trinomial is not reducible in any algebraic field, in contrast to the conditions in the first case.

Having in the above mentioned two different special cases of (1), we now take $s \geqq 3$ in it with $c \neq 0$ which we shall refer to as the third case. Nearly all the theorems that have so far been obtained covering the second case can be extended[1, 2] to the third case without introducing any essentially new types of theories. This situation points up the important role played by the trinomial equation in the finite field and the particular case where the finite field is the set of residue classes modulo p.

Our remarks concerning the properties of (1) indicate something it is so often possible to do in mathematics: If we have a conditional relation involving several given parameters, it may be impossible to say much about the properties of the relation for the parameters all fixed; however, if we fix some and let some others range over a certain set of values, we are often able to make some definite statements about the resulting set of relations.

Pursuing the general idea above mentioned, consider the congruence with $c/(p-1)$, $m/(p-1)$,

$$1 + ax^c \equiv by^m \pmod{p}, \qquad (2)$$

where $abxy \not\equiv 0 \pmod{p}$, with p an odd prime. We now state two problems concerning (2) which have so far received attention in the literature, namely,

PROBLEM I. *If we keep a, b, c, and m fixed in (2) and let p vary over all primes, what can we say about the possible sets of solutions x, y?*

PROBLEM II. *If $m = c$ with a, b, and p fixed, and we increase m, what about the existence of solutions x, y?*

As for problem I, our remarks concerning (1) give the result that the number of incongruent solutions (x, y) increases as p increases, for p sufficiently large.

As[2] for problem II, if we set in (2), $c = m$, we find if

$$(1 + |a| + |b|)^{\varphi(c)} < p,$$

and $1 + a\alpha^{r_1} - b\alpha^{r_2} \not\equiv 0$ for $\alpha = e^{2i\pi/c}$, with the r's any integers, then (2) *has no solutions*, $xy \not\equiv 0 \pmod{p}$. Here $\varphi(c)$ is the Euler indicator of c. In connection with the above-mentioned two problems we have indicated only two of the main results which so far have been obtained.

In the present paper we shall introduce a new problem concerning (2), namely,

PROBLEM III. *If in (2) a and b are fixed integers, $abxy \not\equiv 0 \pmod{p}$, m is fixed, and p increases together with c subject to the relation $mc = k(p-1)$ with k a fixed integer, what can be said about the number of the sets of solutions x, y?*

We begin by introducing primitive roots and write (2) as, g being a primitive root of p and $k = 1$,

$$1 + g^{i+cr} \equiv g^{j+ms} \pmod{p} \qquad (3)$$

$0 \leqq i \leqq c-1$; $0 \leqq j \leqq m-1$. Hence, the problem of finding the incongruent sets x, y which satisfy (2) reduces to finding the distinct sets r, s which satisfy (3), with r in the set $0, 1, \ldots, m-1$ and s in the set $0, 1, \ldots, c-1$. Represent the number of solutions r, s in (3) by (i, j), then we have if m is odd

$$\sum_{j=0}^{m-1}(i, j) = m - \begin{cases} 0 \text{ if } i \neq c/2, \\ 1 \text{ if } i = c/2, \end{cases} \qquad (4)$$

and if m is even

$$\sum_{j=0}^{m-1}(i, j) = m - \begin{cases} 0 \text{ if } i \neq 0, \\ 1 \text{ if } i = 0, \end{cases} \qquad (5)$$

also, for any m,

$$\sum_{i=0}^{c-1}(i, j) = c - \begin{cases} 0 \text{ if } j \neq 0, \\ 1 \text{ if } j = 0. \end{cases} \qquad (6)$$

To prove this we write

$$t = i + rc, \qquad t' = j + ms,$$

and consider

$$1 + g^t \equiv g^{t'} \pmod{p}.$$

We note that a t' exists corresponding to every t, if and only if $t = (p - 1)/2$, giving $i = cm/2 - rc$; whence, if m is odd $i = c/2$; and if m is even, $i = 0$. For all other values of i, t assumes m values. Similarly we may prove (6).

As we have very little theory to guide us in the study of our particular problem, we have begun by setting up tables[3] giving the exact values of (i, j) for various values of m and c, and i and j. We note immediately that there must be for each c and m at least one value (i, j) such that $(i, j) = 0$. This follows from (6) since if each (i, j) is $\geqq 1$, then the sum in (6) is $\geqq c$, violating the conditions in relation (6) for $j = 0$. Examination of the tables mentioned shows that if m is fixed and c increases, the number of zero values for (i,j) increases and runs from 25 to 35 per cent of the possible values (i,j) for the values m and c used in the tables. For $m = 13$, $p = 937$, there are 302 zero values for (i, j); and for $m = 5$, $p = 991, 256$ such values. The fact that we at least always have one value of (i,i) which is zero for a given m and c and that the number of these cases appears to increase with c leads us to an elementary application of what we have already developed. The properties of primitive roots lead us easily to a proof of the

LEMMA: *Consider* $1 + g^i x^c \equiv g^j y^m \pmod{p}$, *where* $p - 1 = mc$; $0 \leqq i \leqq c - 1$; $0 \leqq j \leqq m - 1$; g *is a primitive root of* p. *If* $(x, p) = p$, $(y, p) = 1$, *then the congruence has solutions if and only if* $j = 0$. *If* $(x, p) = 1$, $(y, p) = p$, *then solutions exist when* m *is odd, if and only if* $i = c/2$; *when* m *is even if and only if* $i = 0$.

Let g be a primitive root of p as before and $(d, p) = 1$ and consider the equation[4]

$$(d + k_1 p) + (dg^i + k_2 p)x^c - (dg^j + k_3 p)y^m = 0. \qquad (7)$$

If we reduce this modulo p, we obtain (3). If we then apply the lemma provided $(i, j) = 0$, and use the lemma to exclude the cases when either x or y is divisible by p, we find that (7) has no solutions in x or y. For example, $19 + 9x^6 = 8y^7$ may be written $(19) + (19 \cdot 5 - 2 \cdot 43)x^6 = (19 \cdot 14 - 6 \cdot 43)y^7$. Reducing modulo 43 and using $g = 28$, this becomes $1 + 28^5 x^6 \equiv 28^4 y^7 \pmod{43}$, which is equivalent to the case (5, 4). But $(5, 4) = 0$, and application of the lemma admits no solutions of the original equation.

We shall now give another proof of a theorem[5] which appears to have fundamental application in attacking our problem. Although we shall employ it later only for the case involving trinomials, we will consider it in connection with equation (1) and investigate the number of distinct

solutions N_s of equation (1), $s \geqq 2$, and assume $p^n - 1 = q_i m_i$ for each i. For our purpose here it is convenient to consider the form

$$g_n^{y_1 m_1 + r_1} + \ldots + g_n^{y_s m_s + r_s} = 1, \tag{8}$$

where g^n is a multiplicative generator of $F(p^n)$, used previously for $n = 1$, that is $g_1 = g$. Let $[r_1, \ldots, r_s]$ denote[6] the number of distinct sets of y's ($y_i = 0, 1, \ldots, q_i - 1$) that satisfy (8); thus, $[r_1, \ldots, r_s]m_1 \ldots m_s$ is the number of sets of non-zero solutions of (1) in the x's.

If α_i is a primitive m_i root of unity and ind a is defined such that $g_n^{\text{ind } a} = a$ for any non-zero a in $F(p^n)$, consider the generalized Jacobi-Cauchy cyclotomic sum

$$\psi(u_1, \ldots, u_s) = \sum_{a_1 + \ldots + a_s = 1} \prod_{i=1}^{s} \alpha_i^{u_i \text{ ind } a_i}, \tag{9}$$

where the a's range over the non-zero elements of $F(p^n)$. Vandiver[7] gave the following expression for the number of non-zero solutions of (1):

$$[r_1, \ldots, r_s] \prod_{i=1}^{s} m_i = \sum_{u_1, \ldots, u_s} \psi(u_1, \ldots, u_s) \prod_{i=1}^{s} \alpha_i^{-u_i r_i}, \tag{10}$$

where each u_i ranges independently over the set $0, 1, \ldots, m_i - 1$.

Let $l_a k_a = m_a$ and consider the expression

$$\sum_{t=0}^{l_a - 1} [r_1, \ldots, r_{a-1}, r_a + tk_a, r_{a+1}, \ldots, r_s] = R. \tag{11}$$

Carrying out the summation by means of the relation (10), we find that R equals

$$M \sum_{u_1, \ldots, u_s} \psi(u_1, \ldots, u_s) \prod_{i=1}^{s} \alpha_i^{-u_i r_i} (1 + \alpha^{k a u_a} + \ldots + \alpha^{(l_a - 1) k a u_a}) = M \sum_{u_1, \ldots, u_s} \psi(u_1, \ldots, u_s) \prod_{i=1}^{s} \alpha_i^{-u_i r_i} N,$$

where $N = (\alpha^{l a k a u_a} - 1)/(\alpha^{u a k a} - 1)$ and $M = 1/\prod_{i=1}^{s} m_i$. Each term in the right-hand member reduces to zero except when $k_a \equiv 0 \pmod{l_a}$, that is, for the values $0, l_a, 2l_a, \ldots, (k_a - 1)l_a$ of u_a.

Hence, if u_a' ranges over these values of u_a,

$$R = l_a M \sum_{u_a'} \psi(u_1, \ldots, u_{a-1}, u_a', u_{a+1}, \ldots, u_s) \cdot \sum_{u_a'} \alpha_a^{u_a' r_a} \prod_{i=1}^{a-1} \alpha_i^{v_i} \prod_{j=a+1}^{s} \alpha_j^{v_j},$$

where $v_t = -u_t r_t$. In the expression $\alpha_a^{u_a' r_a}$, since u_a' ranges over the above-stated multiples of l_a we may replace α_a by a primitive k_ath root of unity, say α_a' and let the corresponding u in ψ range over $0, 1, \ldots, k_a - 1$. We may replace $1/l_a M$ by the product $m_1 \ldots m_{a-1} k_a m_{a+1} \ldots m_s$. This gives the

THEOREM I. *If R is as defined in (11), then R is the number of solutions in the z's of*

$$g^{z_a k_a + r_a} + \sum_{i=1}^{a-1} g_n^{w_i} + \sum_{j=a+1}^{s} g_n^{w_j} = c, \tag{12}$$

where $w_t = z_t m_t + r_t$. By operating in a similar fashion on each term of (8) we have a more general relation involving the term containing m_t, any divisor of it in place of m_t itself.

The first proof of the general result just mentioned was quite elementary, but it never appealed to us as being exactly simple. However, that proof may be extended so that if we have any polynomial

$$f(x_1, x_2, \ldots, x_t),$$

with coefficients in $F(p^n)$ but not necessarily of the type (1), then the theorem may be extended to f if it contains a term $c_t x_t^{a_t}$, but is such that x_t appears in no other term, by operating on this one term as was done to prove the special form of the theorem.

On the other hand, the method of proof of the present paper does not apply at all to the general type of equation just mentioned. However, if we wish to examine the problem of finding an analogue to Theorem I, taking into account the zero as well as the non-zero solutions in (1) (which has apparently not been done), we find that our second, but not the first, proof of the theorem is quite adaptable in view of a theorem given by Weil.[8] Applied to (3) Theorem I gives

$$\sum_{v=0}^{l-1} (r + vc_1, k)_{cm} = (r, k)_{c_1 m}, \tag{13}$$

where $c_1 l = c$ and where now it is necessary to extend our notation as to the number of solutions of (3) by writing $(i, j)_{cm}$ for the number of solutions of (3) and the right-hand member of (13) means the number of solutions of (13) when c_1 replaces c in (3).

As to the tables[3] *of solutions of the* $(i, j)_{cm}$ *previously referred to in this paper, then in view of* (13) *we may quickly calculate from them the values of* $(i, j)_{c_1 m_1}$, *where* c_1/c *and* m_1/m.

Take $s = 2$ in (8), we have

$$g_n^{y_1 m_1 + r_1} + g_n^{y_2 m_2 + r_2} = 1, \tag{14}$$

where now $[r_1, r_2]_{m_1 m_2}$ represents the number of its sets of solutions in the y's. Evidently $[r_1, r_2]_{m_1 m_2} = (r_1 + \epsilon, r_2)_{m_1 m_2}$, where $\epsilon = \text{ind}(-1)$, $r_1 = \text{ind } a$, $r_2 = \text{ind } b$ with a and b defined in (2).

By extending the methods employed by Mitchell,[9] Vandiver derived a relation involving numbers of solutions[10] of trinomial non-homogenous equations which may be applied to Problem III. However, we have found

some different types of relations by another method. Employing extensions of methods given in our last reference together with use of (13) yields (details of proof to be given elsewhere),

$$c - m + \sum_{i=0}^{m-1} [0, i]_{cm}{}^2 = \sum_{j,\ d} [d, j]_{cc}{}^2;\ c = c_1 m,\ cm + 1 = p^n, \quad (15)$$

where j ranges over 0, 1, . . ., $c - 1$, and d over every multiple of m in the same range. Now if we had let d range over *all* integers in the set 0, 1, . . ., $c - 1$, then the right-hand member of (15) may be evaluated explicitly[1] (ref. 1, p. 242) in terms of c and m. The last relation (15) is a step beyond this idea, as it is possible to evaluate the left-hand member for certain sets of values of p.

[1] Vandiver, H. S., these PROCEEDINGS, **33,** 236–242 (1947); **36,** 144–151 (1950). Hua, L. K., and Vandiver, H. S., *Ibid.*, **34,** 258–263 (1948); **35,** 89–95, 481–487 (1949). Faircloth, O. B., *Canad. J. Math.*, **4,** 343–351 (1952). Note also references in these papers to former literature. In the first Hua-Vandiver reference the finite field mentioned in (1) is taken as a set of residue classes with respect to an ideal prime modulus in any commutative ring R with a unity element provided the norm of the ideal is finite. The general result is given in Theorem II of that reference.

[2] Vandiver, H. S., these PROCEEDINGS, **32,** 103 (1946). Ankeny, N. C., *Ibid.*, **38,** 881 (1952), Lemma 2.

[3] Tables were set up with $m = 3$: 7, 13, 19, 31, 37, 43, 61, 67, 73, 79, 97, 103, 109, 127, 139, 163; with $m = 4$: 13, 37, 61, 73, 97; with $m = 6$: 37, 61, 73, 97; with $m = 5$: 31, 41, 61, 71, 101, 131, 151, 181, 191, 211, 241, 251, 271, 281, 991; with $m = 7$: 29, 43, 71, 113, 127, 197, 211, 239, 281; with $m = 11$: 199, 331, 353, 397, 991, 1013, 1123; with $m = 13$: 547, 599, 937. For $m \neq 6$ and $m > 4$, $p < 900$, all tables appear in the M.A. Thesis of Erna H. Pearson, University of Texas, August, 1946.

In the following tables all cases of zero values for (i, j) yield insoluble equations, except those having $(xy, p) = p$. When $m = 3$, $p = 31$, $(i, j) = 0$ for (2,0), (3,2), (4,1), (5,2), (6,1), (7,1), (8,2), (9,0), (9,2); $(i, j) = 1$ for (0,0), (0,1), (0,2), (1,0), (1,1), (1,2), (2,1), (3,1), (4,0), (5,0), (5,1), (6,0), (7,0), (8,0); $(i, j) = 2$ for (2,2), (3,0), (4,2), (6,2), (7,2), (8,1); $(i, j) = 3$ for (9,1).

When $m = 4$, $p = 37$, $(i, j) = 0$ for (0,1), (0,2), (1,2), (2,3), (3,0), (3,1), (5,1), (6,1), (6,3), (7,0), (8,2), (8,3); (i, j) = 1 for (0,0), (1,0), (1,3), (2,0), (2,1), (4,0), (4,1), (4,2), (4,3), (5,0), (5,2), (7,2), (7,3), (8,0); $(i, j) = 2$ for (0,3), (1,1), (2,2) (3,2), (3,3), (5,3), (6,0), (6,2), (7,1); $(i, j) = 3$ for (8,1).

When $m = 5$, $p = 41$, $(i, j) = 0$ for (0,2), (1,3), (2,1), (3,0), (3,3), (3,4), (4,1), (4,4), (5,0), (5,3), (6,2), (7,1), (7,4); $(i, j) = 1$ for (0,0), (0,1), (0,4), (1,0), (1,1), (1,2), (2,0), (2,2), (2,3), (4,0), (4,3), (5,2), (6,1), (6,3), (6,4), (7,0), (7,2); $(i, j) = 2$ for (0,3), (1,4), (2,4), (3,2), (4,2), (5,1), (5,4), (6,0); $(i, j) = 3$ for (3,1), (7,3).

When $m = 7$, $p = 29$, $(i, j) = 0$ for (0,2), (0,3), (1,3), (1,6), (2,0), (2,2), (2,5), (3,4); $(i, j) = 1$ for (0,0), (0,1), (0,6), (1,0), (1,1), (1,4), (1,5), (2,1), (2,4), (2,6), (3,0), (3,1), (3,2), (3,3), (3,5); $(i, j) = 2$ for (0,4), (0,5), (3,6); $(i, j) = 3$ for (1,2), (2,3).

Referring to the character of the (i, j)'s, we will call *extreme cases* those where for a given i, $(i, j) = 1$ for each j, and also where for a given i there is an $(i, j) = m$. In the case where $m = 2$, the only two possible cases are extreme. For $m = 3$ the extreme cases are common in the tables we set up. For $m > 3$ the first case appears occasionally. Thus, for $m = 5$, $p = 31$, $(4, j)$ is unity for each j; similarly when $m = 5$, $p = 131$, and $i = 4$ and 19; $m = 5$, $p = 151$, $i = 10$ and 20; $m = 5$, $p = 181$, $i = 1$ and 12.

However, the second extreme case did not occur in any of the tables for $m > 3$. For $m = 5$, $p = 71$, the maximum value of the (i, j) is 4. Also, in the case $m = 5$, $p = 991$, the maximum value is 4 and occurred for 7 values of (i, j).

When a solution of (3) exists for a given (i, j), if divisors of m and c are selected such that $m_1c_1 = p_1 - 1$ for another prime p_1, it may result that the second congruence has no solutions; hence, none of the derived equations have solutions. For example, for $m = 5$, $p = 31$, $(4,1) = 1$. Using $g = 17$, we obtain the equation $1 + 7x^5 = 17y^5$, which may have solutions. Selecting $c_1 = 2$, $p_1 = 11$, we reduce this equation modulo 11, obtaining $1 + 7x_1^2 \equiv 6y_1^5 \pmod{11}$. For $g = 2$, this becomes $1 + 2^7x_1^2 \equiv 2^9y_1^5$, or $i = 1$, $j = 4$. But $(1,4) = 0$; hence, the equations have no solutions.

[4] This method was also applied to other types of trinomial equations in Vandiver, *Math. Mag.*, **22**, 185–192 (1948).

[5] Here in our second proof we have given the details only for the case $c \neq 0$, but if we use the relation given by Faircloth and Vandiver, these PROCEEDINGS, **38**, 54, relation (7) (1952), a similar argument can be carried out for $c = 0$.

[6] We found it convenient in setting up the tables concerning (2) to keep the congruence in the form given in (2) instead of in the form (1) where the constant term appears alone on one side of the relation. This was because we availed ourselves initially of the tables of Jacobi (*Werke*, Band 6, 272–274), where he gave the solutions i in the relation $1 + g^p \equiv g^{i'} \pmod{p}$ for $p < 100$. On the other hand, the form (1) when limited to $s = 2$, $c \neq 0$, is often more convenient for other purposes particularly where exponential sums are employed. The relation between the numbers $[i, j]$ and (i, j) as denoting the numbers of solutions in the two cases is given just below the relation (14) of the present paper.

[7] These PROCEEDINGS, **36**, 148 (1950).

[8] *Bull. Am. Math. Soc.*, **55**, 497–508 (1949); given in a simpler form by Faircloth and Vandiver, *loc. cit.*, footnote 5, relation (12).

[9] *Trans. Am. Math. Soc.*, **17**, 165–177 (1916).

[10] These PROCEEDINGS, **38**, 984 (1952), relation (14).

MECHANOCHEMICAL PROPERTIES OF FIBERS OF SURFACE-SPREAD ACTOMYOSIN

BY TERU HAYASHI AND RAJA ROSENBLUTH

DEPT. OF ZOOLOGY, COLUMBIA UNIVERSITY, NEW YORK CITY

Communicated by W. O. Fenn, October 12, 1953

Introduction.—Fibers of actomyosin, formed by collapsing the surface-spread film of this complex protein, have been shown to be capable of isotonic contraction with a load, repeated elongation and re-contraction, and other characteristics similar to the contractile elements *in situ* of living muscle.[1, 2] The use of the surface-spreading technique has been based on the general assumption that the interaction of protein molecules at intracellular interfaces is a plausible mechanism for the formation of the macromolecular aggregates resulting in cell structures.[3] On this assumption, therefore, the film-fibers of actomyosin may be considered to be a crude

model of the physical state and organization of the contractile filaments of fibrils[4] of the muscle cell. It is of some importance to stress that the behavior and properties of these protein fibers be compared, not to whole intact muscle, but to the contractile elements *in situ* of the living muscle, in so far as they can be separated from the structural complexities of the non-contractile portions of the muscle cell.

In the present investigation, experiments involving mechanical stretch and release are presented which reveal properties of the macromolecular organization of the surface-spread actomyosin fiber bearing on recent observations of living muscle.

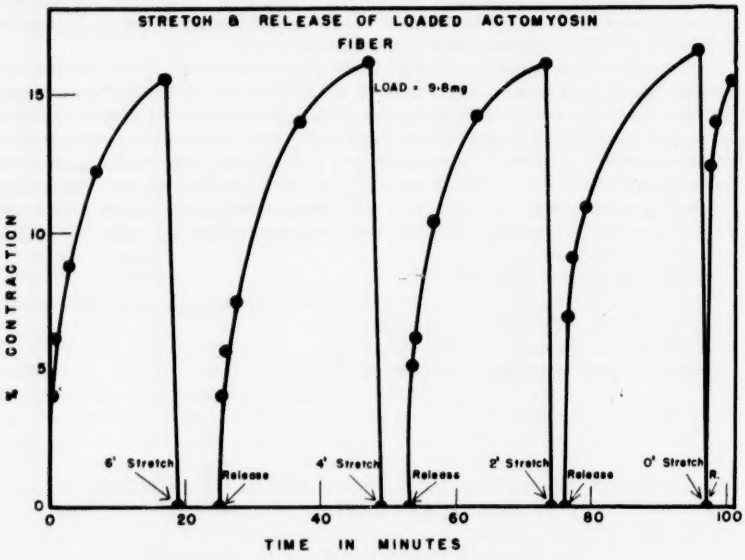

FIGURE 1

The effect of various "hold-times" after stretch of loaded actomyosin fiber in ATP. Fiber continuously bathed in 0.3% ATP in 0.05 *M* KCl, buffered at pH 7.6 in 10 × diluted veronal buffer.

Methods.—The techniques for the formation of film-fibers and subsequent handling for isotonic contraction measurements have been described.[1] For stretching the loaded fiber, a hook was added to the movable platform which engaged the weight hanging on the fiber. A downward movement of the platform thereupon stretched the fiber the required distance, care being taken that the stretch be always vertical. For release, a quick upward movement of the hook and platform disengaged the hook so that fiber and weight hung free. All observations and measurements were done through

a cathetometer with a vernier capable of reading linear distance of 0.02 mm.

Results.—Effect of stretch and release in the presence of ATP: In these experiments, the fiber was allowed to contract isotonically with a medium load (9.8–11.4 mg. in water). The contracted fiber was then stretched to its original length, held at this length for varying periods of time, and then released. During the entire course of the experiment, the fiber was continuously bathed in 0.3% ATP in 0.05 *M* KCl buffered at pH 7.6 with

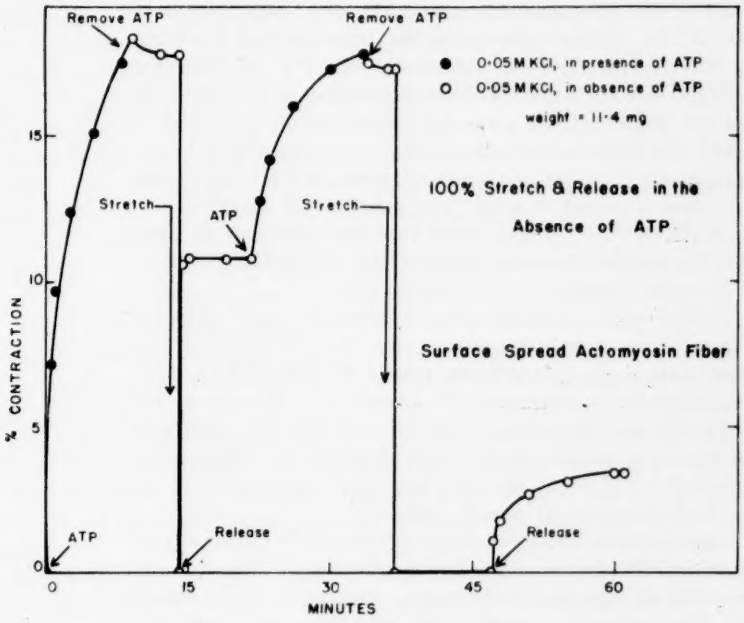

FIGURE 2

Effect of "hold-times" after stretch of actomyosin fibers in absence of ATP. ATP removed during stretch and release, and bathed in 0.05 *M* KCl buffered at pH 7.6 in 10 × diluted veronal buffer.

veronal buffer. The results of a typical experiment are shown in figure 1. The data show clearly that if the fiber is stretched and held for some time (6 minutes) before release, the ensuing recontraction is a smooth curve similar to the original ATP-induced contraction. If, however, the fiber is stretched and released immediately (at extreme right of figure) the ensuing shortening is, for the greater part, a rapid "bounce." Only the last portion shows the slower type of contraction. Between these two extremes of "hold-times" (0 and 6 minutes) the recontractions may be seen to be a com-

bination of the rapid "bounce" and slow contractions, the height of the "bounce" being progressively greater with shorter "hold-times."

The fact that this effect of "hold-time" variation is not due to the progressive aging of the fiber can be simply shown by starting the experiment with zero "hold-time" and progressively increasing the "hold-time." Exactly the same results are obtained.

Stretch and release in the absence of ATP: Figure 2 depicts the results of a typical experiment which began with a loaded isotonic contraction, ATP-induced. The ATP was then removed, leaving the fiber hanging freely in 0.05 *M* KCl at pH 7.6. In this medium, the fiber remains at the shortened length.[2] The fiber is now stretched and quickly released, resulting in a rapid, "bounce-type" recontraction a little more than half way back to the original contracted length. There is no slow recontraction. The ATP is now reintroduced, the fiber contracts to the extreme shortened length, and the ATP is again removed. The fiber is now stretched, held for 12 minutes, and released. There is a small "bounce," and a slight, slow contraction.

The results of the two experiments, taken together, show that the slow recontraction to the extreme shortened length is the ATP-induced contraction, whereas the rapid "bounce" is ATP-independent.

Discussion.—Three general conclusions of interest to muscle physiologist may be drawn from these experiments. (*a*) The ATP-induced contraction of these fibers is not limited by the rate of diffusion of ATP, since (Fig. 1) the recontractions after prolonged immersion in ATP occur at the same rate as the original contraction. This indicates that the slowness of contraction of these actomyosin fibers is due to some inherent factor, possibly an insufficient organization, of these extracted, dissolved, and reassociated (by surface-spreading) protein molecules.

(*b*) A mechanical stretch-and-hold causes a reversal of the chemically induced configurational change during the fiber contraction. This is clearly shown in the ability of such stretched fibers to undergo an ATP-induced recontraction. This enforced reversal is in good agreement with the observation of Abbot, Aubert, and Hill[5] on the absorption of heat with stretch of a muscle during the active contraction phase. They concluded tentatively that the contractile element of muscle is reversibly coupled with a chemical system providing the energy, a conclusion which can be applied admirably to the present results.

(*c*) The actomyosin fiber behaves functionally as though it were composed of contractile "links" and elastic "springs" in a series arrangement. These terms are used simply to facilitate discussion of the behavior of the fibers, and carry no implication as to the chemical configuration or structure of the component molecules. Nonetheless, the results depicted in figures 1 and 2 are adequately explained if we assume the series arrangement of these hypothetical units with the following differing properties.

The "links" react to ATP by contraction, and to rapid (2–5 seconds) mechanical stretch (or a rapid increase of tension) they are a slow-responding system, being relatively hard and inextensible in the small times involved. Given time to respond (in a stretch-and-hold), however, they are readily extensible. These properties are shown in media of relatively low ionic concentration (0.05 *M* KCl or 0.05 *M* KCl + 0.3% ATP). The "springs," on the other hand, are ATP-insensitive, and respond rapidly to quick stretch, elongating readily.

Thus, at the moment of completion of any of the stretches shown in figures 1 and 2, the "springs" are extended, accounting for most of the increase in length of the fiber. If the fiber is quickly released after the stretch, there is a rapid elastic shortening of the "springs." The fact that this rapid shortening does not proceed to the completely shortened length of the fiber indicates that even in the short time involved in the stretch, the "links" have opened somewhat. With a prolonged stretch-and-hold, however, the extended "springs," exerting a steady tension on the "links," pull and open these units, thus reversing the ATP-induced contraction and enabling them again to respond to ATP with a slow concentration. In other words, the reversal of contraction by mechanical stretch noted in (*b*) above is limited to the "links."

In 0.3 *M* KCl, a condition which brings about passive elongation of the fiber,[2] it is the "links" which are affected by the increased salt concentration, becoming softly plastic and readily extensible, even to rapid stretches. This is shown by the fact that fibers stretched in 0.3 *M* KCl show no rapid "bounce" following immediate release. In addition, such a stretched fiber is capable of full slow contraction upon the reapplication of ATP in a low salt medium, showing that the "links," with stretch, have reverted to their open state.

Applying this interpretation of "links" and "springs" to whole muscle, it may be seen that the "links" are the true contractile elements. During the actively contracting phase, in the short time involved in a quick stretch, they are relatively hard and inextensible, in agreement with Hill.[6] With a long time-period of sustained stretch they are forced into reversal, as in muscle.[5] In passive elongation these "links" are soft and plastic, like the contractile elements of muscle.[7]

In addition, the presence of the series elastic element in the actomyosin fiber indicates, that, in living muscle, the series elastic component may not be restricted to the tendon,[8] but may be found in the substance of the muscle itself.

If the contractile "links" and series elastic "springs" are substantiated, one would expect these fibers to show the quick-release-recovery effect.[8, 9] This expectation is fully borne out in the isometric studies of these surface-spread fibers by Joseph.[10] Likewise, for precipitated, stretched, and dried

actomyosin fibers, Portzehl[11] has found the quick-release-recovery effect. Her results are fully interpretable on the basis of the "links" and "springs."[12]

The series elastic "springs" may possibly be localized in the intermolecular association of the actomyosin units in this macromolecular organization. Such interlinkages are presumably formed in the surface-spread association of the actomyosin molecules, which would seem to be a plausible physiological condition in light of the heterogeneous nature of the interior of the cell.

Summary.—Stretch and immediate release of contracted surface-spread actomyosin fibers result in a rapid, elastic return to the shortened state. Stretch followed by a prolonged hold before release results in a slow recontraction to the shortened state similar to the original ATP-induced contraction. This slow recontraction is dependent on the presence of ATP, the rapid "bounce" is not. The results are interpreted on the basis of the presence of contractile "links" and elastic "springs" in a series arrangement in the macromolecular organization of the fiber. The "links" and "springs" differ principally in their time characteristic of response, the former being a slow-responding, the latter a fast-responding system to mechanical stretch. The "links" are the contractile elements, being sensitive to both ATP and salt concentration. The data show that the contraction of these "links" may be reversed by mechanical stretch.

[1] Hayashi, T., *J. Gen. Physiol.*, **36,** 139–152 (1952).

[2] Hayashi, T., and Rosenbluth, R., *J. Cell. Comp. Physiol.*, **40,** 495–506 (1952).

[3] Hayashi, T., *Science*, **114,** 684 (1951).

[4] Hall, C. E., Jakus, M. S., and Schmitt, F. O., *Biol. Bull.*, **90,** 32–50 (1946).

[5] Abbott, B. C., Aubert, X. M., and Hill, A. V., *Proc. Roy. Soc. (London)*, **B139,** 86–104 (1951).

[6] Hill, A. V., *Ibid.*, **B141,** 161–178 (1953).

[7] Hill, A. V., *Ibid.*, **B137,** 40–50 (1950).

[8] Hill, A. V., *Ibid.*, **B141,** 104–117 (1953).

[9] Gasser, H. S., and Hill, A. V., *Ibid.*, **B96,** 398–437 (1924).

[10] Joseph, R., Ph.D. thesis, Columbia University, New York (1953).

[11] Portzehl, H., *Z. Naturforsch.*, **6b,** 355–361 (1951).

[12] For the precipitated type of fiber, Portzehl and Weber, *Ibid.*, **5b,** 123 (1950), had obtained isometric tensions as early as 1950, and not in 1951, as was erroneously reported by one of us (Ref. 1).

PHOSPHOMONOESTERASES IN REEF-BUILDING CORALS

BY THOMAS F. GOREAU

UNIVERSITY COLLEGE OF THE WEST INDIES, MONA, JAMAICA, B. W. I.

Communicated by G. E. Hutchinson, October 16, 1953

Alkaline and acid phosphomonoesterases have now been found in a number of West Indian reef corals. This is believed to be the first demonstration of these enzymes in the coelenterata. Although this report is confined to a description of the phosphomonoesterases found in 26 species of corals belonging to eight different families,[1] our evidence also shows that such enzymes exist in at least one zoanthidean, *Palithoa caribaea*, and a hydrocoralline, *Millepora alcicornis*.

Materials and Methods.—With one exception, all the species used for this study were collected from shallow fringing reefs at Lime Cay, near Kingston, and on the North Coast near the town of Ocho Rios. The freshly collected coral was promptly drained and kept in jars on ice for not more than two hours, then stored in deep freeze until ready to use.

The coral tissue homogenate was prepared by carefully cleaning 50 g. of the freshly frozen coral of all the encrusting growths and dead corallum. The remainder was pounded to fine bits in a mortar, triturated in a blendor with 200 ml. distilled water and centrifuged at 2000 r. p. m. for ten minutes. The light brown supernate was then decanted away from the precipitate and stored in a refrigerator with a few milliliters toluene as preservative. The precipitate was seen to be composed of zooxanthellae, nematocysts and finely ground corallum. Phosphatase analyses of the washed precipitate showed low orders of activity which is attributable to remaining bits of coral tissue rather than to intrinsic activity of the zooxanthellae.

The pH optima of the phosphomonoesterases were determined as follows: 5 ml. aliquots of an ice cold suspension containing 25 ml. of the fresh homogenate, 50 ml. 10% beta-sodium glycerophosphate and 100 ml. of a 1:1 0.2 *N* glycine-NaOH buffer were pipetted into volumetric test tubes. Fifteen points were chosen in the pH range 11.50 to 9.60 and an identical number between pH 3.50 to 6.00. The pH in each tube was then carefully adjusted to one of these points with 0.2 *N* NaOH or 0.2 *N* HAc using glass electrodes. The tubes were allowed to incubate in a thermostat at 37°C. and the reaction stopped with TCA at the end of one hour. Final pH was measured at first owing to the possibility of drift, but as this was seldom more than 0.1 unit in the course of an experiment, this step was omitted in most of the final determinations. After stopping the runs, the volumes were made up to 10 ml., and 2 ml. aliquots were taken for colorimetric phosphate analysis according to the method of Taussky and Shorr.[2] There was

usually a slight turbidity in these samples owing to the presence of small amounts of mucopolysaccharide-like substances which were not precipitated by TCA. Controls run under identical conditions but without the phosphate determinations showed that the optical density of the turbid material remained constant over a pH range of 3.40 to 11.80 and that the effect could be corrected for by running the experimental TCA control as the color blank.

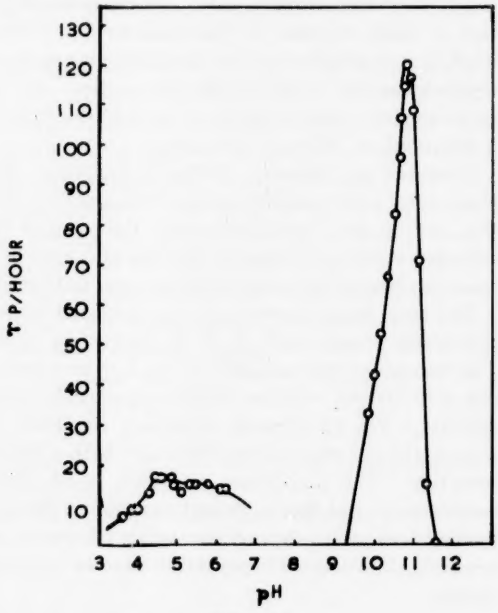

FIGURE 1

Sample plot showing pH optima of P-ases from *Mussa angulosa*

Results.—The activity versus hydrogen ion concentration curves for scleractinian alkaline phosphomonoesterases are markedly different from previously published data which are derived exclusively from mammalian material.[3-5] In all except one of the species examined, the optimum activity is between pH 10.50 and 11.10 (data corrected for sodium error of the glass electrodes). The activity falls off with very great rapidity on either side of the optimum pH, producing in most cases a needle sharp peak (Fig. 1). The mean optimum pH of 25 species, not including *Porites divaricata*, is in the range of 10.85 to 10.90 with relatively small degree of scatter on either side of the mean (Fig. 2).

The acid phosphomonoesterase optima have a much wider scatter in the pH range of 3.60 to 5.50. The peaks are blunt and rounded and the enzyme activity is very variable in intensity relative to the degree of alkaline phosphomonoesterase activity. In four cases the acid phosphomonoesterase activity was not measurable, but it remains uncertain whether this is due to actual absence, excessive dilution, inhibition or deterioration of the enzyme.

The pH optima of the phosphomonoesterases of 26 species of corals are listed in table 1. It will be noted that local representatives of the families Astrangiidae, Trochosmiliidae, Astrocoeniidae, and Seriatoporidae, eight species in all, were not available and had to be omitted from this survey.

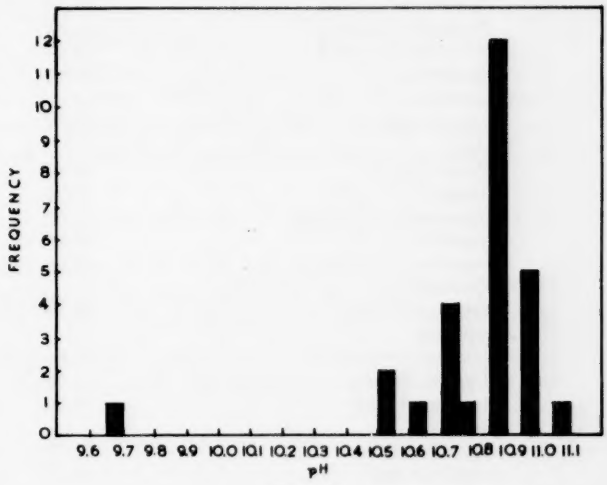

FIGURE 2

Frequency distribution of alkaline P-ase optima from 26 species of Jamaican reef corals.

Discussion.—The exceedingly high pH optima of the alkaline phosphomonoesterases of reef corals are very interesting when considered in the light of possible adaptive advantages they may have for rapid and efficient deposition of $CaCO_3$ into the corallum. Due to the fact that enzyme activity falls off so very rapidly with even small pH changes away from the optimum, and assuming these enzymes to have specific internal functions, it becomes necessary to postulate that very high physiological pH values can occur in the coral polyp. Several mechanisms for achieving this are possible. CO_2 can be lost from the body fluids either through photosynthetic fixation by zooxanthellae or by precipitation into the corallum as carbonate. The same result would also be produced through massive localized produc-

tion of ammonia at night. It is naturally possible to look at the problem from the other side and postulate that carbonate deposition is the mechanism whereby the high pH necessary for the function of these particular

TABLE 1

FAMILY AND SPECIES*	ALKALINE OPTIMUM pH	ACID OPTIMUM pH
Faviidae		
Colpophyllia natans	10.78	4.50
Diploria clivosa	10.86	4.50
Diploria strigosa	10.86	4.50
Diploria labyrinthiformis	10.86	4.50
Manicina areolata	10.86	4.20
Cladocora arbusculata	10.75	..
Montastrea annularis	10.53	4.50
Montastrea cavernosa	10.64	5.50
Favia fragum	10.86	4.50
Oculiniidae		
Oculina diffusa	10.53	5.00
Mussidae		
Mussa angulosa	10.86	5.00
Isophyllastrea rigida	10.75	..
Mycetophyllia lamarkana	10.86	4.50
Isophyllia sinuosa	10.86	4.50
Isophyllia multiflora	10.96	4.90
Caryophylliidae		
Eusmilia fastigiata	10.86	5.50
Acroporiidae		
Acropora cervicornis	10.96	4.00
Acropora palmata	10.96	4.00
Acropora prolifera	10.96	4.00
Agariciidae		
Agaricia agaricites	10.75	..
Agaricia fragilis	10.86	..
Siderastreidae		
Siderastrea siderea	10.86	3.60
Siderastrea radians	10.75	3.80
Poritidae		
Porites astreoides	11.07	4.80
Porites porites	10.96	5.00
Porites furcata	10.86	4.50
Porites divaricata	9.70	3.80

* Generic and specific nomenclature was taken from Smith's monograph on Atlantic reef corals.[6] Familial nomenclature for the species cited is according to Vaughan and Wells.[1]

phosphomonoesterases is produced. This may well be the case if these enzymes are not concerned with calcification at all. It is hoped that work now in progress will help to clarify this problem.

The alkaline phosphomonoesterase of *Porites divaricata* appears to be a spe-

cial case that deserves some discussion. The optimum pH in this species is 9.70 whereas the mean value for all the other species is 10.86. The peak is also not so sharp and much wider at the base than the others. There is strong suspicion that this difference may be the result of environmental changes. The specimen of *Porites divaricata* on which these analyses were performed was the only coral specimen in this series which was not collected in shallow, clear and sunny reef waters that are the normal environment of reef building scleractinia. This particular specimen was collected from the shady side of a submerged sea wall, growing at a depth of more than fifteen feet in extremely turbid water at Port Royal. It is hoped that additional specimens will be collected from other localities to investigate the possibility that environmental changes might produce adaptive changes in the functional characteristics of alkaline phosphomonoesterases in corals.

Investigations to determine the specific localizations of these enzymes in coral tissue are now in progress. This work, together with that described above constitutes part of a more generalized research program being carried out on this laboratory on problems of growth and calcium metabolism in reef corals.

[1] Vaughan, T. W., and Wells, J. W., Geol. Soc. of America, Special Paper No. 44 (1943).

[2] Taussky, H. H., and Shorr, E., *J. Biol. Chem.*, **202**, 675 (1953).

[3] Belfanti, S., Contardi, A., and Ercoli, A., *Biochem. J.*, **29**, 517 (1935).

[4] Kroon, D. B., Neumann, H., and Krayenhoff-Sloot, W. J. A. T., *Enzymologia*, **11**, 186 (1944).

[5] Roche, J., and Bullinger, E., *Ibid.*, **7**, 278 (1939).

[6] Smith, F. G. W., *Atlantic Reef Corals*, University of Miami Press (1948).

VITAL STATISTICS OF OUR FOREIGN ASSOCIATES

BY EDWIN B. WILSON

OFFICE OF NAVAL RESEARCH, BOSTON

Read before the Academy, November 9, 1953

Many years ago incident to committee considerations about elections to the Academy, Raymond Pearl[1] prepared reports on "Vital Statistics of the National Academy of Sciences." More recently Fred E. Wright,[2] who served us long as Home Secretary, prepared another analysis. It seems now desirable to prepare a brief analysis about our foreign associates; their numbers are too few to justify either great length or much technique in the treatment.

From such records as appear in our Annual Report supplemented by data available in the office of the Home Secretary and supplied by his staff,[3]

it appears that between 1864 and 1953, both inclusive, the Academy elected 226 foreign associates.[4] Two of these, Messrs. Einstein and Debye, having become American citizens and been transferred to the list of members of the Academy, are not included in this analysis.

The election of foreign associates has been very irregular, commencing with 10 in 1864 and 5 each in 1865 and 1867, but with none thereafter until 1883 when 24 were elected. In the 60 years 1864–1923 there were elections in only 25 years and 138 were elected, an average of 2.3 per year but 5.5 per election. In the 30 years 1924–1953 the procedure was more regular with elections in all save 4 years and a total of 86 elected, an average of 2.9 per year and 3.3 per election, the most in any one year being 7.

For nine periods the number elected, the average age at election, and for the first six periods the average lifetime as foreign associates are:

64–67	1883	87–98	01–04	05–12	13–21	24–34	35–45	46–53
21	24	26	27	21	19	29	30	27
65.1	63.2	63.2	60.2	57.7	64.7	62.9	61.9	59.3
14.2	14.2	8.9	13.8	20.7	14.3	..	..	..

The average age at election for the first 60 years is 62.4 and the average afterlifetime 14.1; the average age at election for the past 30 years is 61.4, the decrease of 1.0 year being only about half the standard deviation of the difference. It may be noted that: (1) The variation in the average age at election for short periods is considerable and that of the actual lifetime as foreign associate even more striking.[5] (2) The numbers involved in the past 30 years are too small to be worth treating by actuarial methods to estimate the current probable afterlifetime for comparison with the figure 14.1 for the first 60 years.

The frequency functions for age at election during the first 60 and the past 30 years, their totals, and the distribution of the grand total of 224 by a normal curve with mean 62 and standard deviation 10 follow:

40-	45-	50-	55-	60-	65-	70-	75-	80-	TOTAL
4	10	17	24	36	15	13	10	9	138
4	5	17	13	16	11	10	7	3	86
8	15	34	37	52	26	23	17	12	224
10	16	28	40	44	38	26	14	8	224

On this tabulation it should be remarked: (1) The two youngest foreign associates at election were the physicists Rutherford (elected in 1911) and Bohr (elected in 1925), both a few months under 40; they have been included in the 40- group. (2) The oldest was the chemist Chevreul elected a few months short of 97 who lived for almost 6 years thereafter; he is included in the 80- group, no other being so old as 85 at election.[6] (3) Although the two frequency distributions in the two periods look different, the second

being slightly bimodal, they differ only about as much as might be expected by chance. (4) This indicates that the habit of the Academy in selecting foreign associates has been tolerably constant in detail with respect to age distribution as well as in the average age at election, which is in line with the finding of Wright[2] with respect to the age distribution of the membership at election. (5) The frequency distribution of the total of 224 by age differs from normal more than by chance, but not significally ($P = 0.12$).

If one should consider that our foreign associates, being drawn predominantly from western Europe,[7] had life expectancies like those of the fellows of the Royal Society of London, one could use the values for those expectancies by L. Solomon[8] to obtain estimates of the average length of time our foreign associates should live after election. Using these figures, I find by interpolation the following expectancies at the stated ages:

42.5	47.5	52.5	57.5	62.5	67.5	72.5	77.5	82.5
30.8	26.5	22.3	18.5	15.0	11.9	9.1	6.8	4.9

Weighting these expectancies with the numbers elected and averaging for the two respective periods of 60 and 30 years, I find 15.6 to compare with a realized value of 14.1 for the first period,[9] and 16.3 for the second for which we shall have no realized value for many years, but if that value bears a relation to 16.3 similar to that of 15.6 to 14.1, we may perhaps expect a figure such as 14.8. At any rate the increase of the indicated average expectation by 0.7 year is consonant with the decrease of 1.0 year in the average age at election found for the later period.

It is clear that so long as expectations of life at ages over 40 and the habits of the Academy in electing foreign associates do not materially change, the election of an average of 3.5 per annum will maintain in an acturial sense the present constitutional limit of 50 in the group.

[1] These PROCEEDINGS, **11**, 752, 757, 760, 765 (1925) and **12**, 258 (1926).

[2] *Ibid.*, **35**, 117 (1949).

[3] The data have been prepared carefully from reliable sources and are certainly accurate enough for the purposes of this note but cannot be guaranteed. The difficulties one encounters may be illustrated by the case of the very illustrious C. S. Sherrington, recently deceased; some important sources reported no date of birth, others reported 1861, 1859, 1857 for the year with missing or differing birthdays within the year.

[4] For 217 associates months of birth were available and were tabulated as: Jan., 13; Feb., 19; Mar., 19; Apr., 19; May, 16; June, 18; July, 18; Aug., 22; Sept., 24; Oct., 20; Nov., 16; Dec., 13. The connectivity of the numbers indicates a seasonal fluctuation although a Chi-square test, treating the items as random, shows only the variance expected by chance; and should one try to eliminate a seasonal, the residual fluctuations might be suspiciously small! The mean day of birth is near enough to July 1 so that for rough work with small numbers for checking purposes the midyear may be taken as the day of birth in dealing with groups.

[5] The variation in the average age at election is only slightly more than that due to chance; the Lexian ratio is about 1.3. The down-trend in the average age though

obvious is not significant, being about 1.4 times its standard deviation. If this insignificant trend be removed, the residuals have a Lexian ratio of 1. The calculations have been carried to only the three places given and therefore the last place in the averages is not certain.

[6] A single case so isolated raises some annoying statistical problems; it accounts for more than 3 months in the average age of election during the first 60 years and for about 0.3 year in the standard deviation of 10 years for the 224 elected in the whole 90 years. As a matter of fact Chevreul was already distinguished before the Academy was founded; he had been elected a foreign member of the Royal Society in 1826 and had received its Copley medal in 1857.

[7] The distribution of the 49 foreign associates of the Academy on July 1, 1953, by residence is: England, 17 (31%); France and Denmark, 4 each; Netherlands and Switzerland, 3 each; Canada, Germany, Norway, Russia, Scotland, and Sweden, 2 each; Argentina, Belgium, Finland, Italy, Japan, and Mexico, 1 each; and 2 are resident in the United States, of whom 1 was elected from China and 1 from England. How different was the distribution reported on our fiftieth anniversary! Of a total then of 38 we find: Germany 14 (37%); England, 9; Netherlands, 3; France, Russia, and Sweden, 2 each; Austria, Italy, Norway, Scotland, South Africa, and Switzerland, 1 each.

[8] *Proceedings of the Royal Society of London*, **A184**, 464–477 (1945).

[9] It will not do to assume that because 15.6 is greater than 14.1 our foreign associates had lower expectancies than the fellows of the Royal Society without examining the corrections analogous to Sheppard's which might have to be applied; but the examination seems unnecessary for our immediate purposes.

ERRATA: LINEAR PARABOLIC DIFFERENTIAL EQUATIONS OF ARBITRARY ORDER; GENERAL BOUNDARY-VALUE PROBLEMS FOR ELLIPTIC EQUATIONS

In the article of the above title appearing in these PROCEEDINGS **39**, 185–190 (1953), the following corrections should be made:

(1) Line 9, page 189, should read "H_b' as the completion of $\tilde{H}_b$ with respect to $\| \ \|$ and H_b as the subset of $H_b' \cap C^{2m}(D)$ for which (A) holds for every $v \epsilon \tilde{H}_b$."

(2) Line 6 of Theorem 2, p. 189: " . . . . and $u - g$ lies in H_b^+, where H_b^+ is the space of functions satisfying the boundary condition for $(\bar{K}, \tilde{H}_b, p)$.

(3) Every proper boundary value problem is strongly proper.

FELIX E. BROWDER

ERRATA: DEVELOPMENT AND GENETICS OF A SEX-INFLUENCED TRAIT IN THE LIVERS OF MICE

In the article of the above title appearing in these PROCEEDINGS **39**, 811–817 (1953), in the next-to-last line on page 813 "0.06 per cent" should read "0.6 per cent."

C. H. DANFORTH

INFORMATION TO CONTRIBUTORS

THE PROCEEDINGS is the official organ of the NATIONAL ACADEMY OF SCIENCES and of the NATIONAL RESEARCH COUNCIL for the publication of brief accounts of important current researches of members of the ACADEMY and of the COUNCIL and of other American investigators. The PROCEEDINGS will aim especially to secure prompt publication of original announcements of discoveries and wide circulation of the results of American research among investigators in other countries and in all branches of science.

ARTICLES should be brief. The viewpoint should be comprehensive in giving the relation of the paper to previous publications of the author or of others and in exhibiting, where practicable, the significance of the work for other branches of science. Elaborate technical details of the work and long tables of data should be avoided, but authors should be precise in making clear the new results and should give some record of the methods and data upon which they are based.

MANUSCRIPTS should be prepared with a current number of the PROCEEDINGS as a model in matters of form, and should be typewritten in duplicate with double spacing, the author retaining one copy. Illustrations should be confined to text figures of simple character, though more elaborate illustration may be allowed in special instances to authors willing to pay for their preparation and insertion. Particular attention should be given to arranging tabular matter in a simple and concise manner.

REFERENCES to literature, numbered consecutively, will be placed at the end of the article and short footnotes should be avoided. It is suggested that references to periodicals be furnished in some detail and in general in accordance with the standard adopted for the Subject Catalogue of the International Catalog of Scientific Literature, viz., name of author, with initials following (ordinarily omitting title of paper), abbreviated name of Journal, with place of publication, series (if any), volume, inclusive pages, year. For example: Montgomery, T. H., *J. Morph.*, Boston, 22, 731–815 (1911); or, Wheeler, W. M., *Konigsberg, Schr. physik. Ges.*, 25, 1–142 (1914).

MANUSCRIPTS will be accepted only from members of the Academy or from chairmen of the divisions of the National Research Council who will assume responsibility for the propriety and scientific standards of the paper and should be addressed to PROCEEDINGS OF THE NATIONAL ACADEMY OF SCIENCES, *2101 Constitution Ave., Washington 25, D. C. Articles of which a member of the Academy is author or a co-author may extend to twelve printed pages, those by non-members only to six printed pages; space above these limits will be billed to the author at $17.50 per page.*

PROOF will ordinarily be sent,—with the understanding that charges for an author's correction shall be billed to him. Authors are therefore requested to make final revisions on the typewritten manuscripts.

REPRINTS should be ordered at the time of submission of manuscript. They will be furnished to authors at cost, approximately as follows.

SCHEDULE OF RATES FOR REPRINTS, CARRIAGE CHARGES EXTRA

No. Copies	50	100	150	200	250
4 pp.	4.90	5.60	6.30	7.00	7.70
8 pp.	9.80	11.20	12.60	14.00	15.40
Covers	3.75	4.80	5.85	6.90	7.95

CONTENTS

	Page
ASTRONOMY.—SATELLITES, COMETS, AND INTERPLANETARY MATERIAL . . . . . *By Gerard P. Kuiper*	1153
ASTRONOMY.—NOTE ON THE ORIGIN OF THE ASTEROIDS. . . . . *By Gerard P. Kuiper*	1159
ASTRONOMY.—MAGELLANIC CLOUDS, VIII. ON THE POPULATION CHARACTERISTICS OF THE TWO CLOUDS . . . . . *By Harlow Shapley*	1161
ASTRONOMY.—MAGELLANIC CLOUDS, IX. THE NEBULOSITIES OF THE SMALL CLOUD . . . . . *By Virginia McKibben Nail, Charles A. Whitney, and Campbell M. Wade*	1168
BIOCHEMISTRY.—THE ENZYMATIC SYNTHESIS OF PORPHYRINS FROM PORPHOBILINOGEN . . . . . *By Lawrence Bogorad and S. Granick*	1176
BIOCHEMISTRY.—COMPETITION AMONG IONIC SPECIES IN CATION ACTIVATION OF ENZYMES . . . . . *By C. E. Hagen and P. C. Jackson*	1188
BIOCHEMISTRY.—ENZYMATIC REACTIONS IN PURINE DECOMPOSITION BY PREPARATIONS OF *Clostridium Acidi-Urici* . *By Norman S. Radin and H. A. Barker*	1196
BOTANY.—EFFECT OF AMINO ACIDS, ESPECIALLY ASPARTIC AND GLUTAMIC ACID AND THEIR AMIDES, ON THE GROWTH OF *Datura Stramonium* EMBRYOS IN VITRO . . . . *By Denise Paris, J. Rietsema, S. Satina, and A. F. Blakeslee*	1205
CHEMISTRY.—THE BEHAVIOR OF MICELLAR ELECTROLYTES IN THE NEIGHBORHOOD OF THE CRITICAL CONCENTRATION . . . . . *By Charles A. Kraus*	1213
ENGINEERING.—ON THE EFFECT OF PRETWISTING ON BENDING . . . . . *By Francis D. Murnaghan*	1218
GENETICS.—THE EFFECT OF GENERATION TIME ON THE DELAYED APPEARANCE OF INDUCED MUTANTS IN *Escherichia Coli* . . . *By Edgar L. Labrum*	1221
GENETICS.—THE RELATIONSHIP BETWEEN KAPPA AND PARAMECIN IN *Paramecium Aurelia* . *By John R. Preer, Jr., Richard W. Siegel, and Pearl S. Stark*	1228
GENETICS.—CROSS REACTIVATION OF GENETIC LOCI OF T2 BACTERIOPHAGE AFTER DECAY OF INCORPORATED RADIOACTIVE PHOSPHORUS . *By Gunther S. Stent*	1234
GENETICS.—EFFECT OF X-RAYS ON CHROMATID ABERRATIONS IN AIR AND IN NITROGEN. . . . . *By C. P. Swanson and Drew Schwarts*	1241
MATHEMATICS.—SPIRAL AND OTHER ASYMPTOTIC PATHS, AND PATHS OF COMPLETE INDETERMINATION, OF ANALYTIC AND MEROMORPHIC FUNCTIONS . . . . . *By F. Bagemihl and W. Seidel*	1251
MATHEMATICS.—THE GLOBAL BEHAVIOR OF DIFFERENTIAL EQUATIONS ON *N*-DIMENSIONAL MANIFOLDS . . . . . *By Felix Haas*	1258
MATHEMATICS.—CONJUGATE NETS, CONFORMAL STRUCTURE, AND INTERIOR TRANSFORMATIONS ON OPEN RIEMANN SURFACES . . . . . *By James Jenkins and Marston Morse*	1261
MATHEMATICS.—ON A DIFFERENTIAL-GEOMETRIC METHOD IN THE THEORY OF ANALYTIC STACKS . . . . . *By K. Kodaira*	1268
MATHEMATICS.—ON A THEOREM OF LEFSCHETZ AND THE LEMMA OF ENRIQUES-SEVERI-ZARISKI . . . . . *By K. Kodaira and D. C. Spencer*	1273
MATHEMATICS.—ON A NEW PROBLEM CONCERNING TRINOMIAL CONGRUENCES INVOLVING RATIONAL INTEGERS . *By Erna H. Pearson and H. S. Vandiver*	1278
PHYSIOLOGY.—MECHANOCHEMICAL PROPERTIES OF FIBERS OF SURFACE-SPREAD ACTOMYOSIN . . . . . *By Teru Hayashi and Raja Rosenbluth*	1285
ZOOLOGY.—PHOSPHOMONOESTERASES IN REEF-BUILDING CORALS . . . . . *By Thomas F. Goreau*	1291
NATIONAL ACADEMY OF SCIENCES.—VITAL STATISTICS OF OUR FOREIGN ASSOCIATES . . . . . *By Edwin B. Wilson*	1295
ERRATA.—LINEAR PARABOLIC DIFFERENTIAL EQUATIONS OF ARBITRARY ORDER; GENERAL BOUNDARY-VALUE PROBLEMS FOR ELLIPTIC EQUATIONS . . . . . *By Felix E. Browder*	1298
ERRATA.—DEVELOPMENT AND GENETICS OF A SEX-INFLUENCED TRAIT IN THE LIVERS OF MICE . . . . . *By C. H. Danforth*	1298

CURRENT PERIODICAL SERIES

PUBLICATION NO: 402

TITLE: NATIONAL ACADEMY OF SCIENCES.
PROCEEDINGS

VOLUME: 40

ISSUES: 1-12

DATE: January-December 1954

Notice: This periodical may be copyrighted, in which case the contents remain the property of the copyright owner. The microfilm edition is reproduced by agreement with the publisher. Duplication or resale without permission is prohibited.

Xerox University Microfilms, Ann Arbor, Michigan

MICROFILMED – 1973